Fate and Impacts of Contaminants of Emerging Concern during Wastewater Treatment

Yanjun Ma

Dissertation submitted to the faculty of the Virginia Polytechnic Institute and State University in partial fulfillment of the requirements for the degree of

Doctor of Philosophy
In
Civil Engineering

Amy J. Pruden-Bagchi
John T. Novak
Linsey C. Marr
Peter J. Vikesland

February 18, 2014
Blacksburg, VA

Keywords: Wastewater treatment, antibiotic resistance genes, engineered nanomaterials, anaerobic digestion, nitrification, toxicity

Fate and Impacts of Contaminants of Emerging Concern during Wastewater Treatment

Yanjun Ma

ABSTRACT

The purpose of this dissertation was to broadly investigate the fate of antibiotic resistance genes (ARGs) and engineered nanomaterials (ENMs) as representative contaminants of emerging concern in wastewater treatment plants (WWTPs). WWTPs may have their performance impacted by ENMs and may also serve as a reservoir and point of release for both ENMs and ARGs into the environment. Of interest were potential adverse effects of ENMs, such as stimulation of antibiotic resistance in the WWTP, toxicity to microbial communities critical for WWTP performance, and toxicity to humans who may be exposed to effluents or aerosols containing ENMs and their transformation products.

Response of nine representative ARGs encoding resistance to sulfonamide, erythromycin and tetracycline to various lab-scale sludge digestion processes were examined, and factors that drove the response of ARGs were discussed. Mesophilic anaerobic digestion significantly reduced *sul*I, *sul*II, *tet*(C), *tet*(G), and *tet*(X) with longer solids retention time (SRT) exhibiting a greater extent of removal. Thermophilic anaerobic digesters performed similarly to each other and provided more effective reduction of *erm*(B), *erm*(F), *tet*(O), and *tet*(W) compared to mesophilic digestion. Thermal hydrolysis pretreatment drastically reduced all ARGs, but they generally rebounded during subsequent anaerobic and aerobic digestion treatments. Bacterial community composition of the sludge digestion process, as controlled by the physical operating characteristics, was indicated to drive the distribution of ARGs present in the produced biosolids, more so than the influent ARG composition.

Effects of silver (nanoAg), zero-valent iron (NZVI), titanium dioxide (nanoTiO_2) and cerium dioxide (nanoCeO_2) nanomaterials on nitrification function and microbial communities were examined in duplicate lab-scale nitrifying sequencing batch reactors (SBRs), relative to control SBRs received no materials or ionic/bulk analogs. Nitrification function was only inhibited by high load of 20 mg/L Ag^+, but not by other nanomaterials or analogs. However, decrease of nitrifier gene abundances and distinct microbial communities were observed in SBRs receiving nanoAg, Ag^+, nanoCeO_2, and bulkCeO_2. There was no apparent effect of nanoTiO_2 or NZVI on nitrification, nitrifier gene abundances, or microbial community structure. A large portion of nanoAg remained dispersed in activated sludge and formed Ag-S complexes, while NZVI, nanoTiO_2 and nanoCeO_2 were mostly aggregated and chemically unmodified. Thus, the nanomaterials appeared to be generally stable in the activated sludge, which may limit their effect on nitrification function or microbial community structure.

Considering an aerosol exposure scenario, cytotoxicity and genotoxicity of aqueous effluent and biosolids from SBRs dosed with nanoAg, NZVI, nanoTiO_2 and nanoCeO_2 to A549 human lung epithelial cells were examined, and the effects were compared relative to outputs from SBRs dosed with ionic/bulk analogs and undosed SBRs, as well as pristine ENMs. Although the pristine nanomaterials showed varying extents of cytotoxicity to A549 cells, and gentoxicity was observed for nanoAg, no significant cytotoxic or genotoxic effects of the SBR effluents or biosolids containing nanomaterials were observed.

Studies presented in this dissertation provided new insights in the fate of ARGs in various sludge digestion processes and ENMs in nitrifying activated sludge system in lab-scale reactors. The study also yielded toxicity data of ENMs to biological wastewater treatment microbial communities and human lung cells indicated by a variety of toxicity markers. The results will aid in identifying appropriate management technologies for sludge containing ARGs and will inform microbial and human toxicity assessments of ENMs entering WWTPs.

ACKNOWLEDGEMENTS

I would like to give all my gratitude to my advisor, Dr. Amy Pruden, for her guidance, advice and support during the past five years, both academically and personally. Thank her for providing me the great research opportunities, and helping me to develop my research and writing skills. I especially appreciate for her patience and encouragement when I encountered difficulties. I would also like to give all my acknowledgments to my committee members, Dr. John Novak, Dr. Linsey Marr and Dr. Peter Vikesland for their time, patience, and valuable advices on my research.

I would like to give my sincere thanks to Dr. Elankumaran Subbiah, for hosting me in his lab to conduct the studies of nanomaterial toxicity, and his generous advices. Also thanks to Dr. Sandeep Kumar and Jagadeeswan Deventhiran of Dr. Subbiah's group for their assistance on the experimental methods.

I would like to give my sincere thanks Eric Vejerano, Jacob Metch, Chris Wilson, Ian Miller and Elena Leon for their hard-working and supporting on this research; Julie Petruska, Jody Smiley, and Jeff Parks for their assistance in setting up experiments and sample analysis, and helping me with all kinds of lab problems.

I would like to give my sincere appreciations to everyone of Dr. Pruden's group, for their friendship, encouragements and helps during the past five years; and the VT SuN group, which is not only very supportive to my research, but also a very good fellowship.

My deepest thanks were also given to my parents, sister, and brother, for their understanding and love all the time; and my church friends, and many other friends in Blacksburg and elsewhere. Thank you for all your caring and encouragements.

Finally, I give my special thanks to my husband Yuchang Wu, for his love, kindness, patience, encouragement, and taking care of our life (including cooking and washing dishes).

TABLE OF CONTENTS

TABLES

FIGURES

ATTRIBUTION

Each coauthor is duly credited for his or her contribution to this work, both in their sharing of ideas and technical expertise.

Amy Pruden, Ph.D. *Professor of Environmental Engineering*
(Principal Investigator) Department of Civil and Environmental Engineering,
Virginia Polytechnic Institute and State University. Blacksburg, VA 24061
Coauthor of chapters 2, 3, 4

Linsey C. Marr, Ph.D. *Professor of Environmental Engineering*
Department of Civil and Environmental Engineering,
Virginia Polytechnic Institute and State University. Blacksburg, VA 24061
Coauthor of chapters 3, 4

Eric P. Vejerano, Ph.D. *Postdoctoral Associate*
Department of Civil and Environmental Engineering,
Virginia Polytechnic Institute and State University. Blacksburg, VA 24061
Coauthor of chapter 3, 4

John T. Novak, Ph.D. *Professor of Environmental Engineering*
Department of Civil and Environmental Engineering,
Virginia Polytechnic Institute and State University. Blacksburg, VA 24061
Coauthor of chapter 2

Christopher A. Wilson, Ph.D.
Department of Civil and Environmental Engineering,
Virginia Polytechnic Institute and State University. Blacksburg, VA 24061
Coauthor of chapter 2

Rumana Riffat, Ph.D. *Professor of Environmental Engineering*
Department of Civil and Environmental Engineering,

George Washington University, Washington, DC 20052

Coauthor of chapter 2

Sebnem Aynur,
Department of Civil and Environmental Engineering,
George Washington University, Washington, DC 20052

Coauthor of chapter 2

Sudhir Murthy, Ph.D. *Innovations Chief*
DC WATER Blue Plains,
Washington, DC 20090

Coauthor of chapter 2

Jacob W. Metch, *Doctoral Student*
Department of Civil and Environmental Engineering,
Virginia Polytechnic Institute and State University. Blacksburg, VA 24061

Coauthor of chapter 3

Ian J. Miller, *Doctoral Student*
School of Pharmacy, University of Wisconsin. Madison, WI 53706

Coauthor of chapter 3

Elena C. Leon, *Undergraduate Student*
Department of materials Science and Engineering,
Stanford University. Stanford, CA 94305

Coauthor of chapter 3

Elankumaran Subbiah, Ph.D. *Associate Professor of Virology*
Department of Biomedical Sciences & Pathobiology,
Virginia Polytechnic Institute and State University. Blacksburg, VA 24061

Coauthor of chapter 4

CHAPTER 1: Introduction

1.1 Background

Contaminants of emerging concern or emerging contaminants (ECs) can be broadly defined as any chemical or biological pollutant that is not commonly monitored in the environment, but has the potential to enter the environment and cause known or suspected adverse ecological and (or) human health effects.[1] ECs include contaminants that are newly released into the environment, and also those that have persisted for a long time, but only recently have been recognized due to development of new detection methods or discovery of new source, exposure routes and effects.[2-4]

A vast group of chemicals of daily use has been identified as ECs, including pharmaceuticals and personal care products (PPCPs), surfactants and surfactant residues, gasoline additives, hormones and other endocrine disrupting compounds (EDCs), drinking water and swimming pool disinfection by-products (DBPs), engineered nanomaterials (ENMs), etc.[5-6] Emerging biological contaminants such as pathogenic microorganisms (bacteria, viruses, and protozoa) and antibiotic resistance genes (ARGs) can also be considered as ECs.[7-9]

To fill the data gap in assessing environmental risks of ECs, research can serve to characterize their transport and fate into the environment, exposure routes to humans and ecosystem, and toxicities under various exposure conditions. Wastewater treatment plants (WWTPs) have been an important research focus, for a large portion of ECs are generated from human use and enter wastewater streams. The current wastewater treatment configurations are usually not designed to remove ECs, and thus release of ECs such as PPCPs, EDCs, ENMs, and ARGs into natural waters through treated wastewater effluent has been widely reported.[10-14] ECs

can also associate with primary and secondary sludge and persist in biosolids for land-application.[15-19] Some ECs can be biologically or chemically transformed during treatment processes; however, the transformation products of some pharmaceuticals were reported to be more toxic than the parent compounds,[20-23] while transformation and toxicity of many other ECs are largely unknown. These findings highlight the need to critically evaluate existing wastewater treatment processes to track transformation and fate of ECs for better assessing their environmental impacts.

On the other hand, biological treatment is the key driving process of wastewater treatment, relying on microbial communities to remove and stabilize contaminants. In particular, nitrifying bacteria, which conduct the critical function of nitrification and oxidize ammonia to nitrite and subsequently nitrate, are highly sensitive to toxic chemicals.[24] As ECs with identified or suspected toxicities increasingly enter the wastewater streams, their potential adverse impacts on the microbial communities and further on the biological wastewater treatment functions are of concern.

In this dissertation, fate and impacts of two representative ECs during wastewater treatment were examined: 1) antibiotic resistance genes (ARGs), which encode bacterial resistance to antibiotics; and 2) engineered nanomaterials (ENMs), which emerged lately with the expanded application of nanotechnology in consumer products.

1.2 Antibiotic Resistance Genes (ARGs)

Antibiotic resistance is causing increasing failure in therapeutic treatment of bacterial diseases and is a major public health issue.[25] It occurred as early as shortly after the introduction of penicillin in the 1940s, and the resistance developed in *Staphylococcus aureus* was later spread to methicillin.[26] In recent years, resistance has been developed in *enterococci* that showed

high-level resistance to the glycopeptides antibiotic vancomycin, which is a drug of "last resort" against multi-resistant *enterococci* and against methicillin-resistant *Staphylococcus aureus*.[27] Multidrug resistance has also been reported to emerge in other organisms.[28,29]

In the early antibiotic era, mutation in target genes under antibiotic pressure was considered the primary cause of antibiotic resistance.[26] But more recent studies suggest that the majority of antibiotic resistance is most likely acquired through horizontal transfer of ARG from other ecologically and taxonomically distant bacteria.[30] The mobile genetic elements mediating horizontal gene transfer include plasmids, transposons, and integrons. All three classes of elements have been reported to play an important role in spread of ARG amongst bacteria.[31-33] Spread of ARGs has not been restricted within pathogens, but widely disseminated to common bacteria.[34] Moreover, recent research has revealed that ARGs have evolved to serve broader purposes for the cell beyond fighting antibiotics, and are also induced in response to general toxicities or other environmental stimuli.[27,35,36]

WWTPs receive large amount of antibiotics, bacteria, and other chemicals; the complex wastewater constituents are favorable for the development and horizontal transfer of ARGs among bacteria.[37] A wide range of ARGs has been detected in wastewater streams.[38,39] Tetracycline and sulfonamide resistance genes have been frequently detected in treated wastewater effluent and biosolids,[9,14,19,40,41] which revealed the potential of WWTPs to disseminate ARGs to the environment.

1.3 Engineered Nanomaterials (ENMs)

Engineered nanomaterials (ENMs) are defined as materials with one or more dimensions on the order of 1-100 nm. They are widely applied in many commercial products due to novel properties that are generally not seen in conventional bulk counterparts.[42] The range of

nanotechnology products is now extensive and can be broken down into a number of different compound classes, including metal oxides, zero-valent metals, semiconductor materials such as quantum dots, carbonaceous nanomaterials and nanopolymers.[43]

The emergence of ENMs inevitably leads to their release into the environment. Studies have documented release of nanosilver from textiles and fabrics during washing,[44,45] and emission of TiO_2 nanoparticles from exterior façade paints to the discharge and into surface waters.[46] A study on the life cycle of ENMs indicated that except for a limited amount of recycling, the majority of nanomaterials in manufactured products will end up in disposal systems, e.g. landfill, incineration and wastewater treatment.[42] In particular, Mueller and Nowack[47] modeled flow of ENMs (nanosilver, nano-TiO_2 and carbon nanotubes) from products to air, soil, and water in Switzerland, and indicated that up to 95% of the nanosilver and nano-TiO_2 in textiles, cosmetics, sprays, cleaning agents, coatings, paints and plastics are released into WWTPs. This finding emphasizes the critical role of WWTPs on the pathway of ENMs to the environment.

The fate of silver, silica, copper, titanium dioxide, cerium oxide nanoparticles and fullerenes following wastewater treatment has been studied, and generally indicated their removal from wastewater streams and association with the sludge, although a small portion still retained in aqueous effluent.[13,17,18,48-51] The extent of different ENMs partitioning into activated sludge was distinct. While ENMs may primarily partition into primary sludge and be routed to anaerobic digestion, partitioning into activated sludge is also important to consider and has been addressed by some studies. For example, a simulated wastewater treatment system removed less carboxy-terminated polymer coated silver nanoparticles (88%) from wastewaters compared with hydroxylated fullerenes (>90%), aqueous fullerenes (>95%), and nano-TiO_2 (>95%).[18] The

association of ENMs with activated sludge could be affected by their properties and constituents of the wastewater matrix. Significant influence of surface charge and the addition of dispersion stabilizing surfactants on the removal of cerium dioxide nanoparticles from wastewater were observed in a model wastewater treatment system.[13] In another study, silica nanoparticles coated with Tween 20 underwent rapid flocculation, while the uncoated nanoparticles did not flocculate in wastewater over typical residence times for primary treatment.[48] Effect of extracellular polymeric substances (EPS) and natural organic matters (NOM) on the removal of ENMs by activated sludge was examined, and aqueous fullerenes showed a change in the degree of removal when the nanomaterial suspensions were equilibrated with NOM or EPS was extracted from the biomass.[52]

Due to the limitation of detection and quantification techniques, as well as the complexity of wastewater and activated sludge matrix, transformation of ENMs during wastewater treatment is largely unknown. A few recent studies identified conversion of nanosilver to silver sulfide (Ag_2S) and subsequent precipitation into activated sludge.[53-55] Zinc oxide (ZnO) nanoparticles were observed to be transformed to three Zn-containing species, ZnS, $Zn_3(PO4)_2$, and Zn associated Fe oxy/hydroxides in a pilot wastewater treatment plant.[55]

The small nano-size and large surface area of ENMs may increase their reactivity and thus have the potential to exert toxicity to biological systems.[56] Toxicity of ENMs to bacteria pure cultures has been documented in a growing number of studies.[57-59] Therefore, it is suspected that accumulation of ENMs in activated sludge may cause adverse effects on the efficiency of wastewater treatment due to their toxicity to bacterial community, especially nitrifying bacteria, which are sensitive to toxic chemicals. Inhibition of nanosilver to nitrification has been observed in *Nitrosomonas europaea* pure culture[60,61] and enriched nitrifying microorganisms.[62] The

inhibitory effect was further verified by shock loading of 0.75 mg/L nanosilver to a lab-scale Modified Ludzacke Ettinger process, which divided the activated sludge chamber to anoxic and aerobic zones aiming at nitrogen and organic removal.[63] In another study, nitrification efficiency in an anaerobic-low dissolved oxygen sequencing batch reactor was greatly decreased by short-term exposure of ZnO nanoparticles.[64] In the same type of wastewater treatment system, TiO_2 nanoparticles had no acute effects on nitrogen removal after short term exposure, but significantly decreased the nitrification efficiency after long-term exposure.[65]

It should be noted that pure culture assays do not always correspond well to complex environments.[66,67] For example, single walled carbon nanotubes (SWCNTs) were reported to exhibit strong antimicrobial activity in pure cultures.[68] However, in one study, the addition of SWCNTs to activated sludge system did not negatively impact the performance of the reactor, and instead improved sludge settleability and dewaterability.[69] The complex wastewater matrix may alter the toxicity of ENMs by transformations. Furthermore, considering the microbial ecology that drives wastewater treatment, microbial toxicity is particularly relevant at the community level. However, to the author's knowledge, microbial community response to ENMs in the wastewater treatment process has not been characterized.

ENM residuals and transformed forms can be released into natural water and soil from wastewater treatment plants through discharge of water effluent and land-application of biosolids, and thus has the potential to be exposed to human and ecosystem. Cytotoxicity and genotoxicity of common metal and carbon based ENMs to a variety of human and animal cells or tissues has been reported.[70-73] However, to the author's knowledge, the toxicity of environmental samples potentially containing ENMs, such as aqueous effluent and biosolids resulted from

wastewater treatment is rarely examined. It is also unknown whether the transformation of ENMs converts them to non-toxic forms or more toxic chemical structures.

1.4 Research Objectives

The overall objectives of this research are to understand fate of ARGs and ENMs during wastewater treatment processes and to evaluate the toxicity of ENMs during and following wastewater treatment.

To achieve this general objective, the following specific objectives were pursued:

1) Examine effects of various sludge digestion processes on ARG removal and corresponding microbial community compositions in digesters with different SRT, temperature, redox, and feed conditions of untreated biosolids versus thermal hydrolysis pretreatment products.

2) Examine effects of ENMs in nitrifying lab-scale sequencing batch reactors (SBRs) on nitrification function, abundance of nitrifying bacteria, and microbial community compositions, and identify possible relationships of nanomaterial transformation state and the effects observed.

3) Assess cytotoxicity and genotoxicity of wastewater effluent and biosolids from SBRs dosed with ENMs, to examine the toxicity of transformed ENM following biological wastewater treatment, and compare with the toxicities of pristine nanomaterials.

1.5 Annotated Dissertation Outline

Chapter 1: *Introduction.*

Chapter 2: *Effect of Various Sludge Digestion Conditions on Sulfonamide, Macrolide, and Tetracycline Resistance Genes and Class 1 Integrons.* This manuscript addressed the first

specific objective, and examined response of nine representative ARGs encoding resistance to sulfonamide, erythromycin, and tetracycline to lab-scale mesophilic, thermophilic anaerobic digesters and a sequential digestion process with thermal hydrolysis pretreatment. Quantitative Polymerase Chain Reaction (Q-PCR) was used to quantify target genes. Microbial communities were characterized by Denaturing Gradient Gel Electrophoresis (DGGE) and sequencing. The role of microbial community compositions in driving the response of ARGs was discussed. The manuscript has been accepted for publication:

Ma, Y.; Wilson, C. A.; Novak, J. T.; Riffat, R.; Aynur, S.; Murthy, S.; Pruden, A., Effect of Various Sludge Digestion Conditions on Sulfonamide, Macrolide, and Tetracycline Resistance Genes and Class I Integrons. *Environ Sci Technol* **2011,** *45* (18), 7855-7861.

Chapter 3: *Microbial Community Response of Nitrifying Sequencing Batch Reactors to Silver, Zero-Valent Iron, Titanium Dioxide, and Cerium Dioxide Nanomaterials.* This manuscript addressed the second specific objective, and examined effect of silver, zero-valent iron, titanium doxide and cerium dioxide nanomaterials on nitrification function, abundance of nitrifying bacteria (Q-PCR) and microbial communities (Pyrosequencing) in lab-scale SBRs. The effects of nanomaterials in SBRs were compared with SBRs receiving no material and ionic/bulk analogs. Transformation of nanomaterials in SBRs was characterized by Transmission Electron Microscopy (TEM) equipped with Energy Dispersive X-ray Spectroscopy (EDS). The relationship of nanomaterial transformation and the observed effects were discussed. The manuscript is currently under peer-review at *Environmental Science & Technology*.

Chapter 4: *Toxicity of Engineered Nanomaterials and Their Transformation Products Following Wastewater Treatment on A549 Human Lung Epithelial Cells.* This manuscript addressed the third specific objective, and evaluated cytotoxicity and genotoxicity to A549 human lung epithelial cells of wastewater effluents and biosolids from SBR conditions studied in Chapter 3. The effects were compared with pristine nanomaterials and ionic/bulk analogs. Cytoxicity to A549 cells was examined by WST-1 assay, and genotoxicity was analyzed by immunofluorescent labeling of γH2AX foci. This manuscript is currently under peer-review at *Environmental Science & Technology Letters*.

Chapter 5: *Conclusions.* This chapter summarized key conclusions drawn from this study, and highlighted the scientific contributions of this study in understanding fate of ARGs and ENMs during wastewater treatment processes, and toxicity implications of ENMs. Future research was suggested based on outputs of this study.

1.6 References

(1) *U. S. Geological Survey (USGS)* website; http://toxics.usgs.gov/regional/emc/, accessed in January, 2014.

(2) Murnyak, G.; Vandenberg, J.; Yaroschak, P. J.; Williams, L.; Prabhakaran, K.; Hinz, J., Emerging contaminants: Presentations at the 2009 Toxicology and Risk Assessment Conference. *Toxicol Appl Pharm* **2011,** *254* (2), 167-169.

(3) Battaglin, W.; Drewes, Jorg.; Bruce, B.; McHugh, M., Introduction: Contaminants of Emerging Concern in the Environment. *Water resources impact* **2007**, *9* (3), 3-4

(4) Daughton, C. G., Non-regulated water contaminants: emerging research. *Environ Impact Asses* **2004,** *24* (7-8), 711-732.

(5) Aguera, A.; Bueno, M. J. M.; Fernandez-Alba, A. R., New trends in the analytical determination of emerging contaminants and their transformation products in environmental waters. *Environ Sci Pollut R* **2013,** *20* (6), 3496-3515.

(6) Petrovic, M.; et al. Emerging Contaminants in Waste Waters: Sources and Occurrence. In *The Handbook of Environmental Chemistry, Volume 5, Part S5/1, Emerging Contaminants from Industrial and Municipal Waste: Occurrence, Analysis and Effects*; Barcelo, D.; Petrovic, M.; Eds.; Springer-Verlag Berlin Heidelberg: New York 2008; pp 3.

(7) Smital, T.; Acute and Chronic Effects of Emerging Contaminants. In *The Handbook of Environmental Chemistry, Volume 5, Part S5/1, Emerging Contaminants from Industrial and Municipal Waste: Occurrence, Analysis and Effects*; Barcelo, D.; Petrovic, M.; Eds.; Springer-Verlag Berlin Heidelberg: New York 2008; pp 126-127.

(8) Younos, T.; Harwood, V. J.; Falkinham III, J. O.; Shen, H., Pathogens in Natural and Engineered Water Systems: Emerging Issues. *Water resources impact* **2007**, *9* (3), 11-14

(9) Pruden, A.; Pei, R. T.; Storteboom, H.; Carlson, K. H., Antibiotic resistance genes as emerging contaminants: Studies in northern Colorado. *Environ Sci Technol* **2006,** *40* (23), 7445-7450.

(10) Watkinson, A. J.; Murby, E. J.; Costanzo, S. D., Removal of antibiotics in conventional and advanced wastewater treatment: Implications for environmental discharge and wastewater recycling. *Water Res* **2007,** *41* (18), 4164-4176.

(11) Joss, A.; Zabczynski, S.; Gobel, A.; Hoffmann, B.; Loffler, D.; McArdell, C. S.; Ternes, T. A.; Thomsen, A.; Siegrist, H., Biological degradation of pharmaceuticals in municipal wastewater treatment: Proposing a classification scheme. *Water Res* **2006,** *40* (8), 1686-1696.

(12) Kuch, H. M.; Ballschmiter, K., Determination of endocrine-disrupting phenolic compounds and estrogens in surface and drinking water by HRGC-(NCI)-MS in the picogram per liter range. *Environ Sci Technol* **2001,** *35* (15), 3201-3206.

(13) Limbach, L. K.; Bereiter, R.; Mueller, E.; Krebs, R.; Gaelli, R.; Stark, W. J., Removal of oxide nanoparticles in a model wastewater treatment plant: Influence of agglomeration and surfactants on clearing efficiency. *Environ Sci Technol* **2008,** *42* (15), 5828-5833.

(14) Auerbach, E. A.; Seyfried, E. E.; McMahon, K. D., Tetracycline resistance genes in activated sludge wastewater treatment plants. *Water Res* **2007,** *41* (5), 1143-1151.

(15) Kinney, C. A.; Furlong, E. T.; Zaugg, S. D.; Burkhardt, M. R.; Werner, S. L.; Cahill, J. D.; Jorgensen, G. R., Survey of organic wastewater contaminants in biosolids destined for land application. *Environ Sci Technol* **2006,** *40* (23), 7207-7215.

(16) McClellan, K.; Halden, R. U., Pharmaceuticals and personal care products in archived US biosolids from the 2001 EPA national sewage sludge survey. *Water Res* **2010,** *44* (2), 658-668.

(17) Kiser, M. A.; Westerhoff, P.; Benn, T.; Wang, Y.; Perez-Rivera, J.; Hristovski, K., Titanium Nanomaterial Removal and Release from Wastewater Treatment Plants. *Environ Sci Technol* **2009,** *43* (17), 6757-6763.

(18) Wang, Y. F.; Westerhoff, P.; Hristovski, K. D., Fate and biological effects of silver, titanium dioxide, and C-60 (fullerene) nanomaterials during simulated wastewater treatment processes. *J Hazard Mater* **2012,** *201*, 16-22.

(19) Munir, M.; Xagoraraki, I., Levels of Antibiotic Resistance Genes in Manure, Biosolids, and Fertilized Soil. *J Environ Qual* **2011,** *40* (1), 248-255.

(20) Radjenovic, J.; Petrovic, M.; Barcelo, D., Complementary mass spectrometry and bioassays for evaluating pharmaceutical-transformation products in treatment of drinking water and wastewater. *Trac-Trend Anal Chem* **2009,** *28* (5), 562-580.

(21) Fatta-Kassinos, D.; Vasquez, M. I.; Kummerer, K., Transformation products of pharmaceuticals in surface waters and wastewater formed during photolysis and advanced oxidation processes - Degradation, elucidation of byproducts and assessment of their biological potency. *Chemosphere* **2011,** *85* (5), 693-709.

(22) Oulton, R. L.; Kohn, T.; Cwiertny, D. M., Pharmaceuticals and personal care products in effluent matrices: A survey of transformation and removal during wastewater treatment and implications for wastewater management. *J Environ Monitor* **2010,** *12* (11), 1956-1978.

(23) la Farre, M.; Perez, S.; Kantiani, L.; Barcelo, D., Fate and toxicity of emerging pollutants, their metabolites and transformation products in the aquatic environment. *Trac-Trend Anal Chem* **2008,** *27* (11), 991-1007.

(24) Lydmark, P.; Almstrand, R.; Samuelsson, K.; Mattsson, A.; Sorensson, F.; Lindgren, P. E.; Hermansson, M., Effects of environmental conditions on the nitrifying population dynamics in a pilot wastewater treatment plant. *Environ Microbiol* **2007,** *9* (9), 2220-2233.

(25) Baquero, F.; Blazquez, J., Evolution of antibiotic resistance. *Trends Ecol Evol* **1997,** *12* (12), 482-487.

(26) Monroe, S.; Polk, R., Antimicrobial use and bacterial resistance. *Curr Opin Microbiol* **2000,** *3* (5), 496-501.

(27) Martinez, J. L., Antibiotics and antibiotic resistance genes in natural environments. *Science* **2008,** *321* (5887), 365-367.

(28) Melano, R.; Corso, A.; Petroni, A.; Centron, D.; Orman, B.; Pereyra, A.; Moreno, N.; Galas, M., Multiple antibiotic-resistance mechanisms including a novel combination of extended-spectrum beta-lactamases in a Klebsiella pneumoniae clinical strain isolated in Argentina. *J Antimicrob Chemoth* **2003,** *52* (1), 36-42.

(29) Levy, S. B., Factors impacting on the problem of antibiotic resistance. *J Antimicrob Chemoth* **2002,** *49* (1), 25-30.

(30) Alonso, A.; Sanchez, P.; Martinez, J. L., Environmental selection of antibiotic resistance genes. *Environ Microbiol* **2001,** *3* (1), 1-9.

(31) Szczepanowski, R.; Braun, S.; Riedel, V.; Schneiker, S.; Krahn, I.; Puhler, A.; Schluter, A., The 120 592 bp lncF plasmid pRSB107 isolated from a sewage-treatment plant encodes nine different anti biotic-resistance determinants, two iron-acquisition systems and other putative virulence-associated functions. *Microbiol-Sgm* **2005,** *151*, 1095-1111.

(32) Knapp, C. W.; Engemann, C. A.; Hanson, M. L.; Keen, P. L.; Hall, K. J.; Graham, D. W., Indirect evidence of transposon-mediated selection of antibiotic resistance genes in aquatic systems at low-level oxytetracycline exposures. *Environ Sci Technol* **2008,** *42* (14), 5348-5353.

(33) Schmidt, A. S.; Bruun, M. S.; Dalsgaard, I.; Larsen, J. L., Incidence, distribution, and spread of tetracycline resistance determinants and integron-associated antibiotic resistance genes among motile aeromonads from a fish farming environment. *Appl Environ Microb* **2001,** *67* (12), 5675-5682.

(34) Chopra, I.; Roberts, M., Tetracycline antibiotics: Mode of action, applications, molecular biology, and epidemiology of bacterial resistance. *Microbiol Mol Biol R* **2001,** *65* (2), 232-260.

(35) Davies, J.; Spiegelman, G. B.; Yim, G., The world of subinhibitory antibiotic concentrations. *Curr Opin Microbiol* **2006**, 9 (5), 445-453.

(36) Qiu, Z. G.; Yu, Y. M.; Chen, Z. L.; Jin, M.; Yang, D.; Zhao, Z. G.; Wang, J. F.; Shen, Z. Q.; Wang, X. W.; Qian, D.; Huang, A. H.; Zhang, B. C.; Li, J. W., Nanoalumina promotes the horizontal transfer of multiresistance genes mediated by plasmids across genera. *P Natl Acad Sci USA* **2012,** *109* (13), 4944-4949.

(37) Baquero, F.; Martinez, J. L.; Canton, R., Antibiotics and antibiotic resistance in water environments. *Curr Opin Biotech* **2008,** *19* (3), 260-265.

(38) Schwartz, T.; Kohnen, W.; Jansen, B.; Obst, U., Detection of antibiotic-resistant bacteria and their resistance genes in wastewater, surface water, and drinking water biofilms. *Fems Microbiol Ecol* **2003,** *43* (3), 325-335.

(39) Volkmann, H.; Schwartz, T.; Bischoff, P.; Kirchen, S.; Obst, U., Detection of clinically relevant antibiotic-resistance genes in municipal wastewater using real-time PCR (TaqMan). *J Microbiol Meth* **2004,** *56* (2), 277-286.

(40) Pei, R. T.; Kim, S. C.; Carlson, K. H.; Pruden, A., Effect of River Landscape on the sediment concentrations of antibiotics and corresponding antibiotic resistance genes (ARG). *Water Res* **2006,** *40* (12), 2427-2435.

(41) Munir, M.; Wong, K.; Xagoraraki, I., Release of antibiotic resistant bacteria and genes in the effluent and biosolids of five wastewater utilities in Michigan. *Water Res* **2011,** *45* (2), 681-693.

(42) Meyer, D. E.; Curran, M. A.; Gonzalez, M. A., An Examination of Existing Data for the Industrial Manufacture and Use of Nanocomponents and Their Role in the Life Cycle Impact of Nanoproducts. *Environ Sci Technol* **2009,** *43* (5), 1256-1263.

(43) Klaine, S. J.; Alvarez, P. J. J.; Batley, G. E.; Fernandes, T. F.; Handy, R. D.; Lyon, D. Y.; Mahendra, S.; McLaughlin, M. J.; Lead, J. R., Nanomaterials in the environment: Behavior, fate, bioavailability, and effects. *Environ Toxicol Chem* **2008,** *27* (9), 1825-1851.

(44) Benn, T. M.; Westerhoff, P., Nanoparticle silver released into water from commercially available sock fabrics. *Environ Sci Technol* **2008,** *42* (11), 4133-4139.

(45) Geranio, L.; Heuberger, M.; Nowack, B., The Behavior of Silver Nanotextiles during Washing. *Environ Sci Technol* **2009,** *43* (21), 8113-8118.

(46) Kaegi, R.; Ulrich, A.; Sinnet, B.; Vonbank, R.; Wichser, A.; Zuleeg, S.; Simmler, H.; Brunner, S.; Vonmont, H.; Burkhardt, M.; Boller, M., Synthetic TiO(2) nanoparticle emission from exterior facades into the aquatic environment. *Environ Pollut* **2008,** *156* (2), 233-239.

(47) Mueller, N. C.; Nowack, B., Exposure modeling of engineered nanoparticles in the environment. *Environ Sci Technol* **2008,** *42* (12), 4447-4453.

(48) Jarvie, H. P.; Al-Obaidi, H.; King, S. M.; Bowes, M. J.; Lawrence, M. J.; Drake, A. F.; Green, M. A.; Dobson, P. J., Fate of Silica Nanoparticles in Simulated Primary Wastewater Treatment. *Environ Sci Technol* **2009,** *43* (22), 8622-8628.

(49) Ganesh, R.; Smeraldi, J.; Hosseini, T.; Khatib, L.; Olson, B. H.; Rosso, D., Evaluation of Nanocopper Removal and Toxicity in Municipal Wastewaters. *Environ Sci Technol* **2010,** *44* (20), 7808-7813.

(50) Westerhoff, P.; Song, G. X.; Hristovski, K.; Kiser, M. A., Occurrence and removal of titanium at full scale wastewater treatment plants: implications for TiO2 nanomaterials. *J Environ Monitor* **2011,** *13* (5), 1195-1203.

(51) Gomez-Rivera, F.; Field, J. A.; Brown, D.; Sierra-Alvarez, R., Fate of cerium dioxide (CeO_2) nanoparticles in municipal wastewater during activated sludge treatment. *Bioresource Technol* **2012,** *108*, 300-304.

(52) Kiser, M. A.; Ryu, H.; Jang, H. Y.; Hristovski, K.; Westerhoff, P., Biosorption of nanoparticles to heterotrophic wastewater biomass. *Water Res* **2010,** *44* (14), 4105-4114.

(53) Kim, B.; Park, C. S.; Murayama, M.; Hochella, M. F., Discovery and Characterization of Silver Sulfide Nanoparticles in Final Sewage Sludge Products. *Environ Sci Technol* **2010,** *44* (19), 7509-7514.

(54) Kaegi, R.; Voegelin, A.; Sinnet, B.; Zuleeg, S.; Hagendorfer, H.; Burkhardt, M.; Siegrist, H., Behavior of Metallic Silver Nanoparticles in a Pilot Wastewater Treatment Plant. *Environ Sci Technol* **2011,** *45* (9), 3902-3908.

(55) Ma, R.; Levard, C.; Judy, J.D.; Unrine, J.M.; Durenkamp, M.; Ben Martin, Jefferson, B.; Lowry, G.V., Fate of Zinc Oxide and Silver Nanoparticles in a Pilot Wastewater Treatment Plant and in Processed Biosolids. *Environ Sci Technol* **2014**, doi.org/10.1021/es403646.

(56) Nel, A.; Xia, T.; Madler, L.; Li, N., Toxic potential of materials at the nanolevel. *Science* **2006,** *311* (5761), 622-627.

(57) Sondi, I.; Salopek-Sondi, B., Silver nanoparticles as antimicrobial agent: a case study on E-coli as a model for Gram-negative bacteria. *J Colloid Interf Sci* **2004,** *275* (1), 177-182.

(58) Li, M.; Zhu, L. Z.; Lin, D. H., Toxicity of ZnO Nanoparticles to Escherichia coil: Mechanism and the Influence of Medium Components. *Environ Sci Technol* **2011,** *45* (5), 1977-1983.

(59) Pelletier, D. A.; Suresh, A. K.; Holton, G. A.; McKeown, C. K.; Wang, W.; Gu, B. H.; Mortensen, N. P.; Allison, D. P.; Joy, D. C.; Allison, M. R.; Brown, S. D.; Phelps, T. J.;

Doktycz, M. J., Effects of Engineered Cerium Oxide Nanoparticles on Bacterial Growth and Viability. *Appl Environ Microb* **2010,** *76* (24), 7981-7989.

(60) Arnaout, C. L.; Gunsch, C. K., Impacts of Silver Nanoparticle Coating on the Nitrification Potential of *Nitrosomonas europaea*. *Environ Sci Technol* **2012**, *46 (10)*, 5387-5395.

(61) Radniecki, T. S.; Stankus, D. P.; Neigh, A.; Nason, J. A.; Semprini, L., Influence of liberated silver from silver nanoparticles on nitrification inhibition of *Nitrosomonas europaea*. *Chemosphere* **2011**, *85 (1)*, 43-49.

(62) Choi, O.; Deng, K. K.; Kim, N. J.; Ross, L.; Surampalli, R. Y.; Hu, Z. Q., The inhibitory effects of silver nanoparticles, silver ions, and silver chloride colloids on microbial growth. *Water Res* **2008**, *42 (12)*, 3066-3074.

(63) Liang, Z. H.; Das, A.; Hu, Z. Q., Bacterial response to a shock load of nanosilver in an activated sludge treatment system. *Water Res* **2010,** *44* (18), 5432-5438.

(64) Zheng, X. O.; Wu, R.; Chen, Y. G., Effects of ZnO Nanoparticles on Wastewater Biological Nitrogen and Phosphorus Removal. *Environ Sci Technol* **2011,** *45* (7), 2826-2832.

(65) Zheng, X.; Chen, Y. G.; Wu, R., Long-Term Effects of Titanium Dioxide Nanoparticles on Nitrogen and Phosphorus Removal from Wastewater and Bacterial Community Shift in Activated Sludge. *Environ Sci Technol* **2011,** *45* (17), 7284-7290.

(66) Neal, A. L., What can be inferred from bacterium-nanoparticle interactions about the potential consequences of environmental exposure to nanoparticles? *Ecotoxicology* **2008,** *17* (5), 362-371.

(67) Kang, S.; Mauter, M. S.; Elimelech, M., Microbial Cytotoxicity of Carbon-Based Nanomaterials: Implications for River Water and Wastewater Effluent. *Environ Sci Technol* **2009,** *43* (7), 2648-2653.

(68) Kang, S.; Pinault, M.; Pfefferle, L. D.; Elimelech, M., Single-walled carbon nanotubes exhibit strong antimicrobial activity. *Langmuir* **2007,** *23* (17), 8670-8673.

(69) Yin, Y.; Zhang, X., Evaluation of the impact of single-walled carbon nanotubes in an activated sludge wastewater reactor. *Water Sci Technol* **2008,** *58* (3), 623-628.

(70) Yang, H.; Liu, C.; Yang, D. F.; Zhang, H. S.; Xi, Z. G., Comparative study of cytotoxicity, oxidative stress and genotoxicity induced by four typical nanomaterials: the role of particle size, shape and composition. *J Appl Toxicol* **2009,** *29* (1), 69-78.

(71) Lindberg, H. K.; Falck, G. C. M.; Suhonen, S.; Vippola, M.; Vanhala, E.; Catalan, J.; Savolainen, K.; Norppa, H., Genotoxicity of nanomaterials: DNA damage and micronuclei induced by carbon nanotubes and graphite nanofibres in human bronchial epithelial cells in vitro. *Toxicol Lett* **2009,** *186* (3), 166-173.

(72) Jia, G.; Wang, H. F.; Yan, L.; Wang, X.; Pei, R. J.; Yan, T.; Zhao, Y. L.; Guo, X. B., Cytotoxicity of carbon nanomaterials: Single-wall nanotube, multi-wall nanotube, and fullerene. *Environ Sci Technol* **2005,** *39* (5), 1378-1383.

(73) Balasubramanyam, A.; Sailaja, N.; Mahboob, M.; Rahman, M. F.; Hussain, S. M.; Grover, P., In vivo genotoxicity assessment of aluminium oxide nanomaterials in rat peripheral blood cells using the comet assay and micronucleus test. *Mutagenesis* **2009,** *24* (3), 245-251.

CHAPTER 2: Effect of Various Sludge Digestion Conditions on Sulfonamide, Macrolide and Tetracycline Resistance Genes and Class I Integrons

Yanjun Ma, Christopher A. Wilson, John T. Novak, Rumana Riffat, Sebnem Aynur, Sudhir Murthy, and Amy Pruden

2.1 Abstract

Wastewater treatment processes are of growing interest as a potential means to limit the dissemination of antibiotic resistance. This study examines the response of nine representative antibiotic resistance genes (ARGs) encoding resistance to sulfonamide (*sul*I, *sul*II), erythromycin (*erm*(B), *erm*(F)) and tetracycline (*tet*(O), *tet*(W), *tet*(C), *tet*(G), *tet*(X)) to various laboratory-scale sludge digestion processes. The class I integron gene (*int*I1) was also monitored as an indicator of horizontal gene transfer potential and multiple antibiotic resistance. Mesophilic anaerobic digestion at both 10 and 20 day solids retention times (SRTs) significantly reduced *sul*I, *sul*II, *tet*(C), *tet*(G) *and tet*(X) with longer SRT exhibiting a greater extent of removal; however, *tet*W, *erm*B *and erm*F genes increased relative to the feed. Thermophilic anaerobic digesters operating at 47 ℃, 52 ℃ and 59 ℃ performed similarly to each other and provided more effective reduction of *erm*(B), *erm*(F), *tet*(O) and *tet*(W) compared to mesophilic digestion. However, thermophilic digestion resulted in similar or poorer removal of all other ARGs and *int*I1. Thermal hydrolysis pretreatment drastically reduced all ARGs, but they generally rebounded during subsequent anaerobic and aerobic digestion treatments. To gain insight into potential mechanisms driving ARG behavior in the digesters, the dominant bacterial communities were compared by denaturing gradient gel electrophoresis. The overall results suggest that bacterial community composition of the sludge digestion process, as controlled by

the physical operating characteristics, drives the distribution of ARGs present in the produced biosolids, more so than the influent ARG composition.

2.2 Introduction

Numerous studies have demonstrated that antibiotic resistant bacteria are present and can proliferate in wastewater treatment plants (WWTPs).[1-3] Given the potential detriment to human health as a result of the growing problem of antibiotic resistance, the fate of antibiotic resistant bacteria emanating from WWTPs is of interest. WWTPs produce two primary product streams, reclaimed water, which is typically returned directly to aquatic receiving environments or used for irrigation purposes, and biosolids, of which about 55% are land-applied as a beneficial soil amendment and the remainder disposed of in land-fills or by incineration.[4]

Antibiotic resistance is imparted to bacteria by their carriage of DNA encoding antibiotic resistance, or antibiotic resistance genes (ARGs). In one study, nine out of ten tetracycline ARGs assayed were commonly detected in WWTP effluent compared to only two out of ten in neighboring Wisconsin lakes,[5] suggesting that WWTPs may be a significant source of ARGs to the aquatic environment. Further, in a recent study it was found that the molecular signature of ARG occurrence at human-impacted sites along a Colorado river more closely matched those of WWTPs than neighboring animal feeding operation lagoons or the upstream pristine portion of the river.[6] With respect to biosolids, elevated levels of tetracycline ARGs *tet*(O), *tet*(W) and the sulfonamide ARG *sul*I were observed in certain soil types after land application.[7] Such findings highlight the need to critically evaluate existing WWTP treatment processes for their potential to attenuate ARGs and limit dissemination to the environment.

In a positive sense, WWTPs may present the opportunity to minimize potential risk to human health, ideally through simple, effective, and economical modifications. In particular,

treatment processes that go beyond traditional disinfection and actually destroy DNA are of interest, given that ARGs can persist and are highly prone to uptake by downstream bacteria via horizontal gene transfer.[8-10] Characterizing the effectiveness of WWTP processes in terms of the fate of ARGs is also of value considering that pure-culture based methods overlook the vast pool of uncultured organisms.[11] Although about one to three orders of magnitude of *tet* ARG reduction has been observed in full-scale WWTP, *tet* ARGs are still present at about 10^2 to 10^6 copies per milliliter in effluent waters[5,12] and about 10^8 to 10^9 copies per gram of treated biosolids.[5,7] Thus sludge digestion represents a potentially key process for reducing the spread of ARGs.

The most widely applied sludge digestion technology is mesophilic producing class B biosolids. However, increasing demand for higher quality biosolids and more rigorous inactivation of pathogens has driven interest in alternative methods, such as thermophilic digestion,[13] dual-stage treatment,[14] and digestion combined with pretreatments and polishing steps.[15] Of these, only the effect of thermophilic digestion on ARGs has been reported.[16] In this study it was observed that anaerobic thermophilic treatment was markedly effective in reducing tetracycline ARGs relative to mesophilic digestion in full-scale digesters. Subsequently the thermophilic phenomenon was confirmed in lab-scale anaerobic digesters operated over a range of temperatures (22 ℃, 37 ℃, 46 ℃, and 55 ℃).[17] While these findings promise a practical approach to reduce the load of ARGs released to the environment, it is important that the effect be demonstrated over a broad range of ARGs and is extended to other treatments. Moreover, the potential for horizontal transfer of ARGs within bacterial communities during various treatment processes is also of interest. Varied response of ARGs to biological treatment has been observed in other studies.[18,19]

In this study, optimally-functioning lab-scale digesters were investigated under the following conditions: (i) mesophilic anaerobic digestion at 10 and 20 days SRT; (ii) thermophilic anaerobic digestion at 47 ℃, 52 ℃ and 59 ℃; and (iii) sequential thermal hydrolytic pretreatment followed by mesophilic anaerobic and aerobic digestion. Nine ARGs encoding sulfonamide resistance (*sul*I and *sul*II), macrolide resistance (*erm*(B) and *erm*(F)), and three sub-classes of tetracycline resistance (ribosomal protection: *tet*(O) and *tet*(W); tetracycline efflux: *tet*(C) and *tet*(G); tetracycline transformation: *tet*(X)) were quantified by quantitative polymerase chain reaction (Q-PCR) during steady-state operation. Additionally, the integrase gene *int*I1 of Class I integrons was tracked as an indicator of horizontal gene transfer potential. Bacterial communities were characterized by denaturing gradient gel electrophoresis (DGGE) to illustrate their role in driving ARG response to various treatment conditions. Thus, this study provides insight into the potential of a broad range of sludge digestion techniques to reduce several representative antibiotic resistance elements across various classes and resistance mechanisms.

2.3 Materials and Methods

2.3.1 Description of Sludge Treatment Processes

The feed sludge to all treatment processes was from the DCWATER Blue Plains WWTP consisting of a 1:1 ratio of primary and secondary solids, with a combined total solids (TS) concentration of approximately 3%. One mesophilic anaerobic digester was operated at George Washington University at 35 ℃ with an active volume of 10 L and SRT of 10 days. All other mesophilic and thermophilic digesters were operated at Virginia Tech, using identical reactor configurations and temperature control systems. These included a mesophilic anaerobic digester operated at 35 ℃ with an active volume of 10L and SRT of 20 days, and three thermophilic

digesters operated at 47 ℃, 52 ℃, and 59 ℃, respectively, with active volumes of 12 L and 15 day SRTs.

For the sequential process, the feed sludge was dewatered to approximately 15% TS by DCWATER, shipped on ice to RDP technologies, Inc. (Norristown, PA) and subjected to thermal hydrolysis pretreatment at 150 ℃/4.80 bar for 30 min, followed by an immediate flash to ambient temperature and pressure. The sludge hydrolysate (12% TS) was then shipped overnight on ice to Virginia Tech where it was treated by anaerobic digestion at 37 ℃ with an active volume of 15 L and SRT of 15 days. To further destroy solids and remove ammonia, an aerobic digestion post-treatment followed at 32 ℃ with an active volume of 5 L and SRT of 5 days.

Feeding and wasting was performed once per day at an amount of 0.5 L for the 20 day SRT mesophilic digester, 0.8 L for thermophilic digesters, and 1 L for all other digesters to maintain the designated SRT. Volatile solids reduction (VSR) was approximately 50%, 30-40%, and 56-62% by the mesophilic digesters, the thermophilic digesters, and the sequential digestion process, respectively. All digesters were operated for over one year and had achieved optimal steady-state performance in terms of VSR and gas production at the time the present ARG reduction study commenced.

2.3.2 Sample Collection and DNA Extraction

Samples collected in this study included the following: (i) feed sludge; (ii) effluent of the two mesophilic digesters; (iii) effluent of the three thermophilic digesters; (iv) effluent of thermal hydrolysis pretreatment and downstream anaerobic and aerobic digesters. Samples were collected over four sampling events with a time interval of at least one SRT. Each sludge sample was centrifuged at 5,000 rpm for 15 min, and 0.4 g of the pellet was subsampled for DNA extraction using a FastDNA SPIN Kit for Soil (MP Biomedicals) and stored at -20 ℃ for further

analysis. The pellet was also subsampled and dried at 105 ℃ overnight to measure the dry solid content.

2.3.3 Detection and Quantification of ARGs

PCR assays were performed to detect one methicillin (*mec*A), one vancomycin (*van*A), two sulfonamide (*sul*I, *sul*II), three erythromycin (*erm*(A), *erm*(B), *erm*(F)), and twelve tetracycline (*tet*(A), *tet*B(P), *tet*(C), *tet*(E), *tet*(G), *tet*(M), *tet*(O), *tet*(Q), *tet*(S), *tet*(T), *tet*(W), *tet*(X)) ARGs. Nine ARGs (*sul*I, *sul*II, *erm*(B), *erm*(F), *tet*(O), *tet*(W), *tet*(C), *tet*(G) and *tet*(X)) that were frequently detected representing a range of resistance mechanisms, as well as the integrase gene of class 1 integrons (*int*I1) and 16S rRNA genes were further quantified by Q-PCR. Primers, annealing temperatures, and reaction matrix are described in the Supporting Information (Tables S2.1-S2.3). All standard curves of Q-PCR were constructed from serial dilutions of cloned genes ranging from 10^8 to 10^2 gene copies per μL. The presence of PCR inhibitors was checked by serially diluting select samples and comparing PCR efficiencies with standards. It was found that a dilution of 1:50 worked well to minimize inhibitory effects and was applied across samples. Samples were analyzed in triplicate in at least three independent Q-PCR runs, with a standard curve and negative control included in each run.

2.3.4 DGGE Analysis

The bacterial community was characterized by DGGE. 16S rRNA genes in each effluent sample were amplified using primers I-341fGC and I-533r and previously described conditions.[20] The PCR reaction matrix is described in the Supporting Information (Table S2.2). DGGE was performed at 57 ℃ with a D-Code system (Bio-Rad) employing 8% (w/v) polyacrylamide gels with a denaturant gradient from 20% to 55%. PCR products were electrophoresed at 100 V for

10 min and then 60 V for 15 h. The gel was stained with SYBRGold (Molecular Probes, Inc., Eugene, OR) and documented using the Chemidoc XRS Gel Documentation System (Bio-Rad). Quantity One 1-D analysis software (BioRad) was used to identify the bands in the gel and obtain the intensity profiles for each of the lanes. The relative diversity was calculated using the Shannon diversity index as previously described.[21]

2.3.5 Cloning and Sequencing Analysis

Based on the DGGE profiles obtained, five representative samples were selected for further analysis by cloning: the 52 ℃ thermophilic anaerobic digester, the 10 and 20 day SRT mesophilic anaerobic digesters, and the sequential anaerobic and aerobic digesters following thermal hydrolytic pretreatment. The 16S rRNA genes were amplified using primers 8F and 1492R (Table S2.1, Table S2.2), and cloned into *Escherichia coli* using the TOPO TA Cloning Kit for Sequencing (Invitrogen, Carlsbad, CA). Fifty clones generated from each sample were analyzed further by DGGE, as described above, to identify inserts that corresponded to dominant bands of each digester sample. The corresponding M13 PCR products were sequenced by the Virginia Bioinformatics Institute sequencing facility. The closest matches to known microorganisms were determined using the BLAST alignment tool at the National Center for Biotechnology Information Website (http://www.ncbi.nlm.nih.gov/BLAST/). The online environmental analysis software FastUniFrac (http://bmf2.colorado.edu/fastunifrac/) was used to perform Principal Coordinate Analysis (PCoA). For data submission of FastUniFrac, a phylogenetic tree was constructed from the sequence alignment generated using Clustal X 2.0.11.

2.3.6 Data Analysis

To report an average performance of various sludge treatment processes, multiple sampling events were treated as replicates. Averages and standard errors of all data were determined using Microsoft Excel 2007. *t* tests were conducted by R 2.8.1 (http://cran.r-project.org/bin/windows/base/old/2.8.1/) to determine whether Q-PCR based ARG and *int*I1 quantities were significantly different between samples. Correlation tests were also performed to reveal relevance of *int*I1 and ARG occurrence. A *p*-value of <0.05 was considered to indicate significance.

2.4 Results

2.4.1 ARG Occurrence

A broad range of ARGs were detected in the sludge samples, including two *sul* (*sul*I and *sul*II), three *erm* (*erm*(A), *erm*(B), and *erm*(F)) and nine *tet* (*tet*(C), *tet*B(P), *tet*(E), *tet*(G), *tet*(O), *tet*(Q), *tet*(T), *tet*(W), and *tet*(X)) ARGs. The *van*A and *mec*A genes encoding vancomycin and methicillin resistance, respectively, were not detected in any sludge samples in spite of PCR optimization and serial dilution to eliminate possible inhibition by the matrix.

2.4.2 Response of ARGs to Treatments

Nine ARGs (*sul*I, *sul*II, *erm*(B), *erm*(F), *tet*(O), *tet*(W), *tet*(C), *tet*(G), and *tet*(X)) that were frequently detected and represented a range of resistance mechanisms were further quantified to examine their response to various treatment conditions. In order to compare absolute reductions of ARGs, gene quantities are presented normalized to grams of dry solids. Quantities of the nine ARGs in the feed sludge ranged from 10^8 to 10^{10} copies/g dry solids (Table S2.4). ARG quantities after anaerobic digestions with varied SRT and temperatures are

compared in Figure 2.1. Quantitative changes of ARGs during the sequential process are shown in Figure 2.2. Gene quantities are also normalized to 16S rRNA genes as an indicator of the proportion of bacteria carrying ARGs (Figure S2.1, Figure S2.2). In terms of ARGs normalized to grams of total solids, highly similar performance was observed between the 10 and 20 day SRT mesophilic anaerobic digesters operated at 35 ℃. In both conditions, *sul*I, *sul*II, *tet*(C), *tet*(G), and *tet*(X) genes reduced in response to treatment, while *erm*(B), *erm*(F) and *tet*(W) ARGs increased (Figure 2.1). All net changes in concentration were statistically significant ($p < 0.05$) except *tet*(C) and *tet*(W) in the 20 day SRT digester ($p = 0.45$ and 0.20, respectively). Only *tet*(O) responded differently between the two mesophilic digesters: it reduced in the 20 day SRT digester ($p = 0.0005$), but increased in the 10 day SRT digester ($p = 0.0014$).

The three thermophilic digesters operated at 47 ℃, 52 ℃ and 59 ℃ also performed similarly to each other. In all three thermophilic digesters, *sul*I, *sul*II, *erm*(B), *erm*(F), *tet*(O), t*et*(W), and *tet*(G) genes significantly decreased ($p < 0.05$). The exceptions were *tet*(C) and *tet*(X). *tet*(C) increased after digestion at 52 ℃ and 59 ℃ ($p < 0.05$) and was not significantly different from the feed in the 47 ℃ digester ($p = 0.78$). *tet*(X) decreased in the 59 ℃ digester ($p < 0.05$), but increased in the 47 ℃ digester ($p < 0.05$) and was not statistically different from the feed after digestion at 52 ℃ ($p = 0.98$).

Thermal hydrolysis pretreatment resulted in remarkable reduction of all the nine ARGs ($p < 0.05$) with the range of reduction from 1.59 to 2.60 log unit (Figure 2.2). However, most of the ARGs were observed to rebound after subsequent anaerobic digestion except *sul*I and *tet*(G), which were not significantly different from quantities in thermal hydrolytically treated influent ($p = 0.68$ and 0.86, respectively). During aerobic digestion following the anaerobic digestion, *sul*I, *sul*II, *tet*(C), *tet*(G), and *tet*(X) genes continued to increase ($p < 0.05$), while *erm*(B),

erm(F), *tet*(O) and *tet*(W) genes decreased ($p < 0.05$).

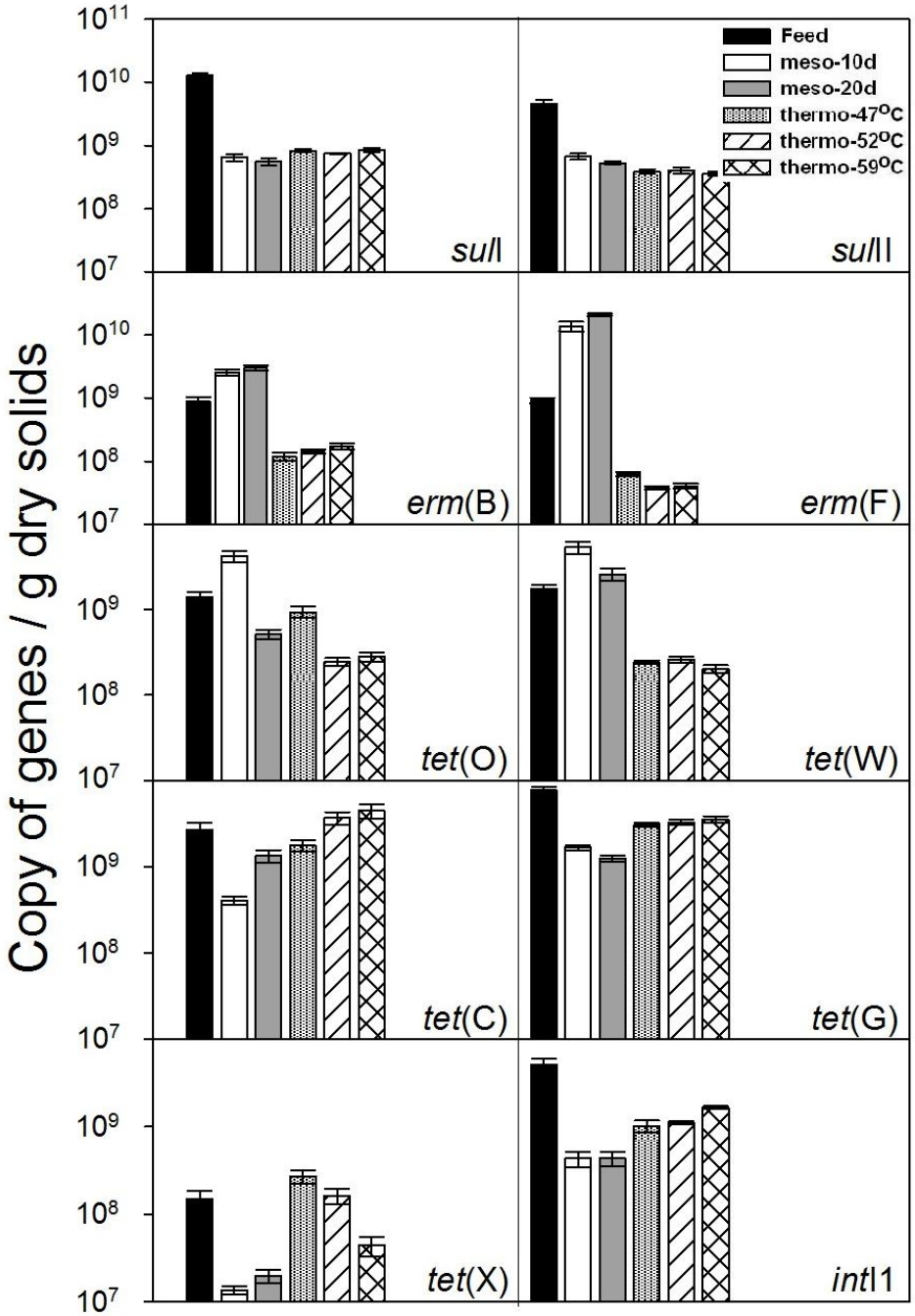

Figure 2.1 Quantities of ARG and *int*I1 gene in the feed sludge (Feed) and effluent of the 10 day SRT mesophilic (meso-10d), 20 day SRT mesophilic (meso-20d), and 47 ℃, 52 ℃ and 59 ℃ thermophilic (thermo) digesters. Error bars indicate standard errors of 9 Q-PCR measurements for each of the 4 sampling events (n=36). The average quantities of ARG and *int*I1 in feed sludge are reported in Table S2.4.

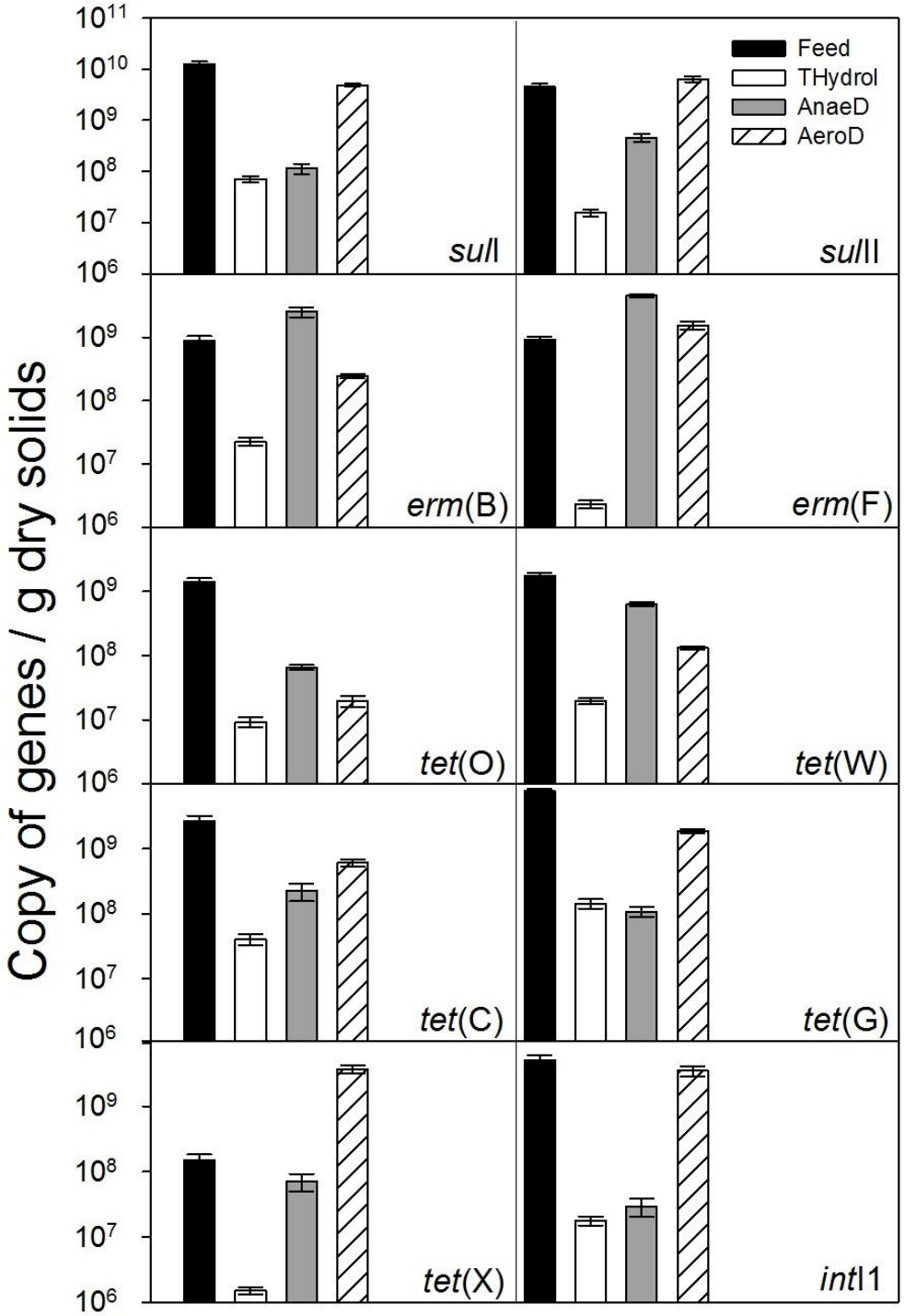

Figure 2.2 Quantities of ARG and *int*I1 in the feed sludge (Feed), sludge pretreated by thermal hydrolysis (THydrol), effluent of the mesophilic digester receiving pretreated sludge (AnaeD), and the subsequent aerobic digester (AeroD). Error bars indicate standard errors of 9 Q-PCR measurements for each of the 4 sampling events (n=36). The average quantities of ARG and *int*I1 in the feed sludge are reported in Table S2.4.

When ARGs were normalized to 16S rRNA genes, rather than grams of solids, the effect of the various treatment processes on ARGs maintained a remarkably similar trend (Figures S2.1, Figure S2.2), with only two exceptions. Firstly, 20 day SRT mesophilic anaerobic digesters yielded significantly greater reduction of *sul*I, *sul*II and *tet*(G) than the 10 day SRT digester ($p < 0.05$). Secondly, because all DNA is similarly affected by hydrolysis, normalization of ARGs to 16S rRNA genes masked the effect of the thermal hydrolytic pretreatment on ARGs (Figure S2.2).

2.4.3 Response of intI1 to Treatments

Significant reduction of *int*I1 was observed in all of the five anaerobic digesters operated at varied SRT and temperatures ($p < 0.05$, Figure 2.1). During the sequential process, a large portion of *int*I1 (2.46 log unit) was removed during thermal hydrolysis pretreatment ($p < 0.05$, Figure 2.2). However, a corresponding rebound and continuous increase of *int*I1 gene was observed in the following anaerobic and aerobic digestions ($p < 0.05$).

2.4.4 Characterization of Bacterial Community

The bacterial community was characterized by DGGE to gain insight into the potential role of microbial ecology in driving the ARG response to biological treatment. The mesophilic anaerobic digesters yielded the greatest number of bands and consequently the highest diversity indices ($H = 1.45$ and 1.51, respectively), relative to the thermophilic digesters ($H = 1.17$, 1.22, and 1.19 at 47 ℃, 52 ℃ and 59 ℃, respectively). Very few bands were yielded by hydrolytically pretreated sludge ($H = 0.69$), but diversity increased markedly in the subsequent anaerobic and aerobic digesters ($H = 1.31$ and 1.33, respectively).

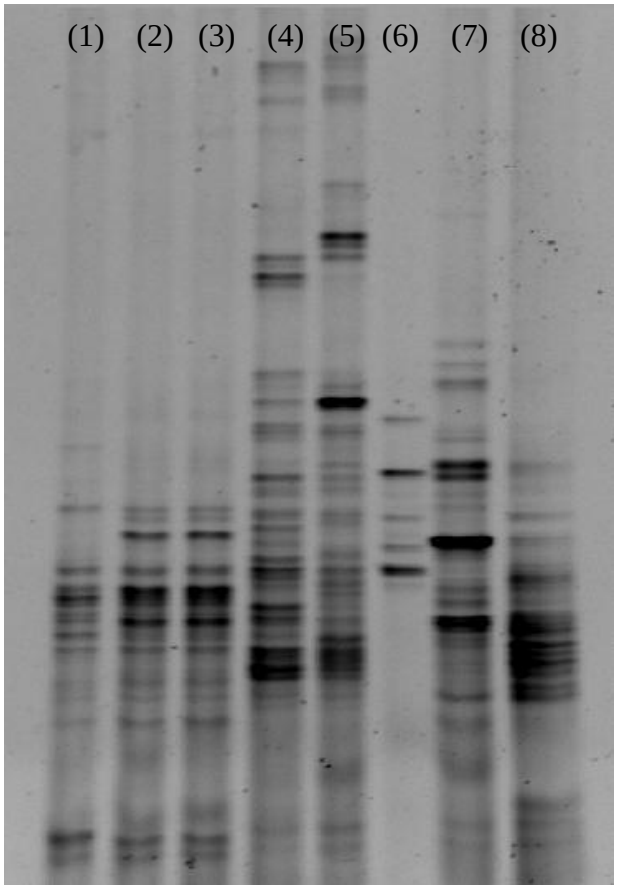

Figure 2.3 Denaturing gradient gel electrophoresis (DGGE) of bacterial community in each treatment process. 1) thermophilic digester at 47 ℃; 2) thermophilic digester at 52 ℃; 3) thermophilic digester at 59 ℃; 4) mesophilic digester at 10 day SRT; 5) mesophilic digester at 20 day SRT; 6) sludge pretreated by thermal hydrolysis; 7) mesophilic digester receiving pretreated sludge; 8) aerobic digester receiving feed from 7).

16S rRNA genes that migrated to the same position as bands in the digester DGGE profiles were sequenced (Table S2.5). Relative intensities of the corresponding DGGE bands were used to estimate the fraction of the community represented by each sequence (Figure S2.3). Most identified bacteria belonged to four phyla: *Firmicutes*, *Proteobacteria*, *Bacteroidetes*, and *Chloroflexi*, which have previously been reported to be dominant in other sludge samples.[22,23] *Firmicutes* and *Proteobacteria* occupied the largest fraction of dominant bacterial community in the thermophilic anaerobic digester. All four phyla were found in the mesophilic anaerobic

digesters. Most bacteria identified in the anaerobic digester following thermal hydrolysis pretreatment were *Firmicutes*, while the bacterial community became evenly distributed among phyla in the downstream aerobic digester.

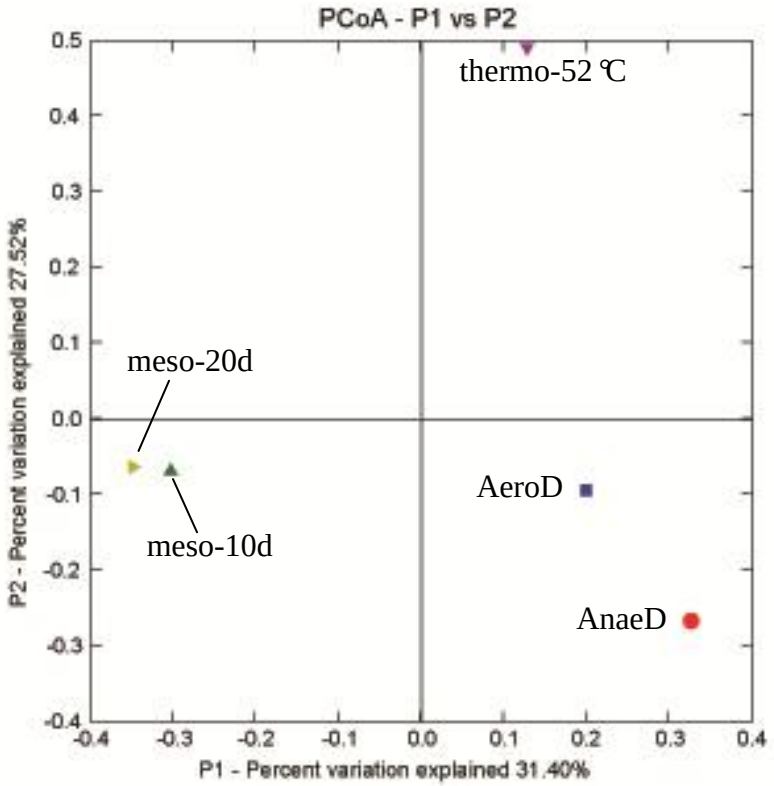

Figure 2.4 First two axes of Principal Coordinate Analysis (PCoA) of 16S rRNA gene sequence data using FastUniFrac. The 52 ℃ thermophilic digester (thermo-52℃), the 10 day SRT mesophilic digester(meso-10d), the 20 day SRT mesophilic digester (meso-20d), the mesophilic digester following thermal hydrolytic pretreatment (AnaeD), and the subsequent aerobic digester (AeroD) correspond to lanes 2, 4, 5, 7 and 8 in Fig. 2.3.

The phylogenetic distance of samples was characterized by PCoA (Figure 2.4). Digester samples tended to cluster by treatment temperatures as well as by characteristics of the feed sludge. The Phylogenetic make-up of the thermophilic anaerobic digester was distinct from that of the other digesters. Digesters at mesophilic temperature but following thermal hydrolytic

pretreatment were clearly differentiated from mesophilic digesters receiving waste solids directly. There was only a slight distinction between the sequential anaerobic and aerobic digesters following hydrolytic pretreatment, and the 10 day and 20 day SRT mesophilic digesters were clustered closely to each other.

2.5 Discussion

This study demonstrates that sludge digestion stands in a key position to alter the loadings of ARGs exiting wastewater treatment plants. Digesters can act to physically destroy extracellular DNA through hydrolysis and biodegradation, which generally would be expected to occur at higher rates with increased temperature. At the same time, ARGs may be harbored by host bacterial cells and subject to amplification via cell growth or horizontal gene transfer or attenuation via differential survival with respect to the digester operating conditions. The fact that ARG removal did not follow a simple trend with temperature emphasizes the importance of advancing understanding of the role of bacterial community composition in the amplification or attenuation of ARGs in sludge digesters.

2.5.1 Effect of SRT

ARG quantities normalized to 16S rRNA genes revealed a greater removal efficiency of *sul*I, *sul*II and *tet*(G) by the 20 day SRT mesophilic anaerobic digester relative to its 10 day SRT counterpart. The fact that this difference was not observable when ARGs were normalized to grams of solids suggests that a greater proportion of inert solids characteristic of longer SRTs masked the effect. In either case, the two mesophilic anaerobic digesters operated at 10 and 20 day SRT yielded strikingly similar patterns of ARG response to treatment, i.e. the same ARGs increased or decreased in both, with *tet*(O) the only exception. The similarity of the bacterial

communities was also remarkable, as indicated by their phylogenetic composition (Figure 2.4, Figure S2.3). It is likely that similar bacterial community composition, which largely determines available ARG hosts, drove their congruent response to treatments, with SRT impacting the extent of changes. Future studies incorporating a wider range of SRTs would be of interest, as well as more deeply exploring the potential effects of host range versus the extent of solids destruction.

2.5.2 Effect of Temperature

Results of this study suggest that the thermophilic anaerobic digesters at 47 ℃, 52 ℃ and 59 ℃ provided superior removal for *erm*(B), *erm*(F), *tet*(O) and *tet*(W) genes, relative to mesophilic digesters. This is consistent with the observations of Ghosh et al.[16] and Diehl and LaPara[17] with respect to *tet*(O) and *tet*(W) ARGs and further extends their encouraging findings to *erm* ARGs. DGGE revealed markedly lower bacterial diversity in the thermophilic versus the mesophilic digester, as illustrated by the number of bands detected (Figure 2.3) and the phylogenetic distribution of dominant bacteria identified (Figure S2.3). While individual ARG hosts may theoretically maintain abundance in spite of low diversity, this situation diminishes the overall probability of encountering a compatible host via horizontal gene transfer. Thus, restriction of the ARG host range may be a significant mechanism of attenuation in thermophilic digesters. Furthermore, higher temperature offers additional benefits of enhancing biological and chemical reaction rates.[13] Such factors may have together contributed to the more effective removal of *erm*(B), *erm*(F), *tet*(O) and *tet*(W) ARGs under higher temperature operation.

Diehl and LaPara[17] observed increasing removal rates and efficiencies of all five *tet* ARGs investigated (*tet*(A), *tet*(L), *tet*(O), *tet*(W) and *tet*(X)) as a function of temperature in lab-scale anaerobic digesters operated at 15 day SRT. Although the operating conditions were

similar, the trend was not identical in the present study. Within the thermophilic temperature range (47 ℃, 52 ℃, and 59 ℃), the responses of ARGs in this study were notably consistent. Meanwhile, highly similar bacterial communities within the three digesters were observed by DGGE analysis (Figure 2.3). These observations further support the conclusion that bacterial community composition played an important role in driving similar response of ARGs to treatments. Considering that temperature was the only variable between the three thermophilic digesters, these observations also reveal the high repeatability of the digesters operating in this study.

Furthermore, in this study thermophilic digestion was more effective for *erm*(B), *erm*(F), *tet*(O) and *tet*(W); but did not achieve greater attenuation of the other ARGs relative to mesophilic digestion. While *sul*I and *sul*II genes were reduced to a statistically equivalent extent ($p > 0.05$) by both digestion processes, quantities of *tet*(C), *tet*(G) and *tet*(X) were generally lower in the effluent of the two mesophilic digesters than in the three thermophilic digesters ($p < 0.05$, except $p = 0.25$ for *tet*(C) in 20 day mesophilic versus 47 ℃ thermophilic digester and $p = 0.26$ for *tet*(X) in 10 day mesophilic versus 59 ℃ thermophilic digester). Notably, *tet*(C) increased during the 52 ℃ and 59 ℃ digestions, while *tet*(X) increased during the 47 ℃ digestion ($p < 0.05$). *tet*(X) in particular exhibited precisely the opposite trend in the present study relative to that of Diehl and LaPara. Although a different forward primer for *tet*(X) was employed (Table S2.1), it is not expected that the specificity would be impacted given that it was designed from the same *tet*(X) sequence variant (GenBank # M37699). Considering that the temperature range of the Diehl and LaPara study (22 ℃, 37 ℃, 46 ℃, and 55 ℃) was comparable to the present study, this suggests that other factors may also be important. In addition to a distinct feed sludge, the amount and frequency of sludge replacement in the Diehl

and LaPara study was somewhat atypical, with 33% of the reactor volume replaced every 5 days, whereas in the present study, 5-6.7% of the sludge volume was replaced each day. Although this technically results in the same net SRT, larger and less frequent volume replacement approaches a plug flow reactor regime, which may impose feast and famine conditions on the bacterial community or even subject it to shock loads of toxins.

2.5.3 Effect of Thermal Hydrolysis Pretreatment

Thermal hydrolysis pretreatment was initially introduced to sludge digestion for the purpose of improving dewaterability and accelerating the rate-limiting step of hydrolysis of organic matter. The high temperature and pressure generally acts to sterilize the sludge, destroy cell walls, and release readily degradable components. This study confirmed that DNA is also susceptible to hydrolytic destruction. Interestingly, the anaerobic digester following thermal hydrolysis pretreatment, although also operated at mesophilic temperature, was clearly distinct from the mesophilic digesters receiving untreated sludge (Figure 2.3, Figure 2.4). The dominant bacteria in the anaerobic digester following thermal hydrolysis pretreatment mainly belonged to *Firmicutes* (Figure S2.3), indicating a favorable environment for fermentation after hydrolysis having largely been executed during pretreatment. It is also noted in the PCoA that the sequential anaerobic and aerobic digesters were clustered closely to each other (Figure 2.4), although they have contrasting redox conditions. This is likely an indication of the persistence of the DNA of dead or inactive bacteria through the relatively short 5 day SRT of the aerobic post-treatment digester.

Arguably, the most significant finding of this study is that most ARGs rebounded during anaerobic digestion following thermal hydrolytic pretreatment. The overall rebound effect following pretreatment illustrates that the microbial community composition of the digester

seemingly dominates the behavior of ARGs relative to influent ARG concentrations. ARG distribution and concentration is likely driven by the characteristics of the seed culture and ARG carriers subsequently respond to the selection pressures imposed by the digester operating conditions. However, the potential for persistence of residual DNA and horizontal gene transfer cannot be precluded. It would be interest to conduct future studies in which the seed culture is carefully selected to be devoid of ARGs, with the feed concentration of ARGs systematically manipulated.

In spite of the rebound effect, all ARGs were still lower in the digester receiving thermal hydrolytically pretreated sludge than in the mesophilic digesters receiving untreated sludge ($p < 0.05$), except *sul*II and *erm*(B), which rebounded to quantities that were statistically equivalent to the 20 day SRT mesophilic digester ($p = 0.07$ and 0.28, respectively). Perhaps the lower diversity of bacteria, mostly dominated by *Firmicutes*, provided a narrower host range for ARGs, in a similar fashion to the phenomenon suggested for the thermophilic digesters. An alternate explanation may be that the higher ARG concentrations present in the feed of the conventional mesophilic digesters did provide some contribution to the effluent ARG levels.

Further support for the importance of bacterial community composition is the fact that ARG behavior in subsequent the aerobic digester was distinct: *sul*I, *sul*II, *tet*(C), *tet*(G) and *tet*(X) ARGs continued to increase ($p < 0.05$), while *erm*(B), *erm*(F), *tet*(O) and *tet*(W) ARGs decreased ($p < 0.05$). Aerobic conditions select for distinct bacteria and generally a wider host range. For example, *tet*(X) encodes an oxygenase enzyme and though it is found in the obligately anaerobic *Bacteroides*, the enzyme itself theoretically requires oxygen to function.[24] Though Diehl and LaPara[17] observed stable *tet*(X) levels during various aerobic digestions, aerobic

conditions appeared to exert a strong selection pressure on *tet*(X) under the conditions of the present study.

2.5.4 Correlation of *int*I1 with ARGs

The class I integron plays an important role in gene transfer among bacteria. It is frequently reported to carry one or more gene cassettes that encode antibiotic resistance.[25,26] Thus documenting behavior of *int*I1 may provide insight to ARG dissemination potential. In this study, correlation analysis was performed to relate *int*I1 and ARG occurrence. Only *sul*I was found to positively correlate with *int*I1 occurrence in the feed and effluent of digesters (R^2 = 0.88, $p < 0.05$), which is consistent with *sul*I typically being associated with class I integrons.[27] Significant correlation was not found between *int*I1 and other ARGs. Notably, *int*I1 rebounded together with ARGs during the anaerobic digestion following thermal hydrolysis pretreatment, and increased by ~2 log units in the aerobic digester, which was the largest increase of any ARG. This suggests that the horizontal gene transfer may be a key process during sludge digestion and is worthy of further study.

2.6 Acknowledgment

Funding for this research was provided by the National Science Foundation, CBET CAREER award # 0547342. The findings of this study do not necessarily reflect the views of the foundation. The authors also thank Dr. Daniel Gallagher (Virginia Tech) for assistance with statistical analysis.

2.7 References

(1) Zhang, Y. L.; Marrs, C. F.; Simon, C.; Xi, C. W., Wastewater treatment contributes to selective increase of antibiotic resistance among Acinetobacter spp. Sci Total Environ 2009, 407 (12), 3702-3706.

(2) Baquero, F.; Martinez, J. L.; Canton, R., Antibiotics and antibiotic resistance in water environments. *Curr Opin Biotech* **2008,** *19* (3), 260-265.

(3) D'Costa, P. M.; Vaz-Pires, P.; Bernardo, F., Antimicrobial resistance in Enterococcus spp. isolated in inflow, effluent and sludge from municipal sewage water treatment plants. *Water Res* **2006,** *40* (8), 1735-1740.

(4) A National Biosolids Regulation, Quality, End Use and Disposal Survey. North East Biosolids and Residuals Association. 2007. http:// www.nebiosolids.org/uploads/pdf/NtlBiosolidsReport-20July07.pdf (accessed Jan 27, 2010).

(5) Auerbach, E. A.; Seyfried, E. E.; McMahon, K. D., Tetracycline resistance genes in activated sludge wastewater treatment plants. *Water Res* **2007,** *41* (5), 1143-1151.

(6) Storteboom, H.; Arabi, M.; Davis, J. G.; Crimi, B.; Pruden, A., Tracking Antibiotic Resistance Genes in the South Platte River Basin Using Molecular Signatures of Urban, Agricultural, And Pristine Sources. *Environ Sci Technol* **2010,** *44* (19), 7397-7404.

(7) Munir, M.; Xagoraraki, I., Levels of Antibiotic Resistance Genes in Manure, Biosolids, and Fertilized Soil. *J Environ Qual* **2011,** *40* (1), 248-255.

(8) Courvalin, P., Transfer of Antibiotic-Resistance Genes between Gram-Positive and Gram-Negative Bacteria. *Antimicrob Agents Ch* **1994,** *38* (7), 1447-1451.

(9) Salyers, A. A.; Shoemaker, N. B., Resistance gene transfer in anaerobes: New insights, new problems. *Clin Infect Dis* **1996,** *23*, S36-S43.

(10) Davison, J., Genetic exchange between bacteria in the environment. *Plasmid* **1999,** *42* (2), 73-91.

(11) Riesenfeld, C. S.; Goodman, R. M.; Handelsman, J., Uncultured soil bacteria are a reservoir of new antibiotic resistance genes. *Environ Microbiol* **2004,** *6* (9), 981-989.

(12) Borjesson, S.; Mattsson, A.; Lindgren, P. E., Genes encoding tetracycline resistance in a full-scale municipal wastewater treatment plant investigated during one year. *J Water Health* **2010,** *8* (2), 247-256.

(13) Zabranska, J.; Dohanyos, M.; Jenicek, P.; Ruzicikova, H.; Vranova, A., Efficiency of autothermal thermophilic aerobic digestion and thermophilic anaerobic digestion of municipal wastewater sludge in removing Salmonella spp. and indicator bacteria. *Water Sci Technol* **2003,** *47* (3), 151-156.

(14) Cheunbarn, T.; Pagilla, K. R., Anaerobic thermophilic/mesophilic dual-stage sludge treatment. *J Environ Eng-Asce* **2000,** *126* (9), 796-801.

(15) Muller, J. A., Prospects and problems of sludge pretreatment processes. *Water Sci Technol* **2001,** *44* (10), 121-128.

(16) Ghosh, S.; Ramsden, S. J.; LaPara, T. M., The role of anaerobic digestion in controlling the release of tetracycline resistance genes and class 1 integrons from municipal wastewater treatment plants. *Appl Microbiol Biot* **2009,** *84* (4), 791-796.

(17) Diehl, D. L.; LaPara, T. M., Effect of Temperature on the Fate of Genes Encoding Tetracycline Resistance and the Integrase of Class 1 Integrons within Anaerobic and Aerobic Digesters Treating Municipal Wastewater Solids. *Environ Sci Technol* **2010,** *44* (23), 9128-9133.

(18) Pei, R.; Cha, J.; Carlson, K. H.; Pruden, A., Response of antibiotic resistance genes (ARG) to biological treatment in dairy lagoon water. *Environ Sci Technol* **2007,** *41* (14), 5108-5113.

(19) Storteboom, H. N.; Kim, S. C.; Doesken, K. C.; Carlson, K. H.; Davis, J. G.; Pruden, A., Response of antibiotics and resistance genes to high-intensity and low-intensity manure management. *J Environ Qual* **2007,** *36* (6), 1695-1703.

(20) Watanabe, K.; Kodama, Y.; Harayama, S., Design and evaluation of PCR primers to amplify bacterial 16S ribosomal DNA fragments used for community fingerprinting. *J Microbiol Meth* **2001,** *44* (3), 253-262.

(21) Cox, G. W. Laboratory Manual of General Ecology. W.C. Brown, Dubuque, IA, 1972.

(22) Riviere, D.; Desvignes, V.; Pelletier, E.; Chaussonnerie, S.; Guermazi, S.; Weissenbach, J.; Li, T.; Camacho, P.; Sghir, A., Towards the definition of a core of microorganisms involved in anaerobic digestion of sludge. *Isme J* **2009,** *3* (6), 700-714.

(23) Bibby, K.; Viau, E.; Peccia, J., Pyrosequencing of the 16S rRNA gene to reveal bacterial pathogen diversity in biosolids. *Water Res* **2010,** *44* (14), 4252-4260.

(24) Roberts, M. C., Resistance to tetracycline, macrolide-lincosamide-streptogramin, trimethoprim, and sulfonamide drug classes. *Mol Biotechnol* **2002,** *20* (3), 261-283.

(25) Henriques, I. S.; Fonseca, F.; Alves, A.; Saavedra, M. J.; Correia, A., Occurrence and diversity of integrons and beta-lactamase genes among ampicillin-resistant isolates from estuarine waters. *Res Microbiol* **2006,** *157* (10), 938-947.

(26) Mendes, R. E.; Castanheira, M.; Toleman, M. A.; Sader, H. S.; Jones, R. N.; Walsh, T. R., Characterization of an integron carrying bla(IMP-1) and a new aminoglycoside resistance gene, aac(6')-31, and its dissemination among genetically unrelated clinical isolates in a Brazilian hospital. *Antimicrob Agents Ch* **2007,** *51* (7), 2611-2614.

(27) Partridge, S. R.; Tsafnat, G.; Coiera, E.; Iredell, J. R., Gene cassettes and cassette arrays in mobile resistance integrons. *Fems Microbiol Rev* **2009,** *33* (4), 757-784.

2.8 Supplemental Materials

Table S2.1 Primer sequences and annealing temperatures of PCR and Q-PCR assays

Primer	Target gene	Primer / Probe sequence (5'- 3')	Annealing Temp. (℃)	Source of reference
*van*A-Fw	*van*A	CTGTGAGGTCGGTTGTGCG	60	*(1)*
*van*A-Rv		TTTGGTCCACCTCGCCA		
*mec*A-Fw	*mec*A	CGCAACGTTCAATTTAATTTTGTTAA	60	*(1)*
*mec*A-Rv		TGGTCTTTCTGCATTCCTGGA		
*sul*I- Fw	*sul*I	CGCACCGGAAACATCGCTGCAC	69.9	*(2)*
*sul*I- Rv		TGAAGTTCCGCCGCAAGGCTCG		
*sul*II- Fw	*sul*II	TCCGGTGGAGGCCGGTATCTGG	67.5	*(2)*
*sul*II- Rv		CGGGAATGCCATCTGCCTTGAG		
erm(A)-Fw	*erm*(A)	GAAATYGGRTCAGGAAAAGG	55	*(3)*
Erm(A)-Rv		AAYAGYAAACCYAAAGCTC		
erm(B)- Fw	*erm(*B)	GATACCGTTTACGAAATTGG	58	*(3)*
erm(B)- Rv		GAATCGAGACTTGAGTGTGC		
erm(F)- Fw	*erm*(F)	CGACACAGCTTTGGTTGAAC	56	*(3)*
erm(F)- Rv		GGACCTACCTCATAGACAAG		
tet(A)-Fw	*tet*(A)	GCGCGATCTGGTTCACTCG	61	*(4)*
tet(A)-Rv		AGTCGACAGYRGCGCCGGC		
*tet*B(P)-FW	*tet*B(P)	AAAACTTATTATATTATAGTC	46	*(5)*
*tet*B(P)-Rv		TGGAGTATCAATAATATTCAC		
tet(C)- Fw	*tet*(C)	GCGGGATATCGTCCATTCCG	70	*(4)*
tet(C)- Rv		GCGTAGAGGATCCACAGGACG		
tet(E)- Fw	*tet*(E)	GTTATTACGGGAGTTTGTTGG	61	*(4)*
tet(E)- Rv		AATACAACACCCACACTACGC		
tet(G)- Fw	*tet*(G)	GCAGAGCAGGTCGCTGG	64.2	*(4)*
tet(G)- Rv		CCYGCAAGAGAAGCCAGAAG		
tet(M)- Fw	*tet*(M)	ACAGAAAGCTTATTATATAAC	55	(5)

tet(M)- Rv		TGGCGTGTCTATGATGTTCAC		
tet(O)- Fw	*tet*(O)	ACGGARAGTTTATTGTATACC	50.3	*(5)*
tet(O)- Rv		TGGCGTATCTATAATGTTGAC		
tet(Q)- Fw	*tet*(Q)	AGAATCTGCTGTTTGCCAGTG	63	*(5)*
tet(Q)- Rv		CGGAGTGTCAATGATATTGCA		
tet(S)- Fw	*tet*(S)	GAAAGCTTACTATACAGTAGC	50	*(5)*
tet(S)- Rv		AGGAGTATCTACAATATTTAC		
tet(T)- Fw	*tet*(T)	AAGGTTTATTATATAAAAGTG	46	*(5)*
tet(T)- Rv		AGGTGTATCTATGATATTTAC		
tet(W)- Fw	*tet*(W)	GAGAGCCTGCTATATGCCAGC	60	*(5)*
tet(W)- Rv		GGGCGTATCCACAATGTTAAC		
tet(X)- Fw	*tet*(X)	CAATAATTGGTGGTGGACCC	64.5	*(6)*
tet(X)- Rv		TTCTTACCTTGGACATCCCG		
HS463a	*int*I1	CTGGATTTCGATCACGGCACG	60	*(7)*
HS464		ACATGCGTGTAAATCATCGTCG		
1369F	16S rRNA	CGGTGAATACGTTCYCGG	60	*(8)*
1492R		GGWTACCTTGTTACGACTT		

Table S2.2 PCR reaction matrix[a]

Reagent	Amount or concentration in 25 μL master mix
10 × buffer	2.5 μL
5 × buffer	5 μL
2 μL Mg^{2+}	2 μL
dNTPs	0.2mM
Forward and reverse primer	0.25 μM
Taq DNA polymerase	1.75U
Formamide[b]	0.25 μL
DNA template	1 μL

[a] PCR assays were carried out using a MasterTaq kit (Eppendorf, Westbury, NY).

[b] Formamide is added for 16S rRNA PCR only.

Table S2.3 Q-PCR reaction matrix

Reagent	Concentration in 20 μL master mix
Forward and reverse primers	0.3 μM
SsoFast EvaGreen Supermix	1 ×

Table S2.4 Average quantities of ARG and *int*I1 in feed sludge

Gene	Quantity (copy of genes / g dry solids)
*sul*I	$(1.27 \pm 0.13) \times 10^{10}$
*sul*II	$(4.55 \pm 0.64) \times 10^{9}$
erm(B)	$(8.92 \pm 1.55) \times 10^{8}$
erm(F)	$(9.20 \pm 0.94) \times 10^{8}$
tet(O)	$(1.39 \pm 0.20) \times 10^{9}$
tet(W)	$(1.75 \pm 0.22) \times 10^{9}$
tet(C)	$(2.67 \pm 0.56) \times 10^{9}$
tet(G)	$(7.69 \pm 0.79) \times 10^{9}$
tet(X)	$(1.50 \pm 0.33) \times 10^{8}$
*int*I1	$(5.13 \pm 0.80) \times 10^{9}$

Table S2.5 Closest match microorganisms of sequenced clones

Sample	Phylogenetic affiliation		Closest match microorganism (accession number)	% of identity
	Phylum	Class		
thermo-52 ℃	Firmicutes	Clostridia	Clostridium sp. PML3-1 (EF165015)	94%
	Firmicutes	Clostridia	Coprothermobacter proteolyticus DSM 5265 (CP001145)	98%
	Firmicutes	Clostridia	Clostridium sp. ZH11 (HM103331)	87%
	Firmicutes	Clostridia	Coprothermobacter sp. GK5	98%
	Proteobacteria	α-Proteobacteria	Rhodobacter sp. TCRI 14 (AB017799)	96%
	Proteobacteria	β-Proteobacteria	Pseudorhodoferax soli strain TBEA3 (EU825700)	98%
	Proteobacteria	β-Proteobacteria	Comamonas denitrificans strain 110 (AF233876)	97%
	Proteobacteria	β-Proteobacteria	Acidovorax sp. 3T2-6	100%
	Proteobacteria	β-Proteobacteria	Uncultured Methylophilus sp. (FM175198)	97%
	Proteobacteria	β-Proteobacteria	Uncultured soil bacterium clone M22_Pitesti (DQ378242)	97%
	Proteobacteria	β-Proteobacteria	Uncultured bacterium clone Rap1_6A (EF192877)	98%
	Proteobacteria	β-Proteobacteria	Alcaligenes faecalis strain SAG5 (GQ422443)	98%
	TM7	unclassified	Uncultured TM7 bacterium (CU917719)	97%
	Planctomycetes	Planctomycetacia	Uncultured planctomycete clone PLA10 (AF525965)	96%
	Acidobacteria	unclassified	Acidobacteria bacterium enrichment culture clone Ac-F6 (GQ902908)	100%
meso-10d	Bacteroidetes	Bacteroidia	Uncultured Bacteroidetes bacterium clone QEEA3AF11 (CU918774)	100%
	Bacteroidetes	unclassified	Uncultured Bacteroidetes bacterium (CU924056)	99%

	Chloroflexi	Anaerolineae	Uncultured Chloroflexi bacterium (CU917962)	99%
	Firmicutes	Clostridia	Uncultured bacterium clone BXHA73 (GQ480020)	100%
	Firmicutes	Clostridia	Clostridia bacterium enrichment culture clone WSC-8 (HM635205)	90%
	Firmicutes	Mollicutes	Mycoplasma mycoides subsp. mycoides SC str. Gladysdale MU clone SC5 (CP002107)	82%
	Proteobacteria	α-Proteobacteria	Methylocella silvestris BL2 (CP001280)	98%
	Proteobacteria	β-Proteobacteria	Beta proteobacterium BP-5 (AY145571)	98%
	Proteobacteria	δ-Proteobacteria	Syntrophus sp. enrichment culture clone MB1_1 (AM933651)	99%
	unclassified	unclassified	Uncultured bacterium gene clone:BSA2B-20 (AB175392)	99%
	unclassfied	unclassfied	Uncultured bacterium clone G1 (EU551100)	96%
meso-20d	Bacteroidetes	Bacteroidia	Ruminofilibacter xylanolyticum strain S1 (DQ141183)	99%
	Chloroflexi	Anaerolineae	Uncultured Chloroflexi bacterium clone QEDN11DD10 (CU926916)	100%
	Firmicutes	Clostridia	Candidate division OP9 clone OPB47 (AF027082)	92%
	Firmicutes	Clostridia	Desulfosporosinus sp. 44a-T3a (AY082482)	87%
	Firmicutes	Clostridia	Syntrophomonas sp. TB-6 (AB098336)	91%
	Firmicutes	Erysipelotrichi	Erysipelothrix sp. Oita0548 (EF494749)	86%
	Proteobacteria	α-Proteobacteria	Methylocella silvestris BL2 (CP001280)	97%
	Proteobacteria	α-Proteobacteria	Beijerinckiaceae bacterium LAY (FR686345)	98%
	Proteobacteria	β-Proteobacteria	Alcaligenes sp. VV1 (EU817657)	98%
	Bacteroidetes	Bacteroidia	Dysgonomonas sp. Dy73 (AB547446)	99%
	Bacteroidetes	Bacteroidia	Bacteroides sp. (AB003390)	93%
	Planctomycetes	Planctomycetacia	Uncultured planctomycete clone	99%

			5GA_Pla_HKP_19 (GQ356166)	
	unclassified	unclassified	Uncultured WWE1 bacterium, clone QEDN11CH09 (CU925933)	100%
	unclassified	unclassified	Uncultured WWE1 bacterium clone QEEA1CH01 (CU918787)	98%
AnaeD	Bacteroidetes	Bacteroidia	Prevotella sp. 326-8 (FJ848548)	84%
	Firmicutes	Clostridia	Peptostreptococcaceae bacterium SK031 (AB377177)	93%
	Firmicutes	Clostridia	Caldanaerocella colombiensis strain P4.4 (AY464940)	93%
	Firmicutes	Clostridia	Uncultured bacterium clone 166_BE1_21 (FJ825480)	100%
	Firmicutes	Clostridia	Uncultured Firmicutes bacterium (FJ440067)	89%
	Firmicutes	Clostridia	Peptostreptococcaceae bacterium 19gly3 (AF550609)	95%
	Firmicutes	Clostridia	Clostridium ultunense strain DSM 10521 (GQ461825)	96%
	Firmicutes	Clostridia	Clostridiales bacterium oral clone P4GC_38 P4 (AY207058)	88%
	Firmicutes	Lactobacillales	Streptococcus bovis strain 15MP (EU075037)	85%
	Firmicutes	Mollicutes	Acholeplasma modicum (M23933)	93%
	Firmicutes	unclassified	Uncultured Firmicutes bacterium (CU918150)	99%
	unclassified	unclassified	Uncultured bacterium (FJ205862)	99%
AeroD	Bacteroidetes	Flavobacteria	Aequorivita sp. R-36724 (FR691437)	94%
	Firmicutes	Clostridia	Peptostreptococcaceae bacterium SK031 (AB377177)	92%
	Firmicutes	Clostridia	Uncultured bacterium clone 166_BE1_21 (FJ825480)	99%
	Firmicutes	Clostridia	Sedimentibacter sp. enrichment culture clone	88%

			B19 (GU645041)	
	Firmicutes	Clostridia	Tepidanaerobacter sp. T1 (FJ620692)	99%
	Proteobacteria	α-Proteobacteria	Parvibaculum lavamentivorans DS-1 (CP000774)	98%
	Proteobacteria	α-Proteobacteria	Paracoccus solventivorans (AY014175)	100%
	Proteobacteria	β-Proteobacteria	Pusillimonas terrae strain SAG3 (GQ422442)	98%
	Proteobacteria	β-Proteobacteria	Pusillimonas sp. H11 (GQ254281)	97%
	Proteobacteria	γ-Proteobacteria	Pseudomonas pseudoalcaligenes strain 23 (EU780001)	96%
	Cyanobacteria	Oscillatoriales	Oscillatoria sp. (AJ133106)	90%
	unclassified	unclassified	Uncultured bacterium clone 30 (AY853673)	98%
	unclassified	unclassified	Uncultured bacterium clone GW-33 (EU407216)	96%

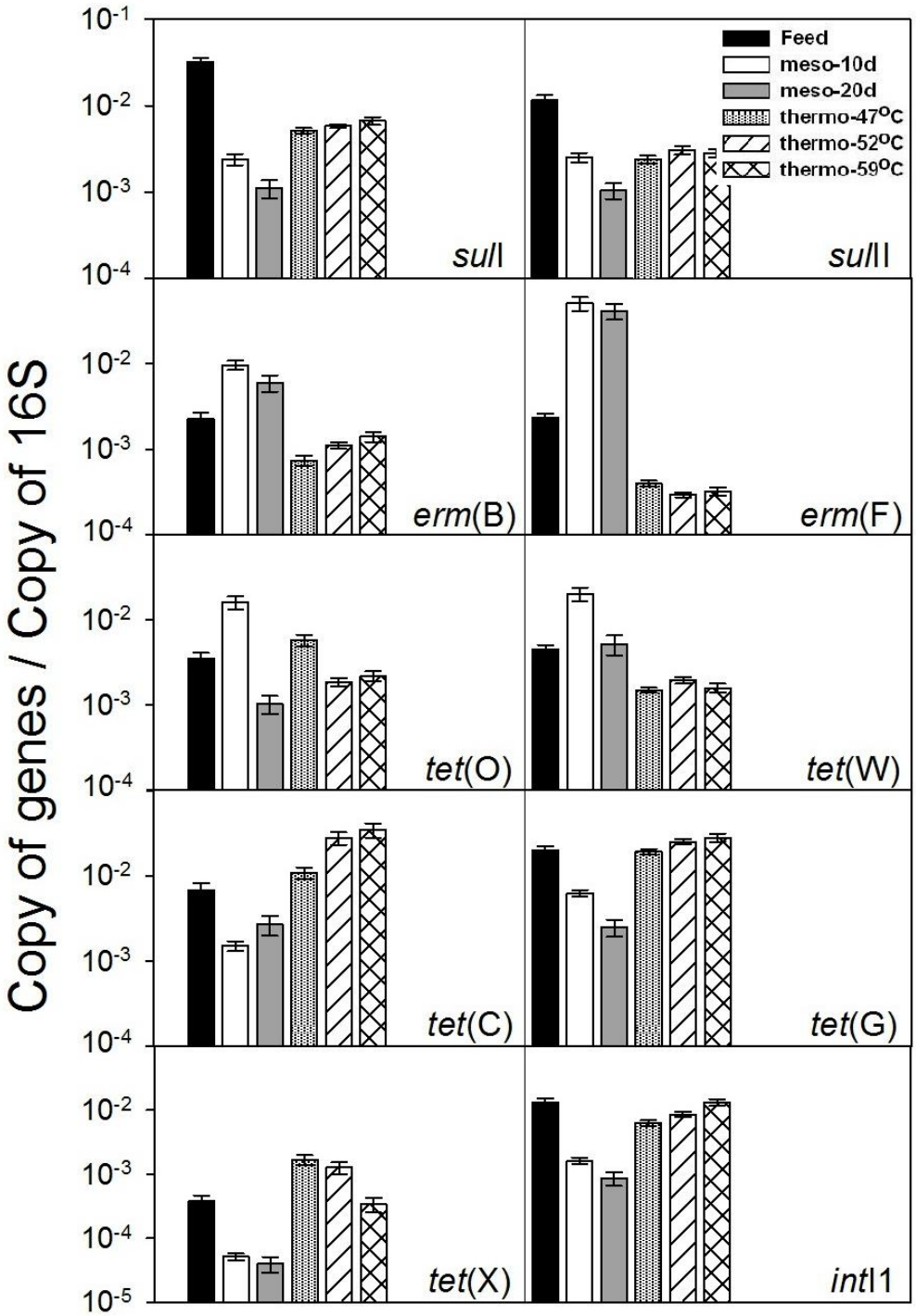

Figure S2.1 Quantities of ARG and *int*I1 gene normalized to 16S rRNA genes in the feed sludge (Feed) and effluent of the 10 day SRT mesophilic (meso-10d), 20 day SRT mesophilic (meso-20d), and 47 ℃, 52 ℃ and 59 ℃ thermophilic (thermo) digesters. Error bars indicate standard errors of 9 Q-PCR measurements for each of the 4 sampling events (n = 36).

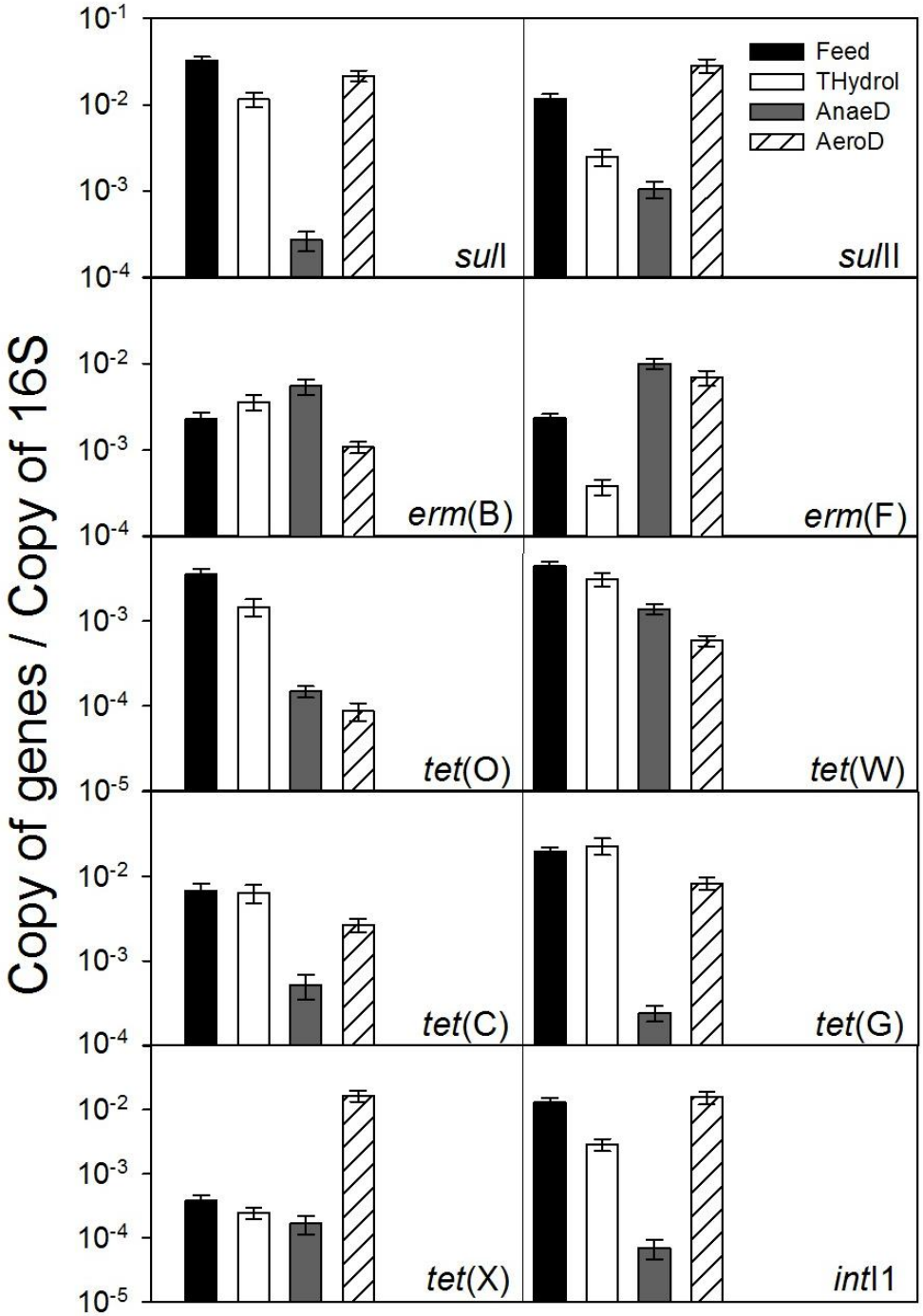

Figure S2.2 Quantities of ARG and *int*I1 normalized to 16S rRNA genes in the feed sludge (Feed), sludge pretreated by thermal hydrolysis (THydrol), effluent of the mesophilic digester receiving pretreated sludge (AnaeD), and the subsequent aerobic digester (AeroD). Error bars indicate standard errors of 9 Q-PCR measurements for each of the 4 sampling events (n = 36).

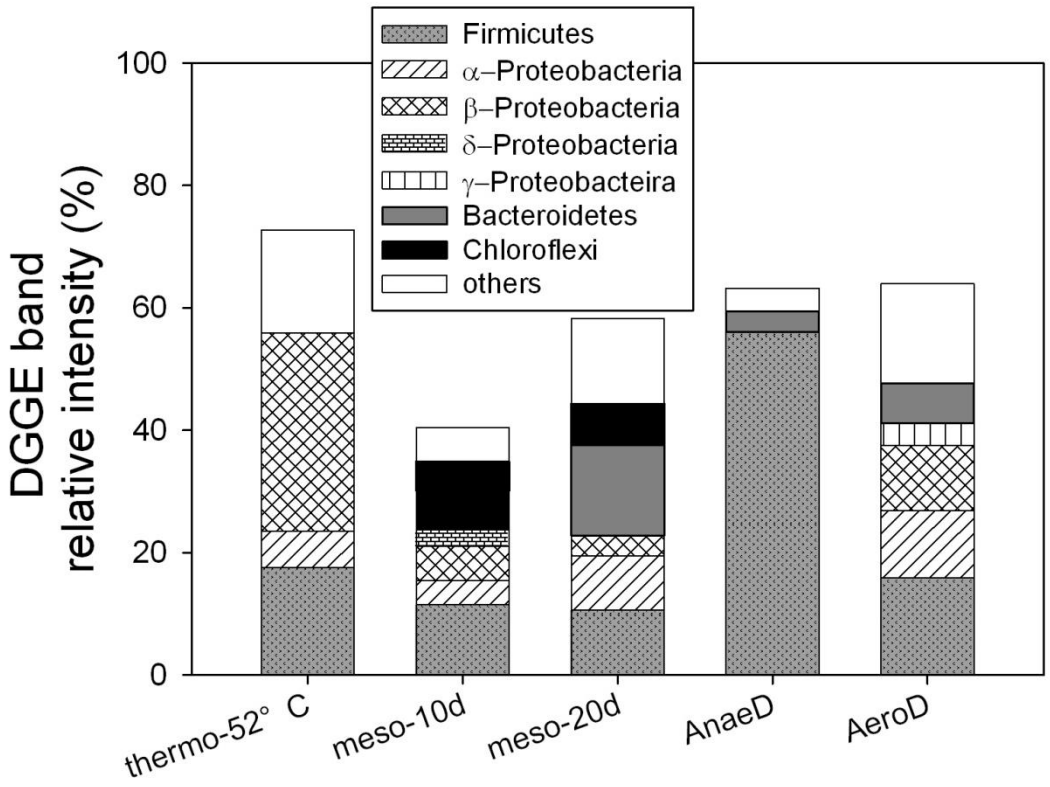

Figure S2.3 Classification of dominant bacteria in the 52 ℃ thermophilic digester (thermo-52 ℃), the 10 day SRT mesophilic digester (meso-10d), the 20 day SRT mesophilic digester (meso-20d), the mesophilic digester following thermal hydrolytic pretreatment (AnaeD), and the subsequent aerobic digester (AeroD) corresponding to lanes 2, 4, 5, 7 and 8 in Figure 2.3. 16S rRNA gene clones that migrated to the same position as bands in the digester DGGE profiles were sequenced. Fifty clones were analyzed for each digester.

References

(1) Volkmann, H.; Schwartz, T.; Bischoff, P.; Kirchen, S.; Obst, U., Detection of clinically relevant antibiotic-resistance genes in municipal wastewater using real-time PCR (TaqMan). *J Microbiol Meth* **2004,** *56* (2), 277-286.

(2) Pei, R. T.; Kim, S. C.; Carlson, K. H.; Pruden, A., Effect of River Landscape on the sediment concentrations of antibiotics and corresponding antibiotic resistance genes (ARG). *Water Res* **2006,** *40* (12), 2427-2435.

(3) Chen, J.; Yu, Z. T.; Michel, F. C.; Wittum, T.; Morrison, M., Development and application of real-time PCR assays for quantification of erm genes conferring resistance to macrolides-lincosamides-streptogramin B in livestock manure and manure management systems. *Appl Environ Microb* **2007,** *73* (14), 4407-4416.

(4) Aminov, R. I.; Chee-Sanford, J. C.; Garrigues, N.; Teferedegne, B.; Krapac, I. J.; White, B. A.; Mackie, R. I., Development, validation, and application of PCR primers for detection of tetracycline efflux genes of gram-negative bacteria. *Appl Environ Microb* **2002,** *68* (4), 1786-1793.

(5) Aminov, R. I.; Garrigues-Jeanjean, N.; Mackie, R. I., Molecular ecology of tetracycline resistance: Development and validation of primers for detection of tetracycline resistance genes encoding ribosomal protection proteins. *Appl Environ Microb* **2001,** *67* (1), 22-32.

(6) Ng, L. K.; Martin, I.; Alfa, M.; Mulvey, M., Multiplex PCR for the detection of tetracycline resistant genes. *Mol Cell Probe* **2001,** *15* (4), 209-215.

(7) Hardwick, S. A.; Stokes, H. W.; Findlay, S.; Taylor, M.; Gillings, M. R., Quantification of class 1 integron abundance in natural environments using real-time quantitative PCR. *Fems Microbiol Lett* **2008,** *278* (2), 207-212.

(8) Suzuki, M. T.; Taylor, L. T.; DeLong, E. F., Quantitative analysis of small-subunit rRNA genes in mixed microbial populations via 5 '-nuclease assays. *Appl Environ Microb* **2000,** *66* (11), 4605-4614.

CHAPTER 3: Microbial Community Response of Nitrifying Sequencing Batch Reactors to Silver, Zero-Valent Iron, Titanium Dioxide and Cerium Dioxide Nanomaterials

Yanjun Ma, Jacob W. Metch, Eric P. Vejerano, Ian J. Miller, Elena C. Leon, Linsey C. Marr, and Amy Pruden

3.1 Abstract

As nanomaterials in consumer products increasingly enter wastewater treatment plants, there is concern that they may have adverse effects on biological wastewater treatment. Effects of silver (nanoAg), zero-valent iron (NZVI), titanium dioxide (nanoTiO_2) and cerium dioxide (nanoCeO_2) nanomaterials on nitrification and microbial community structure were examined in duplicate lab-scale nitrifying sequencing batch reactors (SBRs) relative to control SBRs that received no nanomaterials or bulk/ionic analogs. Nanomaterial/analog doses started at 0.1 mg/L and were sequentially increased every 14 days to 1, 10, and 20 mg/L. Nitrification function was not measurably inhibited in the SBRs by any of the dosed materials based on ammonia, nitrite, or nitrate levels. However, decreased nitrifier gene abundances (qPCR of *amo*A and *Nitrobacter* 16S rRNA genes) and distinct bacterial communities (pyrosequencing of 16S rRNA genes) were observed in SBRs dosed with nanoAg, Ag^+, nanoCeO_2, and bulkCeO_2, relative to controls, with the most pronounced effects associated with Ag^+. There was no apparent effect of nanoTiO_2 or NZVI on nitrification, nitrifier gene abundances, or microbial community structure. Because nanoAg and nanoCeO_2 indicated the greatest potential effects, experiments were repeated for these two nanomaterials and their analogs at a continuous high load of 20 mg/L over 42 days. While the high load Ag^+ condition rapidly lost nitrification functionality, there was no

measureable effect of continuous high loads of the other dosed materials on nitrification function or levels of nitrification gene markers. TEM-EDS analysis indicated that a large portion of nanoAg remained dispersed in the activated sludge and formed Ag-S complexes, while NZVI, nanoTiO_2 and nanoCeO_2 were mostly aggregated and chemically unmodified. Thus, the nanomaterials appeared to be generally stable in the activated sludge, which may have limited their effect on nitrification function and microbial community structure. Experiments carried out over longer term or shock load conditions may elicit a stronger effect.

3.2 Introduction

As nanotechnology-based consumer products enter into widespread use, a large portion of nanomaterials will enter wastewater treatment plants.[1-2] As a gateway of controlling nanomaterial release into the natural environment, wastewater treatment processes have been observed to remove the majority of nanomaterials in aqueous effluents, primarily concentrating them into the activated sludge phase.[3-4] Compared with traditional bulk materials, the nano-size range imparts unique properties, including greater reactivity and thus more potential toxicity to biological systems.[5] Toxicity of nanomaterials to microbes has been well-documented in pure culture studies.[6-8] Therefore, there is concern that the accumulation of nanomaterials in activated sludge could have adverse effects on microbes responsible for biological wastewater treatment.

Nitrifying bacteria, including ammonia oxidizing bacteria (AOB) and nitrite oxidizing bacteria (NOB), conduct the critical function of nitrification in biological wastewater treatment to covert ammonia to nitrite and subsequently to nitrate. Nitrifying bacteria are known for slow growth rate and high sensitivity to toxic chemicals.[9] As increasing amounts of nanomaterials enter wastewater, they have the potential to inhibit nitrification function due to toxicity to nitrifying bacteria. Toxic effects of silver nanoparticles have been observed on *Nitrosomonas*

europeae in pure culture[10-11] and enriched nitrifying microorganisms.[12] However, the effects of other nanomaterials on nitrifying bacteria, especially under the real-world complex wastewater matrix and aeration conditions of biological treatment, have not been established.

Impacts of a few nanomaterials, including Ag, TiO_2 and ZnO, on nitrification have been examined in laboratory-scale reactors.[13-16] However, the extent of reported nitrification inhibition has varied and inconsistent trends have been observed with respect to effects of nanomaterial concentrations and individual wastewater treatment processes. In one study, nitrification inhibition was observed in response to a 12-h period of silver nanoparticle shock loading to reach a final peak silver concentration of 0.75 mg/L in a lab-scale Modified Ludzacke-Ettinger process.[13] In another study, continuous loading of 0.1 and 0.5 mg/L silver nanoparticle into sequencing batch reactors (SBRs) reduced ammonia removal rate on the first day, but the SBRs recovered quickly.[14] Nitrification efficiency decreased significantly in an anaerobic-low dissolved oxygen SBR following short-term exposure of 10 and 50 mg/L ZnO nanoparticles,[15] but a similar effect was not observed for short-term exposure of 1 or 50 mg/L TiO_2 nanoparticles in the same type of reactor.[16] Thus, there is a need for broad comparison of a range of nanoparticles on nitrification in complex bioreactors under a common set of conditions. Furthermore, considering that wastewater treatment is a microbial-ecologically driven process, insight into effects of nanomaterials on the broader microbial community is needed.

In this study, effects of silver (nanoAg), zero valent iron (NZVI), titanium dioxide (nanoTiO_2) and cerium dioxide (nanoCeO_2) nanomaterials were investigated in duplicate lab-scale SBRs simulating typical nitrifying activated sludge wastewater treatment. Effects of nanomaterials were compared to control SBRs that were undosed or received bulk or ionic counterparts (Ag^+, Fe^{2+}, bulkTiO_2, or bulkCeO_2). SBRs were re-started prior to each set of

experiments, which were conducted in two phases: 1.) sequentially increased loading after each 14 days with nanomaterial concentrations of 0.1, 1, 10 and 20 mg/L and 2.) continuous high loading at 20 mg/L for nanoAg, nanoCeO_2, and their analogs, which indicated the greatest potential effects based on the sequential loading experiments. Nitrification performance was monitored along with the abundance of gene markers of nitrification by quantitative polymerase chain reaction (q-PCR), while response of microbial communities was characterized by pyrosequencing of bacterial 16S rRNA genes.[17,18] Transmission Electron Microscopy (TEM) equipped with Energy Dispersive X-ray Spectroscopy (EDS) was used to examine aggregation state and interaction of nanomaterials with activated sludge to understand potential relationships between nanomaterial transformation and toxicity effects.

3.3 Materials and Methods

3.3.1 Preparation of Nanomaterial Suspensions

NanoAg was synthesized by the sodium citrate reduction method, yielding a concentration of 100 mg/L.[19] NZVI dispersion with a combination of a biodegradable organic and inorganic stabilizer was purchased from NANO IRON s.o.r. (NANOFER 25S, Rajhrad, Czech Republic). Anatase TiO_2 and CeO_2 nanopowder (Sigma-Aldrich, Saint Louis, MO) were dispersed into nanopure water by sonication for 20 min (90 W, 20 KHz, 20 ℃) at the concentration of 100 mg/L. Freshly prepared nanomaterial dispersions were used to dose SBRs. The properties of the prepared nanomaterial dispersions were confirmed and characterized by TEM. The average sizes of the nanoparticles were 52 ± 12 nm for nanoAg, 46 ± 10 nm for NZVI, 21 ± 12 nm for nanoTiO_2, and 33 ± 12 nm for nanoCeO_2.

3.3.2 Set-up of Sequencing Batch Reactors (SBRs)

Lab-scale SBRs were set up in 3 L glass beakers (Fisher, Suwanee, GA) with an active volume of 2 L in a temperature controlled room at 20 ℃. Each SBR was operated with two 12 h cycles per day with solids retention time (SRT) of 23 days and hydraulic retention time (HRT) of 2 days. Each cycle consisted of 0.1 h feeding, 10.82 h aeration, 0.05 h mixed liquor wasting (solids wasting), 0.75 h settling, and 0.33 h decant. Waste sludge was returned at a rate of 0.10 to maintain the biomass. The SBRs were seeded with return nitrifying activated sludge from a local municipal wastewater treatment plant. A synthetic wastewater (Table S3.1 and S3.2) served as feed with an initial chemical oxygen demand (COD) of 450 mg/L and total nitrogen (TN) of 55 mg/L. Upon reaching steady state, pH of the SBRs was in the range of 7.4-7.7, mixed liquor suspended solids (MLSS) 3000-4000 mg/L, and mixed liquor volatile suspended solids (MLVSS) 2200-3400 mg/L. SBRs were acclimated until ammonium nitrogen removal of >98% was achieved (typically 3-5 weeks) before dosing of nanomaterials. Each nanomaterial was tested individually, with the SBRs re-started prior to the next experiment in order to attain equivalent performance among the SBRs and avoid effects of prior nanomaterials before testing the subsequent nanomaterial.

3.3.3 Sequential Load of Nanomaterials

Three conditions were examined in duplicate SBRs: nanomaterial, corresponding bulk or ionic material [Ag^+ as $AgNO_3$ (Fisher, Suwanee, GA); Fe^{2+} as $FeSO_4$ (Fisher, Suwanee, GA); bulkTiO_2 (Fisher, Suwanee, GA); bulkCeO_2 (Sigma-Aldrich, Saint Louis, MO)], and undosed controls. The dosing of nanomaterials and bulk/ionic materials was initiated at an influent concentration of 0.1 mg/L and sequentially increased after each 14 days to 1 mg/L, 10 mg/L and

finally 20 mg/L. Nanomaterial and bulk/ionic material dispersions or solutions were directly dosed to the reactors at the feeding time of each cycle.

3.3.4 High Load of Nanomaterials

Based on results of sequential load experiments, nanoAg, nanoCeO_2 and the bulk/ionic analogs were selected for high load experiments. Upon reaching steady-state, 20 mg/L nanoAg, Ag^+, nanoCeO_2 and bulkCeO_2 dispersions or solutions were dosed to each reactor at the feeding time of each cycle for a total of 42 days.

3.3.5 Analytical Methods

Nitrification was monitored by quantifying concentrations of nitrite nitrogen (NO_2^--N), nitrate nitrogen (NO_3^--N) and ammonia nitrogen (NH_3-N) in the aqueous effluent by Ion Chromatography (Thermo Scientific, Tewksbury, MA) and using an Ammonia Nitrogen Test Kit (Hach, Loveland, CO). pH, MLSS and MLVSS of SBRs were monitored regularly as indicators of reactor performance using standard methods.[20] Partitioning of nanomaterials and bulk/ionic materials in effluents and activated sludge were analyzed using ICP-MS (Thermo Scientific, Tewksbury, MA) by quantification of Ag, Fe, Ti and Ce. Aqueous effluents were filtered through 0.45 μm mixed-cellulose ester (MCE) membrane filters (EMD Millipore, Billerica, MA) prior to analysis. Activated sludge containing nanoAg was digested with 1:3 hydrochloric to Nitric acid (v/v), and activated sludge containing NZVI, nanoTiO_2, and nanoCeO_2 was digested by 1:1 sulfuric to nitric acid (v/v). The digested samples were diluted and filtered through 0.45 μm MCE membrane filters (EMD Millipore, Billerica, MA) for ICP-MS.

3.3.6 q-PCR

Activated sludge was sampled from each SBR just prior to commensing dosing and every 7 days during both sequential load and high load experiments. Total nucleic acid was extracted in duplicates from 175 µL activated sludge using a MagMAX^{TM} Total Nucleic Acid Isolation Kit (Life technologies, Grand Island, NY) following the manufacturer's instruction. To monitor the abundance of nitrifying bacteria, *amo*A genes encoding the active-site polypeptide of ammonia monooxygenase, 16S rRNA genes of *Nitrobactor* and *Nitrospira* (two common genera of NOB), and universal bacterial 16S rRNA genes were quantified by q-PCR using previously reported primers.[21-24] All q-PCR standard curves were constructed from serial dilutions of cloned genes ranging from 10^8 to 10^2 gene copies per µL. The presence of PCR inhibitors was checked by serially diluting a representative sub-set of samples and comparing PCR efficiencies with standards. It was found that a 1:50 dilution performed well to minimize inhibitory effects and was applied across samples. Samples were analyzed in triplicate with a standard curve and negative control included in each run. Gene copy numbers of *amo*A and *Nitrobacter* and *Nitrospira* 16S rRNA genes were normalized to universal bacterial 16S rRNA genes. Averages and standard deviations of all data were determined using Microsoft Excel® 2007. *t* tests were conducted using R 2.8.1 software (http://cran.r-project.org/bin/windows/base/old/2.8.1/) to determine statistical differences between samples at at a significance level of 0.05 ($p < 0.05$).

3.3.7 Pyrosequencing

Nucleic acid extracts corresponding to just prior to dosing and at the end of both sequential load and high load experiments were diluted to 20 ng/µL and subjected to pyrosequencing of 16S rRNA genes using primers 341F/907R on a Roche 454 FLX Titanium platform (Roche, Nutley, NJ) by the Research and Testing Laboratory (Lubbock, TX). Duplicate

extracts were combined for pyrosequencing analysis. The retrieved sequences were processed using MOTHUR 1.32.1 software according to published methods[25] and on-line 454 SOP accessed in 2013 (http://www.mothur.org/wiki/454_SOP). In brief, primers and barcodes were removed, and sequences with ambiguous base pairs, more than two mismatches in the primer sequence, more than one mismatch in the barcode sequence, more than nine homopolymers, or less than 150 base pairs were filtered out. Alignment of sequences was carried out using SILVA reference database (http://www.mothur.org/wiki/Silva_reference_alignment). Chimeras were removed using UCHIME. Sequences corresponding to mitochondria, chloroplast, Archaea, Eukarya or unknown were removed. This processing resulted in an average of 3,541 sequences per sample (n = 64, sd = 2108). The sequences were subsampled to the smallest library size and the phylotype was assigned at the genus level. A total of 315 genera were identified. Inverse Simpson diversity index ($1/\lambda = 1\Big/\sum_{i=1}^{S} p_i^2$) was calculated by MOTHUR for each sample.[26] Multidimensional Scaling (MDS) analysis was performed using Primer 6 software (Primer-E, Plymouth, UK) to compare similarities of microbial community compositions between samples based on the calculation of Bray-Curtis coefficient.[27]

3.3.8 TEM-EDS mapping

Activated sludge from SBRs dosed with nanoAg, NZVI, nanoTiO_2, and nanoCeO_2 were freeze-dried for TEM grid preparation as previously described.[28] A JEOL 2100 TEM operated at 200 kV was used to detect and characterize aggregation state of nanoparticles in the activated sludge. The microscope was equipped with EDS which was used to analyze the chemistry of the particles of interest under the scanning TEM (STEM) mode.

3.4 Results and Discussion

3.4.1 Effects of Nanomaterials on Nitrification

In the sequential load experiments, NH_3-N and NO_2^--N effluent concentrations remained near the detection limit in all SBRs throughout the dosing (data not shown). This indicates that nitrification functionality was not impacted by dosing of nanomaterials or bulk/ionic analogs when the load was sequentially increased. There was similarly no effect of nanomaterials in the high load experiments for nanoAg or nanoCeO_2, with NH_3-N and NO_2^--N consistently near the detection limit (data not shown). Nitrification was also not significantly impacted by high load bulkCeO_2; however, in the high load Ag^+ condition, effluent NH_3-N rose above 10 mg/L and NO_3^--N decreased to ~15 mg/L within seven days (Figure 3.1A). NO_2^--N concentrations remained near the detection limit all through the dosing, indicating that NO_2^- oxidization was not impacted even by Ag^+ (Figure 3.1B). The SBRs receiving the high load of Ag^+ failed at about 14 days, with high COD (109 and 92 mg/L) and turbid effluent, while the remaining SBRs continued to operate at high load with no apparent inhibitory effects on nitrification.

Overall, the impacts of the nanomaterials and bulk/ionic analogs on nitrification appeared to be negligible under the conditions of this study, with the exception of Ag^+. Although nanoAg was reported to elicit greater inhibition to nitrification than Ag^+ in studies of nitrifying bacterial enrichments,[12-13] inhibition of nitrification by nanoAg was not observed under the complex SBR conditions in this study. In a lab-scale Modified Ludzack-Ettinger process, nitrification was inhibited by a 12-h period of nanoAg shock loading to reach a final peak silver concentration of 0.75 mg/L.[13] However, nanoAg did not elicit an apparent effect on nitrification function in this study, even when the concentration was as high as 20 mg/L. The present study was consistent

with another study that dosed 0.1 and 0.5 mg/L of nanoAg to lab-scale SBRs and reported no significant effect on NH_3 removal.[14]

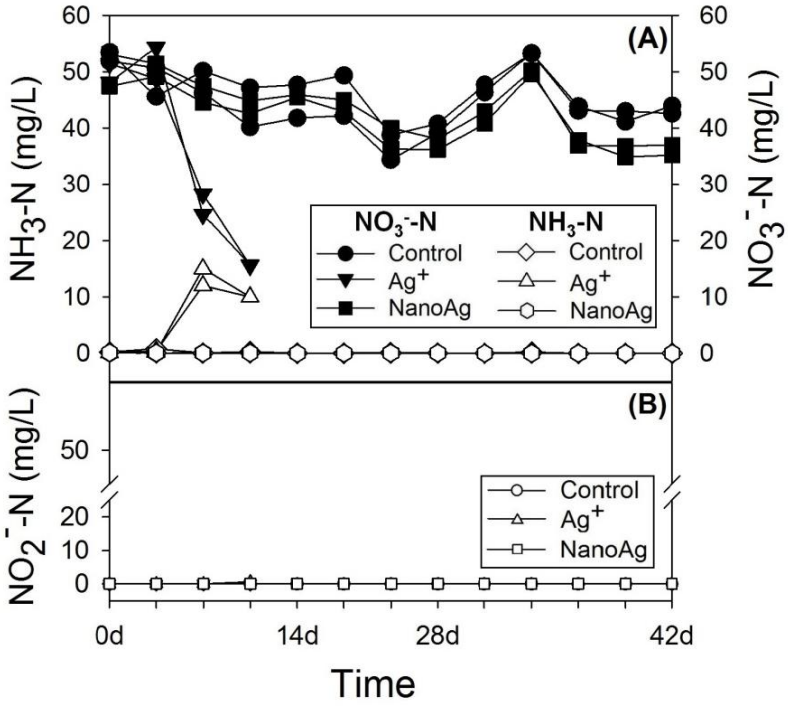

Figure 3.1 Concentrations of (A) NH_3-N, NO_3^--N and (B) NO_2^--N in duplicate SBRs dosed with continuous high load of 20 mg/L nanoAg or Ag^+ relative to undosed controls.

Although nanoTiO_2 was observed to inhibit nitrification at 50 mg/L in lab-scale anaerobic-low dissolved oxygen SBRs dosed over a 70 day period,[16] no effects were observed in this study of SBRs dosed with nanoTiO_2 or bulkTiO_2. Garc á and colleagues[29] reported strong inhibition of enriched AOB cultures by nanoCeO_2, but no effects of nanoCeO_2 or bulkCeO_2 on nitrification function were observed in this study. To the authors' knowledge, the effects of NZVI on nitrification and nitrifying bacteria have not been previously reported. In this study, there were no apparent toxic effects of NZVI or Fe^{2+} on nitrification function.

3.4.2 Effects of Nanomaterials on Abundance of Nitrifying Bacteria

In the sequential load experiments, *amo*A gene copy numbers decreased in SBRs dosed with nanoAg and Ag^{+} at the 20mg/L level (Figure 3.2A, $p < 0.05$) and also in NZVI, Fe^{2+}, nanoCeO_2 and bulkCeO_2 SBRs at the end of 20mg/L dosing (Figure 3.2C-D, $p < 0.05$). *amo*A genes were not significantly impacted by dosing of nanoTiO_2 or bulkTiO_2 (Figure S3.1A, $p > 0.05$). *Nitrobacter* 16S rRNA gene copy numbers decreased significantly in SBRs dosed with nanoAg from 10 to 20 mg/L (Figure S3.2A, $p < 0.05$), but were not significantly impacted by Ag^{+} or the other three nanomaterials/bulk/ionic analogs relative to undosed controls (Figure S3.2, $p > 0.05$). *Nitrospira* 16S rRNA gene levels were not impacted by any of the four nanomaterials or bulk/ionic materials relative to undosed controls (Figure S3.3, $p > 0.05$).

A recent study reported no significant changes of *amo*A, *Nitrobacter* and *Nitrospira* 16S rRNA genes during long-term (more than 60 days) continuous loading of 0.1 mg/L nanoAg to a membrane bioreactor.[30] In this study, dosing of nanoAg at 0.1 mg/L in the sequential load also did not noticeably impact *amo*A, *Nitrobacter* and *Nitrospira* 16S rRNA gene levels. However, *amo*A and *Nitrobacter* 16S rRNA gene copy numbers did decrease as the nanoAg loading concentration increased to 20 mg/L. Yang and colleagues[31] also noted *amo*A expression to be sensitive to nanoAg and Ag^{+} in pure cultures of *Nitrosomonas europaea*. Nonetheless, in this study, nitrification function was not observed to correspond to decrease in nitrification marker genes monitored in any of the sequential load experiments. It is possible that the observed decrease in nitrifier marker genes had not reached the threshold of causing actual nitrification inhibition and thus inhibition of nitrification functionality could eventually be observed over longer time scales. It is also possible that other microbes that were not monitored, such as ammonia oxidizing Achaea and other genera of NOB, played an important role in nitrification.

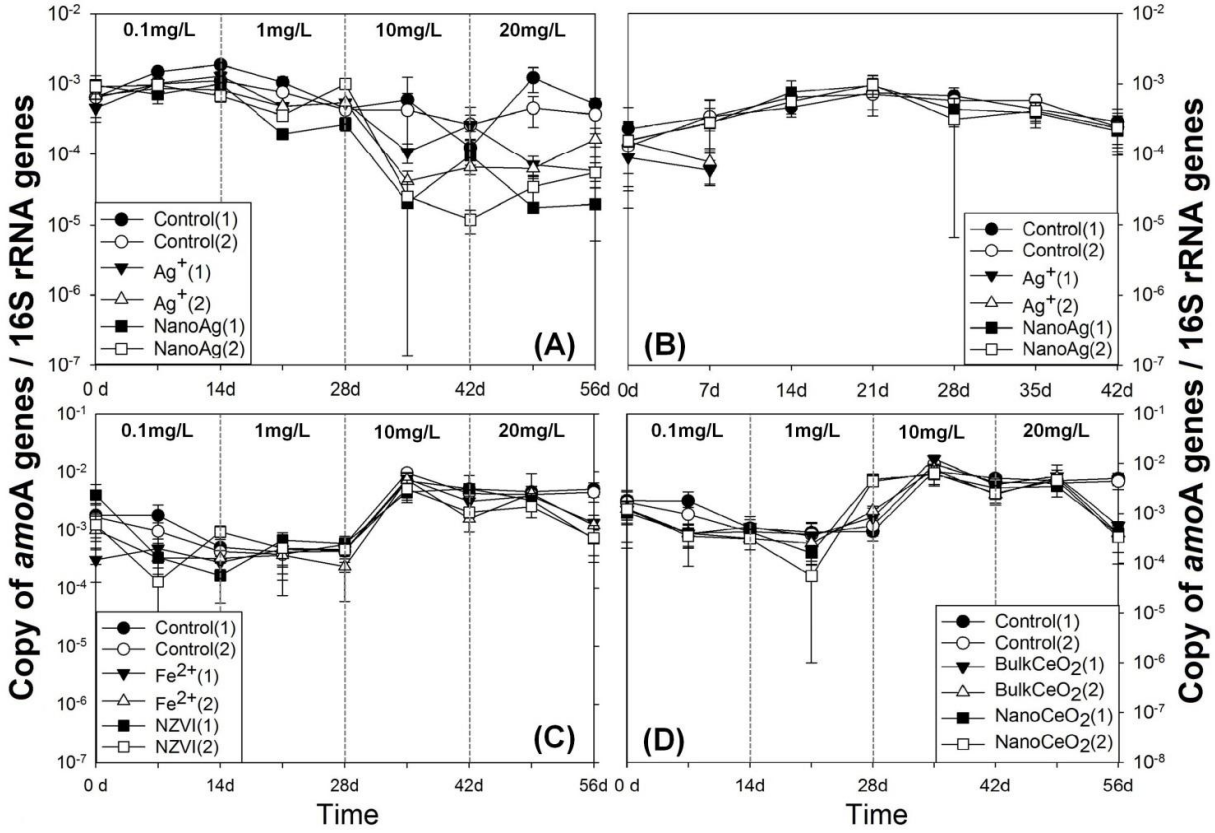

Figure3.2 Quantities of *amo*A genes normalized to 16S rRNA genes in conditions that indicated an effect of the dosed materials: (A) sequential load of nanoAg and Ag^+; (B) high load of nanoAg and Ag^+; (C) sequential load of NZVI and Fe^{2+}; and (D) sequential load of $nanoCeO_2$ and $bulkCeO_2$. Error bars represent standard deviation of duplicate DNA extracts with triplicate q-PCR runs.

In the high load experiment, *amo*A genes decreased significantly in SBRs dosed with Ag^+ compared with SBRs dosed with nanoAg and undosed controls (Figure 3.2B, $p < 0.05$). However, *Nitrobacter* and *Nitrospira* 16S rRNA genes were not significantly impacted (Figure S3.4A-B, $p > 0.05$). The results corresponded well with the observed accumulation of ammonia during high load of Ag^+, while no accumulation of nitrite was observed (Figure 3.1). Although significant decreases of *amo*A genes and *Nitrobacter* 16S rRNA genes were observed at 20 mg/L nanoAg in the sequential load experiments, no effects of nanoAg on any of the three nitrifier

marker genes were observed in the high load experiments (Figure 3.2B, Figure S3.4A-B, $p > 0.05$). Similarly, *amo*A genes decreased by the end of the nanoCeO_2 and bulkCeO_2 sequential load experiments, but none of the three genes were significantly impacted by the high loads (Figure S3.1B, Figure S3.4C-D, $p > 0.05$). Thus, it appeared that sequential load of nanomaterials had a greater impact on the abundance of nitrifying bacteria than the high load condition. Considering that the exposure time of the sequential load (56 days) was longer than the high load (42 days), it may be that the longer exposure time had a stronger influence than exposure concentration or the total nanomaterial loaded (435 versus 840 mg total load). It is also possible that spikes in concentration in the sequential loading conditions triggered a shock response that was not observed under the stable loading conditions of the high load experiment.

In the above-referenced study that observed nitrification inhibition by shock loading of 0.75 mg/L nanoAg to a Modified Ludzacke-Ettinger process, decreases of *Nitrosomonas europaea* and *Nitrospira* populations were observed, while *Nitrobacter* completely washed out.[13] However, in the present study, AOB appeared to be more sensitive than *Nitrobacter* and *Nitrospira*. *amo*A genes were impacted by nanoAg, NZVI, nanoCeO_2 and the bulk/ionic analogs. By contrast, *Nitrobacter* was only impacted by sequential loading of nanoAg, while *Nitrospira* was not impacted by any of the nanomaterials or bulk/ionic materials. Considering the distinct operating conditions of Modified Ludzacke-Ettinger process versus SBR, different process configurations likely vary in their susceptibility to potential microbial nanotoxicity.

3.4.3 Effects of Nanomaterials on Microbial Community Structure

To the knowledge of the authors, pyrosequencing was used for the first time to gain insight into the response of wastewater microbial communities to nanomaterials. Shifts in diversity can serve as an indicator of the overall health of a microbial community.[32] According to

the inverse Simpson diversity index, microbial diversity was the lowest in SBRs dosed with Ag^{+}, in both sequential and high load experiments (Figure S3.5A-B). In the sequential load, one SBR dosed with nanoAg was significantly lower than the initial diversity, but the duplicate SBR maintained the initial level of diversity (Figure S3.5A). The diversities of SBRs dosed with high loads of nanoAg were lower than the undosed controls, but higher than the SBRs dosed with Ag^{+} (Figure S3.4B). No significant changes in microbial diversity were observed in SBRs dosed with NZVI, $nanoTiO_2$, $nanoCeO_2$ or their bulk/ionic analogs (Figure S3.4C-F).

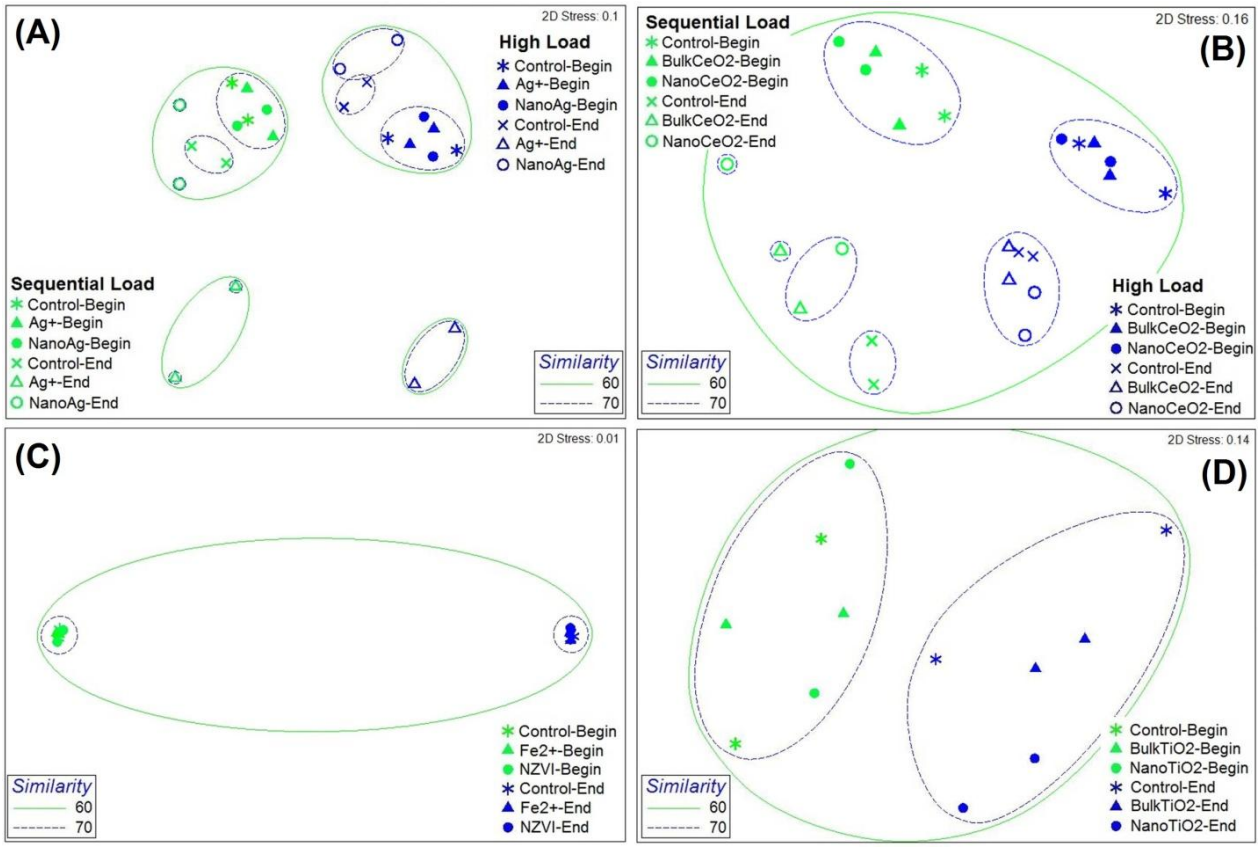

Figure 3.3 Multidimensional Scaling (MDS) analysis of microbial community similarities derived from pyrosequencing of bacterial 16S rRNA genes at the beginning (Begin) and at the end (End) of dosing: (A) sequential load and high load of nanoAg and Ag^{+}; (B) sequential load and high load of $nanoCeO_2$ and $bulkCeO_2$; (C) sequential load of NZVI and Fe^{2+}; (D) sequential load of $nanoTiO_2$ and $bulkTiO_2$.

MDS analysis was used to examine relative similarities of microbial communities at the beginning and the end of dosing. In general, microbial communities at the beginning were clustered closely, with similarities greater than 70%, which confirmed that initial conditions were relatively consistent prior to dosing (Figure 3.3). However, by the end of dosing, microbial communities in all SBRs shifted notably, with similarities less than 70% relative to the initial communities (Figure 3.3).

In the sequential loading experiment, SBRs dosed with Ag^{+} were noted to house distinct microbial communities, with similarities less than 60% relative to SBRs dosed with nanoAg and undosed controls (Figure 3.3A). The SBRs dosed with nanoAg, nanoCeO_2, and bulk CeO_2 also diverged relative to undosed controls, with similarity between 60% and 70% (Figure 3.3A-B). Although the microbial communities at the end of dosing shifted compared with the initial communities in SBRs dosed with NZVI, Fe^{2+}, nanoTiO_2 and bulkTiO_2, with similarities less than 70%, there was no apparent difference among dosed and control SBRs at the end of the experiment (similarities greater than 70%) (Figure 3.3C-D).

Similar to the sequential load experiments, SBRs dosed with the high load of Ag^{+} contained distinct microbial communities relative to SBRs dosed with nanoAg and undosed controls (similarity less than 60%) (Figure 3.3A). SBRs dosed with nanoAg were also distinct from undosed controls, with the similarity between 60% and 70% (Figure 3.3A). For SBRs dosed with nanoCeO_2 and bulkCeO_2 at high load, although there was shift in microbial community structure at the end of dosing relative to the beginning, there was no significant difference relative to undosed controls (similarities greater than 70%) (Figure 3.3B).

Ag^{+} showed the strongest effect on the microbial community diversity and composition, corresponding well with the impacts of nanomaterials on nitrification function and abundance of

nitrifying bacteria. This suggests that nitrification inhibition was associated with reduction of microbial diversity and changes of microbial community compositions, an association observed in one previous study.[16] While nitrification function was associated in microbial shifts in the other conditions investigated in this study, a threshold response might be achieved with longer exposure times.

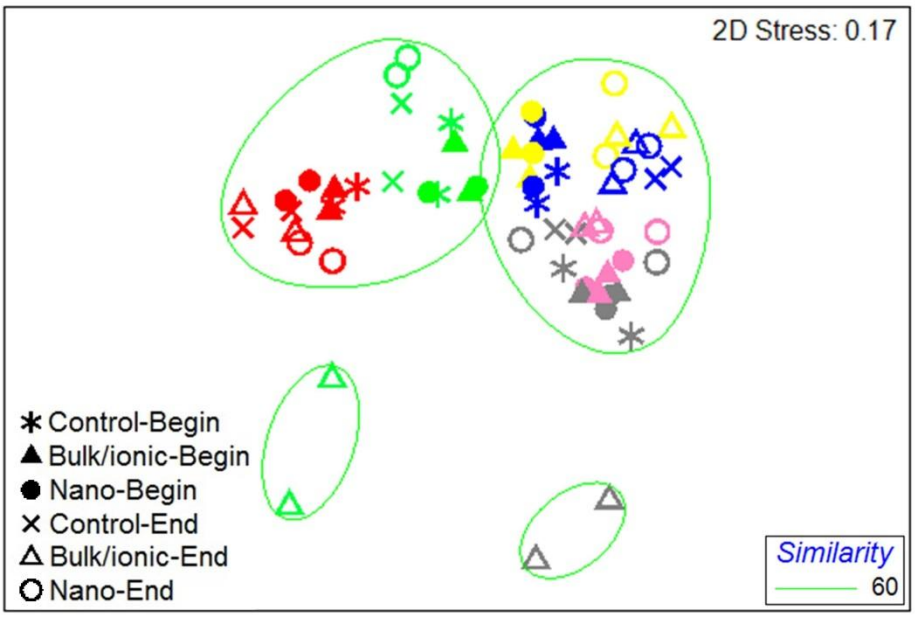

Figure 3.4 Multidimensional Scaling (MDS) analysis of bacterial community similarities derived from pyrosequencing in the beginning (Begin) and at the end (End) of dosing in all sequential load and high load experiments. Green: sequential load of nanoAg and Ag^{+}; Red: sequential load of nanoTiO_2 and bulkTiO_2; Blue: sequential load of NZVI and Fe^{2+}; Yellow: sequential load of nanoCeO_2 and bulk CeO_2; Gray: high load of nanoAg and Ag^{+}; Pink: high load of nanoCeO_2 and bulk CeO_2.

Since SBRs were re-started with each experiment to avoid bias of prior dosed materials, it was of interest to compare the similarities of SBR microbial communities across experiments. Interestingly, variation in the initial microbial community structures were even greater than the

variation associated with dosing of nanomaterials and bulk/ionic analogs, except SBRs dosed with Ag^+ (Figure 3.4). Considering that stable nitrification was achieved at the beginning of each experiment, the specific microbial composition of the communities appeared not to be critical for performance, suggesting functional redundancy. Also, considering that microbial diversity was affected only by Ag^+, while many of the materials influenced microbial community composition, it may be that shift in diversity is a superior indicator of shift in performance.

3.4.4 Nanomaterial Transformation and the Toxicity Effects

Results of ICP-MS indicated that >99% of nanomaterials and bulk/ionic analogs dosed to the SBRs partitioned into the activated sludge, except that the Ag concentration increased to 1.49 and 0.74 mg/L in the aqueous effluent of duplicate SBRs receiving high loads of Ag^+ (data not shown). The results were consistent with other studies indicating that the majority of nanoAg, nanoTiO_2 and nanoCeO_2 is captured by activated sludge during biological wastewater treatment,[3,4,14,30,33] while the fate of NZVI has not previously been reported to the authors' knowledge. However, no functional inhibition to nitrification was observed in spite of accumulation of the nanomaterials in activated sludge. In order to identify possible relationships between nanomaterial transformation state and the effects observed, TEM-EDS was used to detect nanoAg, NZVI, nanoTiO_2 and nanoCeO_2 in activated sludge and to identify nanomaterial transformation by mapping the chemical compositions of particles.

The finding that a large portion of nanoAg remained dispersed was unexpected (Figure S3.6). This was possibly due to the high colloidal stability of nanoAg coated with citrate, which was reported in another study.[10] EDS mapping revealed good spatial correlation of silver with sulfur, but not with chlorine, phosphorus, oxygen or carbon, which could also form complexes with silver (Figure 3.5, Figure S3.7). Studies have shown that sulfidation of nanoAg and

formation of Ag-S complexes could reduce toxicity of nanoAg to microbes,[34-35] and that Ag-S complexes are stable under aerobic conditions.[34] Another recent study also reported that all nanoAg and Ag^+ dosed to a pilot-scale activated sludge plant was converted to Ag_2S.[36] In this study, sulfate was rich in the synthetic wastewater and pyrosequencing showed high abundance of sulfate-reducing bacteria in the activated sludge. Thus Ag-S complexes may have formed and limited the toxicity of nanoAg. Moreover, monodispersed nanoAg has been observed to result in a greater extent of sulfidation than polydispersed, aggregated particles.[35] Therefore, in this study the dispersed particles could favor the occurrence of sulfidation and effectively stabilize nanoAg.

This study supported observations of others that Ag^+ is more toxic than nanoAg.[37] The toxicity of Ag^+ could also be reduced by reaction with sulfide, but one study reported that sulfide could only restrict Ag^+ toxicity within a narrow concentration range.[34] This restriction might explain nitrification inhibition at the high loading of 20 mg/L Ag^+; however, Ag^+ did not inhibit nitrification at 20 mg/L in the experiment with sequential loading. It is possible that as the concentration was sequentially increased from 0.1 mg/L to 20 mg/L, microbes adapted to resist the toxicity under sublethal conditions. Such an effect was suggested in a recent study in which the abundance of the silver resistance gene *sil*E gradually increased during continuous loading of 0.1 mg/L nanoAg to a membrane bioreactor.[30]

In contrast to nanoAg, the other three nanomaterials; NZVI, nanoTiO_2, and nanoCeO_2, were mostly aggregated (Figure 3.6, Figure S3.9-S3.11). According to a previous study, NZVI could be rapidly oxidized under aerobic conditions and inactivate microbes by physical attachment, disruption of the membrane and generation of reactive oxygen species.[6] However, in this study EDS mapping did not indicate correlation of iron with oxygen or other elements

(Figure S3.8), indicating that the particles were not chemically modified. Particle aggregation could possibly reduce the reactivity of NZVI and overall toxicity effects.

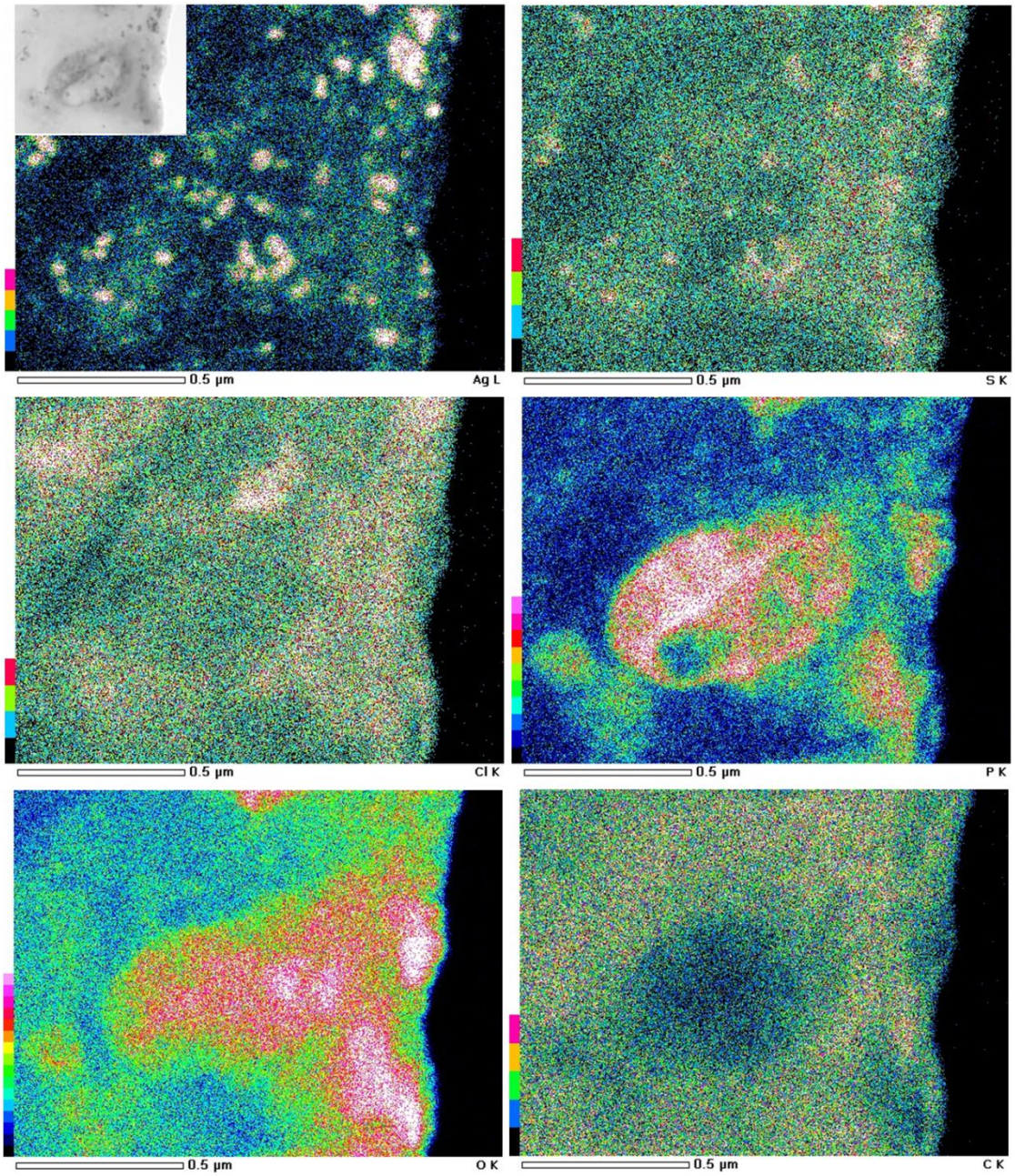

Figure 3.5 EDS maps of silver (Ag), sulfur (S), chlorine (Cl), phosphorus (P), oxygen (O) and carbon (C) in activated sludge after dosing with nanoAg. Color intensity is indicative of the number of X-ray counts. Corresponding STEM images appear in the gray insets.

EDS maps of titanium and cerium spatially correlated only with oxygen, and not with chlorine, sulfur, phosphorus or carbon, suggesting that nanoTiO_2 and nanoCeO_2 remained chemically unmodified (Figure S3.10-S3.11). This was expected considering that nanoTiO_2 and nanoCeO_2 are highly insoluble and thus not likely to be altered in the SBRs. Toxicity of nanoTiO_2 and nanoCeO_2 has mainly been attributed to generation of reactive oxygen species and penetrating the cells due to the small size.[38,39] However, in this study, the toxic effects might have been reduced by aggregation of the nanomaterials.

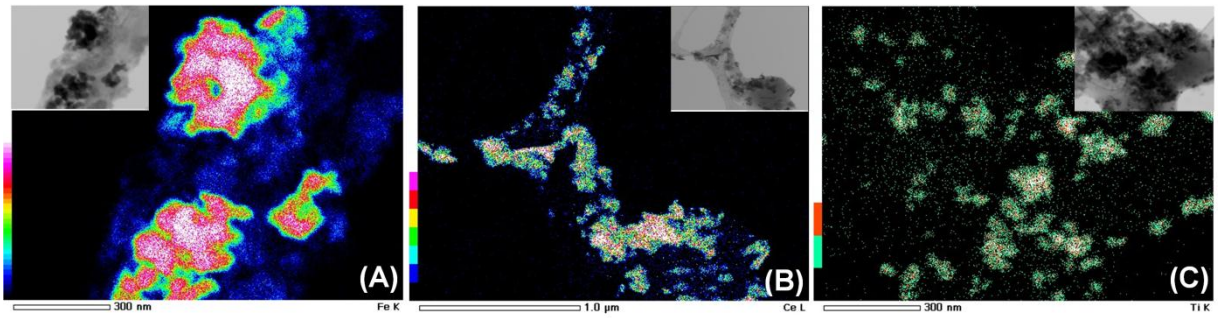

Figure 3.6 EDS maps of: (A) iron, (B) cerium and (C) titanium in activated sludge after dosing of NZVI, nanoCeO_2 and nanoTiO_2. Color intensity is indicative of the number of X-ray counts. Corresponding STEM images appear in the gray insets.

The overall results suggest cautious optimism regarding disposal of nanowaste into wastewater treatment plants and their potential to inhibit key microbial processes. However, considering the effects of nanoAg and nanoCeO_2 on the abundance of nitrifying bacteria and microbial community compositions, long-term study is necessary to verify if continuous exposure to nanomaterials will eventually exert adverse effects on the nitrification. Also, shifting nanomaterial concentrations may be more of a concern than stable loading conditions and is worthy of further investigation.

3.5 Acknowledgments

Funding for this research was provided by the U.S. Environmental Protection Agency Star Grant #834856, the National Science Foundation (NSF) Center for the Environmental Implications of Nanotechnology (CIENT) (EF-0830093), and the Microbiology in the Post-Genome Era NSF REU site at Virginia Tech (NSF Award #1156954), and the Virginia Tech Institute for Critical Technology and Applied Science (ICTAS).

3.6 References

(1) Mueller, N. C.; Nowack, B., Exposure modeling of engineered nanoparticles in the environment. *Environ Sci Technol* **2008**, *42* (12), 4447-4453.

(2) Brar, S. K.; Verma, M.; Tyagi, R. D.; Surampalli, R. Y., Engineered nanoparticles in wastewater and wastewater sludge - Evidence and impacts. *Waste Manage* **2010**, *30* (3), 504-520.

(3) Li, L. X. Y.; Hartmann, G.; Doblinger, M.; Schuster, M., Quantification of Nanoscale Silver Particles Removal and Release from Municipal Wastewater Treatment Plants in Germany. *Environ Sci Technol* **2013,** *47* (13), 7317-7323.

(4) Kiser, M. A.; Westerhoff, P.; Benn, T.; Wang, Y.; Perez-Rivera, J.; Hristovski, K., Titanium Nanomaterial Removal and Release from Wastewater Treatment Plants. *Environ Sci Technol* **2009**, *43* (17), 6757-6763.

(5) Nel, A.; Xia, T.; Madler, L.; Li, N., Toxic potential of materials at the nanolevel. *Science* **2006,** *311* (5761), 622-627.

(6) Diao, M. H.; Yao, M. S., Use of zero-valent iron nanoparticles in inactivating microbes. *Water Res* **2009**, *43* (20), 5243-5251.

(7) Pelletier, D. A.; Suresh, A. K.; Holton, G. A.; McKeown, C. K.; Wang, W.; Gu, B. H.; Mortensen, N. P.; Allison, D. P.; Joy, D. C.; Allison, M. R.; Brown, S. D.; Phelps, T. J.; Doktycz, M. J., Effects of Engineered Cerium Oxide Nanoparticles on Bacterial Growth and Viability. *Appl Environ Microb* **2010**, *76* (24), 7981-7989.

(8) Li, M.; Zhu, L. Z.; Lin, D. H., Toxicity of ZnO Nanoparticles to *Escherichia coli*: Mechanism and the Influence of Medium Components. *Environ Sci Technol* **2011**, *45* (5), 1977-1983.

(9) Lydmark, P.; Almstrand, R.; Samuelsson, K.; Mattsson, A.; Sorensson, F.; Lindgren, P. E.; Hermansson, M., Effects of environmental conditions on the nitrifying population dynamics in a pilot wastewater treatment plant. *Environ Microbiol* **2007**, *9* (9), 2220-2233.

(10) Arnaout, C. L.; Gunsch, C. K., Impacts of Silver Nanoparticle Coating on the Nitrification Potential of *Nitrosomonas europaea*. *Environ Sci Technol* **2012**, *46* (10), 5387-5395.

(11) Radniecki, T. S.; Stankus, D. P.; Neigh, A.; Nason, J. A.; Semprini, L., Influence of liberated silver from silver nanoparticles on nitrification inhibition of *Nitrosomonas europaea*. *Chemosphere* **2011**, *85* (1), 43-49.

(12) Choi, O.; Deng, K. K.; Kim, N. J.; Ross, L.; Surampalli, R. Y.; Hu, Z. Q., The inhibitory effects of silver nanoparticles, silver ions, and silver chloride colloids on microbial growth. *Water Res* **2008**, *42* (12), 3066-3074.

(13) Liang, Z. H.; Das, A.; Hu, Z. Q., Bacterial response to a shock load of nanosilver in an activated sludge treatment system. *Water Res* **2010**, *44* (18), 5432-5438.

(14) Hou, L. L.; Li, K. Y.; Ding, Y. Z.; Li, Y.; Chen, J.; Wu, X. L.; Li, X. Q., Removal of silver nanoparticles in simulated wastewater treatment processes and its impact on COD and NH_4 reduction. *Chemosphere* **2012**, *87* (3), 248-252.

(15) Zheng, X. O.; Wu, R.; Chen, Y. G., Effects of ZnO Nanoparticles on Wastewater Biological Nitrogen and Phosphorus Removal. *Environ Sci Technol* **2011**, *45* (7), 2826-2832.

(16) Zheng, X.; Chen, Y. G.; Wu, R., Long-Term Effects of Titanium Dioxide Nanoparticles on Nitrogen and Phosphorus Removal from Wastewater and Bacterial Community Shift in Activated Sludge. *Environ Sci Technol* **2011**, *45* (17), 7284-7290.

(17) Quince, C.; Lanzen, A.; Curtis, T. P.; Davenport, R. J.; Hall, N.; Head, I. M.; Read, L. F.; Sloan, W. T., Accurate determination of microbial diversity from 454 pyrosequencing data. *Nat Methods* **2009**, *6* (9), 639-641

(18) Ye, L.; Shao, M. F.; Zhang, T.; Tong, A. H. Y.; Lok, S., Analysis of the bacterial community in a laboratory-scale nitrification reactor and a wastewater treatment plant by 454-pyrosequencing. *Water Res* **2011**, *45* (15), 4390-4398.

(19) Lee, P. C.; Meisel, D., Adsorption and Surface-Enhanced Raman of Dyes on Silver and Gold Sols. *J Phys Chem-Us* **1982,** *86* (17), 3391-3395.

(20) APHA. *Standard Methods for the Examination of Water and Wastewater*, 20th ed.; American Public Health Association: Washington, DC, 1998.

(21) Rotthauwe, J. H.; Witzel, K. P.; Liesack, W., The ammonia monooxygenase structural gene amoA as a functional marker: Molecular fine-scale analysis of natural ammonia-oxidizing populations. *Appl Environ Microb* **1997,** *63* (12), 4704-4712.

(22) Degrange, V.; Bardin, R., Detection and Counting of *Nitrobacter* Populations in Soil by PCR. *Appl Environ Microb* **1995,** *61* (6), 2093-2098.

(23) Regan, J. M.; Harrington, G. W.; Noguera, D. R., Ammonia- and nitrite-oxidizing bacterial communities in a pilot-scale chloraminated drinking water distribution system. *Appl Environ Microb* **2002**, *68* (1), 73-81.

(24) Suzuki, M. T.; Taylor, L. T.; DeLong, E. F., Quantitative analysis of small-subunit rRNA genes in mixed microbial populations via 5 '-nuclease assays. *Appl Environ Microb* **2000,** *66* (11), 4605-4614.

(25) Schloss, P. D.; Gevers, D.; Westcott, S. L., Reducing the Effects of PCR Amplification and Sequencing Artifacts on 16S rRNA-Based Studies. *Plos One* **2011**, *6* (12).

(26) Peet, R. K., The Measurement of Species Diversity. *Annual Review of Ecology and Systematics* **1974**, *5*, 285-307.

(27) Bray, J. R., Curtis J., An Ordination of the Upland Forest Communities of Southern Wisconsin. *Ecol Monogr* **1957**, *27*(4), 325-349.

(28) Kim, B.; Park, C. S.; Murayama, M.; Hochella, M. F., Discovery and Characterization of Silver Sulfide Nanoparticles in Final Sewage Sludge Products. *Environ Sci Technol* **2010**, *44* (19), 7509-7514.

(29) Garcia, A.; Delgado, L.; Tora, J. A.; Casals, E.; Gonzalez, E.; Puntes, V.; Font, X.; Carrera, J.; Sanchez, A., Effect of cerium dioxide, titanium dioxide, silver, and gold nanoparticles on the activity of microbial communities intended in wastewater treatment. *J Hazard Mater* **2012,** *199*, 64-72.

(30) Zhang, C.; Liang, Z.; Hu, Z., Bacterial Response to a Continuous Long-term Exposure of Silver Nanoparticles at Sub-ppm Silver Concentrations in a Membrane Bioreactor Activated Sludge System. *Water Research* **2013**, http://dx.doi.org/10.1016/j.watres.2013.10.047.

(31) Yang, Y.; Wang, J.; Xiu, Z. M.; Alvarez, P. J. J., Impacts of silver nanoparticles on cellular and transcriptional activity of nitrogen-cycling bacteria. *Environ Toxicol Chem* **2013**, *32* (7), 1488-1494.

(32) Philippot, L.; Spor, A.; Henault, C.; Bru, D.; Bizouard, F.; Jones, C. M.; Sarr, A.; Maron, P. A., Loss in microbial diversity affects nitrogen cycling in soil. *Isme J* **2013,** *7* (8), 1609-1619.

(33) Limbach, L. K.; Bereiter, R.; Mueller, E.; Krebs, R.; Gaelli, R.; Stark, W. J., Removal of oxide nanoparticles in a model wastewater treatment plant: Influence of agglomeration and surfactants on clearing efficiency. *Environ Sci Technol* **2008,** *42* (15), 5828-5833.

(34) Choi, O.; Cleuenger, T. E.; Deng, B. L.; Surampalli, R. Y.; Ross, L.; Hu, Z. Q., Role of sulfide and ligand strength in controlling nanosilver toxicity. *Water Res* **2009,** *43* (7), 1879-1886.

(35) Reinsch, B. C.; Levard, C.; Li, Z.; Ma, R.; Wise, A.; Gregory, K. B.; Brown, G. E.; Lowry, G. V., Sulfidation of Silver Nanoparticles Decreases Escherichia coli Growth Inhibition. *Environ Sci Technol* **2012,** *46* (13), 6992-7000.

(36) Ma, R.; Levard, C.; Judy, J. D.; Unrine, J. M.; Durenkamp, M.; Martin, B.; Jefferson, B.; Lowry, G. V., Fate of Zinc Oxide and Siver Nanoparticles in a Pilot Wastewater Treatment Plant and in Processed Biosolids. *Environ Sci Technol* **2014**, doi.org/10.1021/es403646.

(37) Xiu, Z. M.; Zhang, Q. B.; Puppala, H. L.; Colvin, V. L.; Alvarez, P. J. J., Negligible Particle-Specific Antibacterial Activity of Silver Nanoparticles. *Nano Lett* **2012**, *12* (8), 4271-4275.

(38) Jin, C.; Tang, Y.; Yang, F. G.; Li, X. L.; Xu, S.; Fan, X. Y.; Huang, Y. Y.; Yang, Y. J., Cellular Toxicity of TiO2 Nanoparticles in Anatase and Rutile Crystal Phase. *Biol Trace Elem Res* **2011**, *141* (1-3), 3-15.

(39) Zhang, H. F.; He, X. A.; Zhang, Z. Y.; Zhang, P.; Li, Y. Y.; Ma, Y. H.; Kuang, Y. S.; Zhao, Y. L.; Chai, Z. F., Nano-CeO2 Exhibits Adverse Effects at Environmental Relevant Concentrations. *Environ Sci Technol* **2011,** *45* (8), 3725-3730.

3.7 Supplemental Materials

Table S3.1 Chemical composition of the synthetic wastewater

Chemical	Formula	Concentration (g/L)
Bactopeptone	/	0.300
Linoleic acid	$C_{18}H_{32}O_2$	0.090
Ammonium sulfate	$(NH_4)_2SO_4$	0.030
Aluminum sulfate octadecahydrate	$Al_2(SO_4)_3 \cdot 18H_2O$	0.037
Calcium chloride dihydrate	$CaCl_2 \cdot 2H_2O$	0.110
Iron chloride	$FeCl_3$	0.017
Magnesium sulfate	$MgSO_4$	0.090
Potassium hydrogen phosphate	K_2HPO_4	0.110
Sodium acetate	NaAc	0.139
Sodium bicarbonate	$NaHCO_3$	0.217
Micronutrients	Table S2	0.1% (v/v)

Table S3.2 Chemical composition of micronutrients

Chemical	Formula	Concentration (g/L)
Citric acid	$C_6H_8O_7$	2.73
Hippuric acid	$C_9H_9NO_3$	2
Trisodium ethylenediaminetetraacetic acid tetrahydrate	$Na_3(EDTA) \cdot 4H_2O$	1.5
Boric acid	H_3BO_3	0.25
Zinc sulfate heptahydrate	$ZnSO_4 \cdot 7H_2O$	0.15
Manganese chloride tetrahydrate	$MnCl_2 \cdot 4H_2O$	0.12
Copper sulfate pentahydrate	$CuSO_4 \cdot 5H_2O$	0.06
Potassium iodide	KI	0.03
Sodium molybdate dihydrate	$Na_2MoO_4 \cdot 2H_2O$	0.03
Cobalt chloride hexahydrate	$CoCl_2 \cdot 6H_2O$	0.03
Nickel chloride hexahydrate	$NiCl_2 \cdot 6H_2O$	0.03
Sodium tungstate tetrahydrate	$NaWO_4 \cdot 2H_2O$	0.03

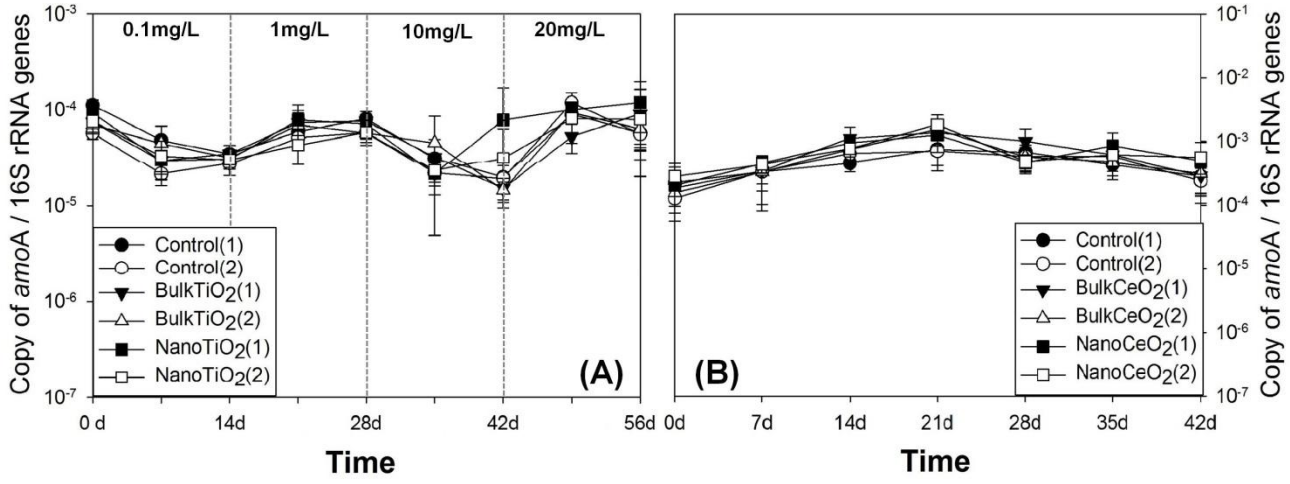

Figure S3.1 *amo*A gene copy numbers normalized to universal bacterial 16S rRNA genes in duplicate nitrifying SBRs during: (A) sequential load of nanoTiO_2 and bulkTiO_2; and (B) high load of nanoCeO_2 and bulkCeO_2 (at 20 mg/L). Error bars represent standard deviation of duplicate DNA extracts with triplicate q-PCR runs.

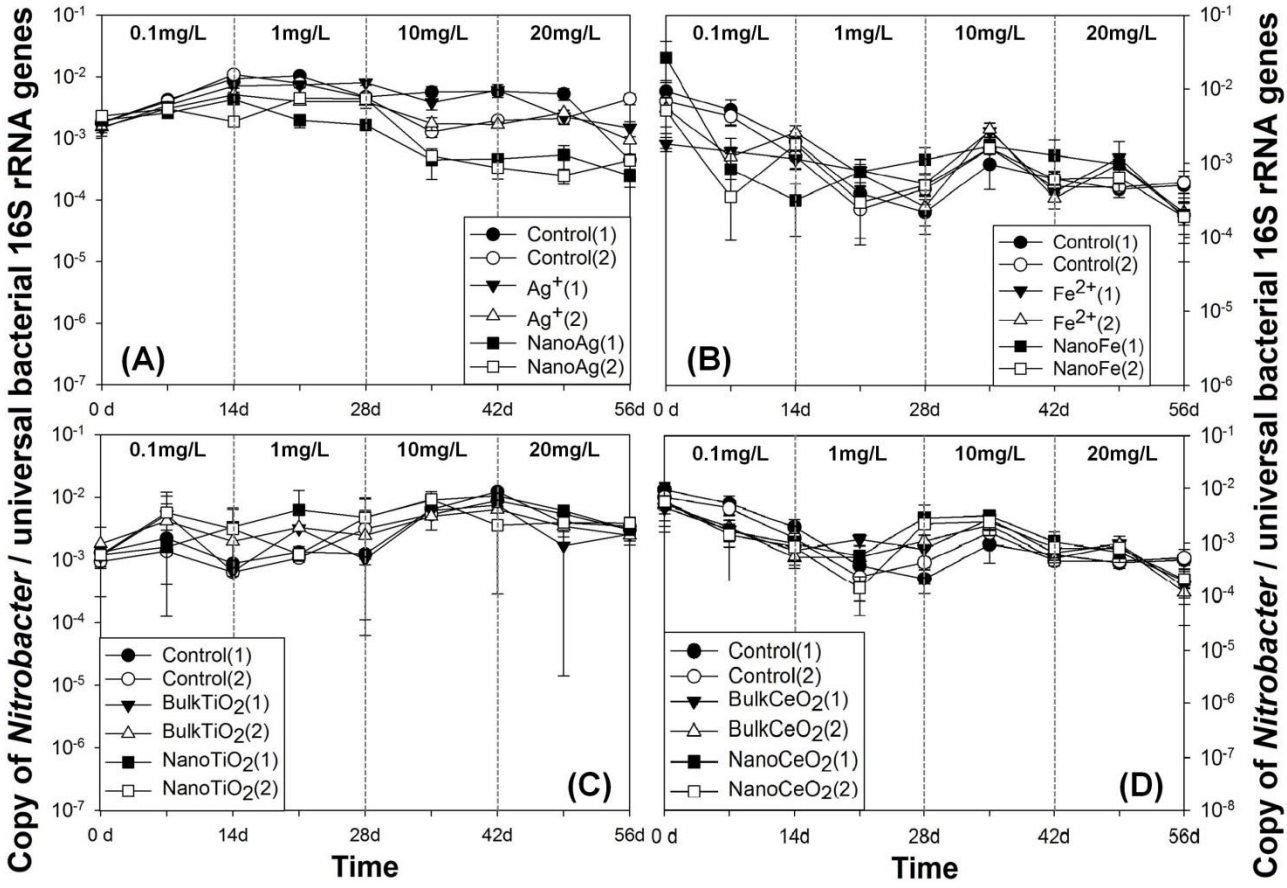

Figure S3.2 ***Nitrobacter*** **16S rRNA gene copy numbers normalized to universal bacterial 16S rRNA genes in duplicate nitrifying SBRs during sequentially increased loading of: (A) nanoAg and Ag^{+}, (B) NZVI and Fe^{2+}, (C) nanoTiO_2 and bulkTiO_2, (D) nanoCeO_2 and bulkCeO_2 Error bars represent standard deviation of duplicate DNA extracts with triplicate q-PCR runs.**

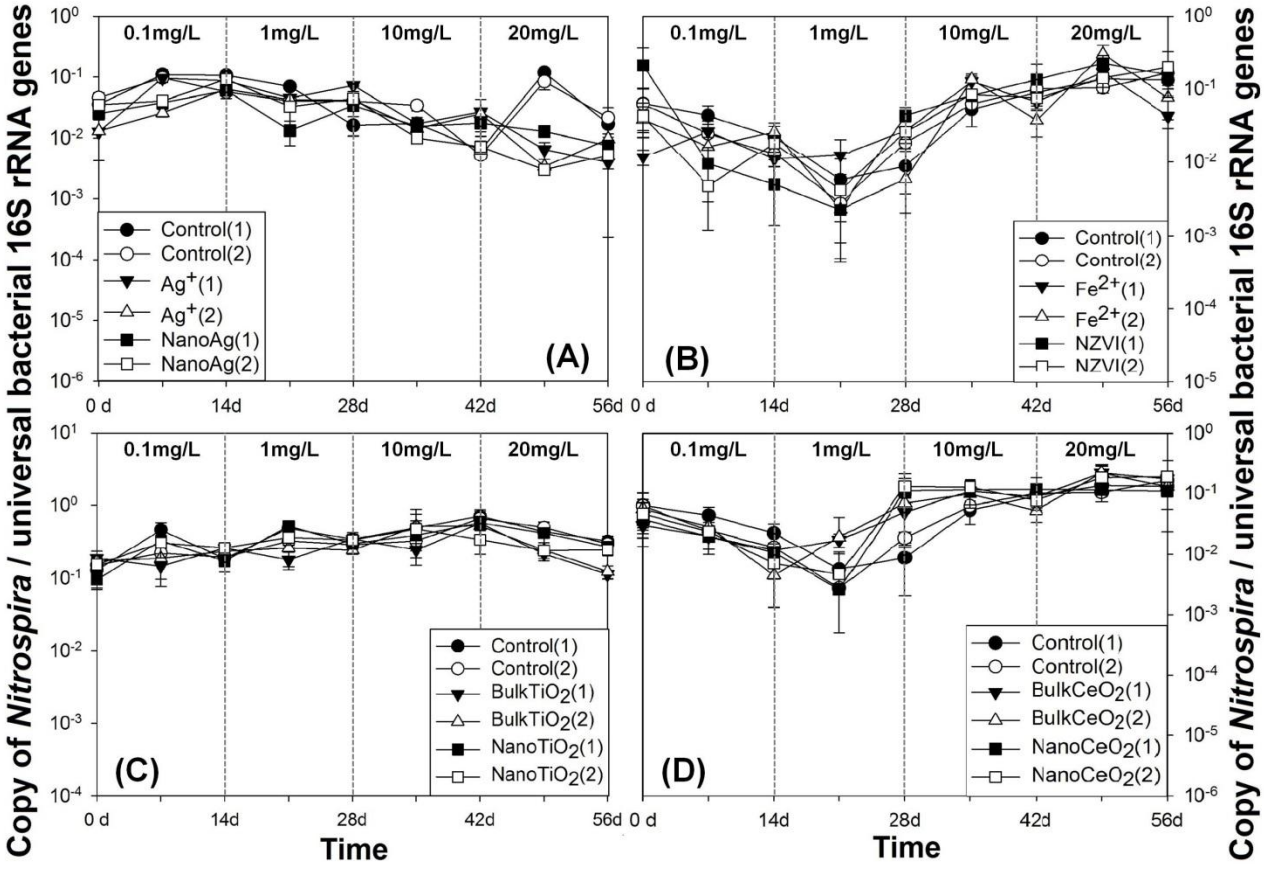

Figure S3.3 ***Nitrospira*** **16S rRNA gene copy numbers normalized to universal bacterial 16S rRNA genes during sequential loading of: (A) nanoAg and Ag^{+}, (B) NZVI and Fe^{2+}, (C) nanoTiO_2 and bulkTiO_2, (D) nanoCeO_2 and bulkCeO_2. Error bars represent standard deviation of duplicate DNA extracts with triplicate q-PCR runs.**

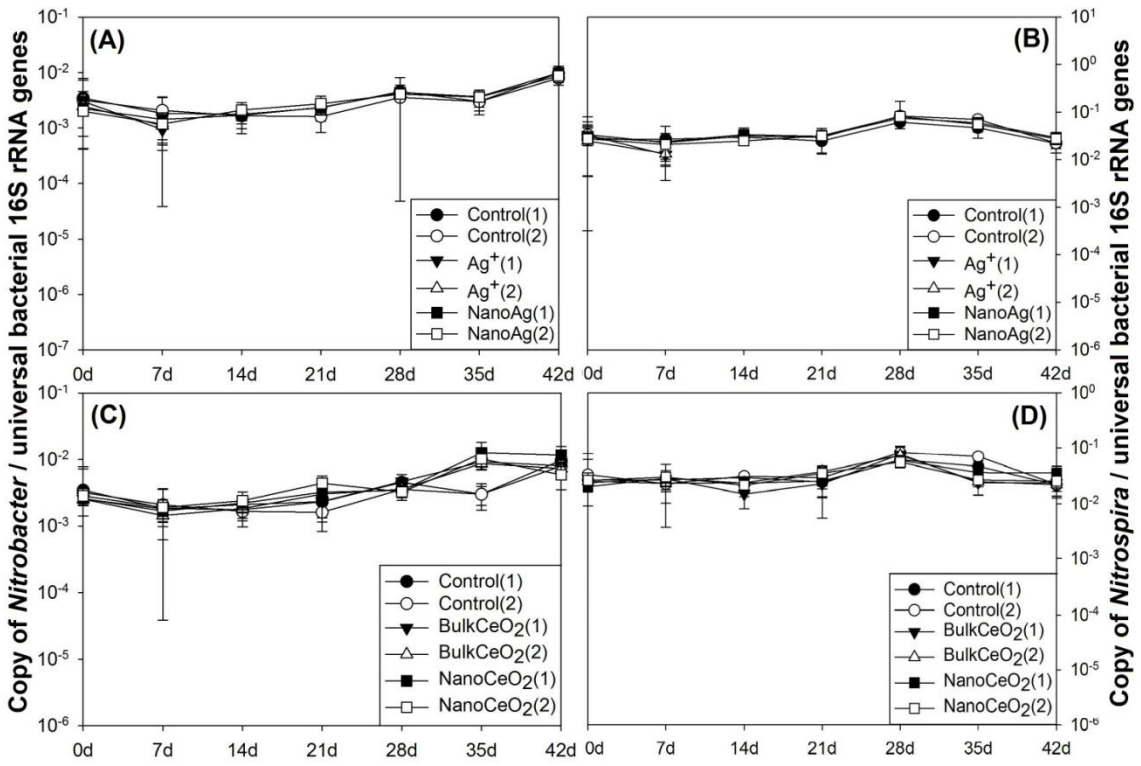

Figure S3.4 ***Nitrobacter*** **(A) and** ***Nitrospira*** **(B) 16S rRNA gene copy numbers normalized to universal bacterial 16S rRNA genes in the high load experiments for nanoAg and Ag^+ and** ***Nitrobacter*** **(C) and** ***Nitrospira*** **(D) 16S rRNA gene copy numbers normalized to universal bacterial 16S rRNA genes in the high load experiments for $nanoCeO_2$ and $bulkCeO_2$. Error bars represent standard deviation of duplicate DNA extracts with triplicate q-PCR runs.**

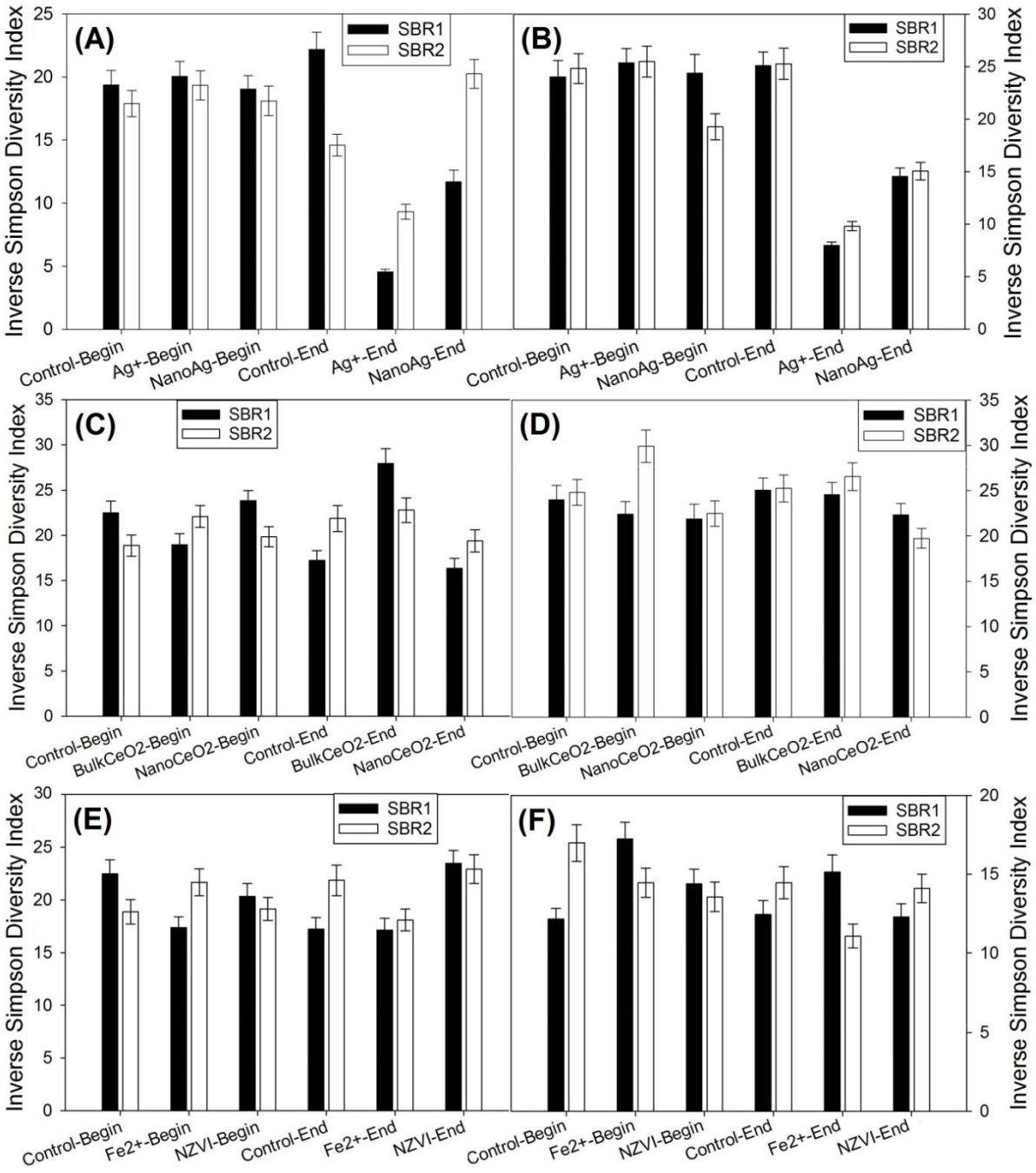

Figure S3.5 Inverse Simpson diversity index of microbial communities at the beginning and at the end of dosing in (A) sequential load of nanoAg and Ag^{+}; (B) high load of nanoAg and Ag^{+}; (C) sequential load of $nanoCeO_2$ and $bulkCeO_2$; (D) high load of $nanoCeO_2$ and $bulkCeO_2$; (E) sequential load of NZVI and Fe^{2+}; and (F) sequential load of $nanoTiO_2$ and $bulkTiO_2$. The calculation was conducted by MOTHUR based on genus level classification of pyrosequencing data.

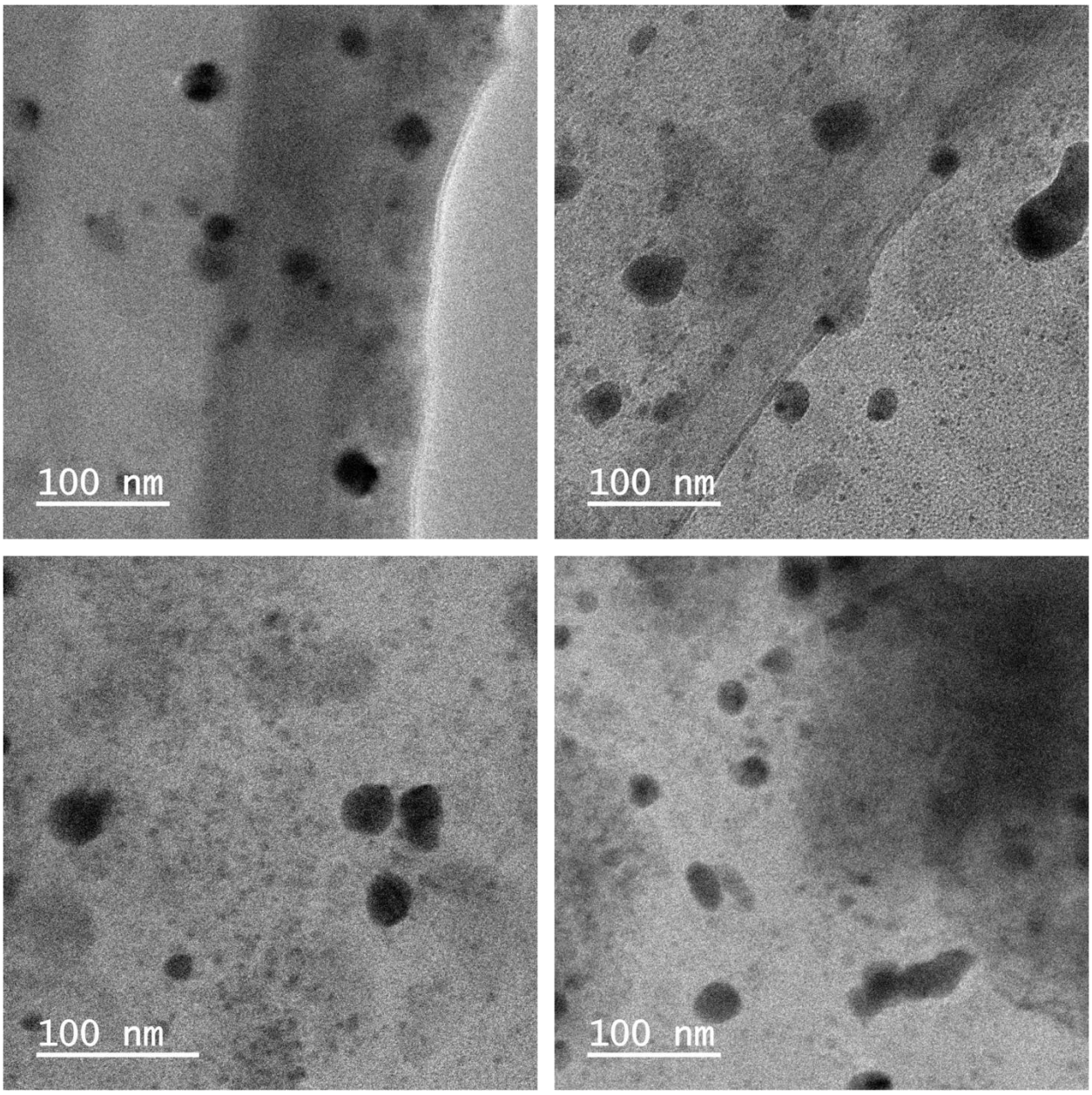

Figure S3.6 TEM images of nanoAg in activated sludge from SBRs dosed with nanoAg.

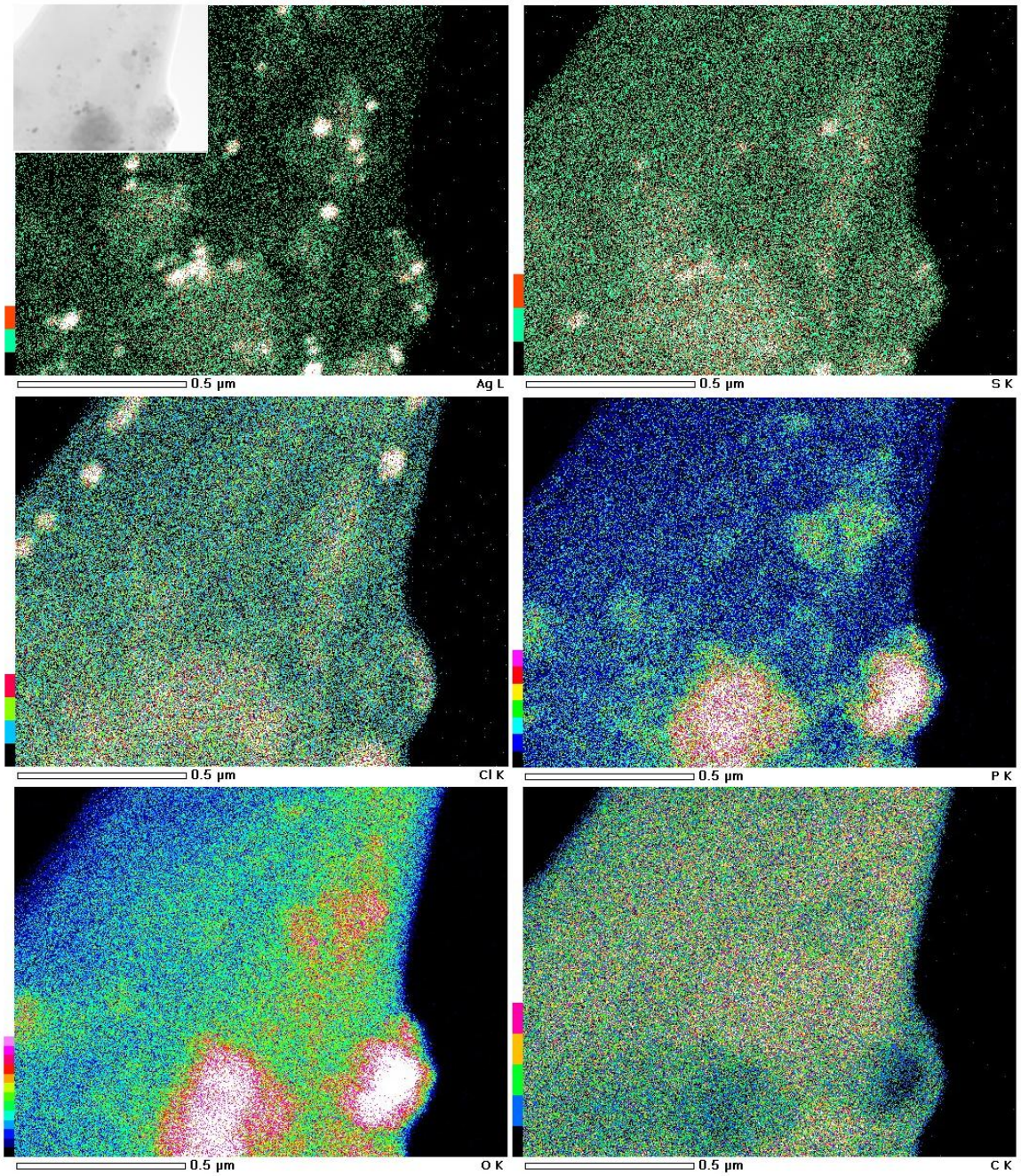

Figure S3.7 Additional EDS maps of silver (Ag), sulfur (S), chlorine (Cl), Phosphorus (P), oxygen (O) and carbon (C) in activated sludge after dosing of nanoAg. Greater color intensity indicates higher X-ray counts. Corresponding STEM images appear in the gray insets.

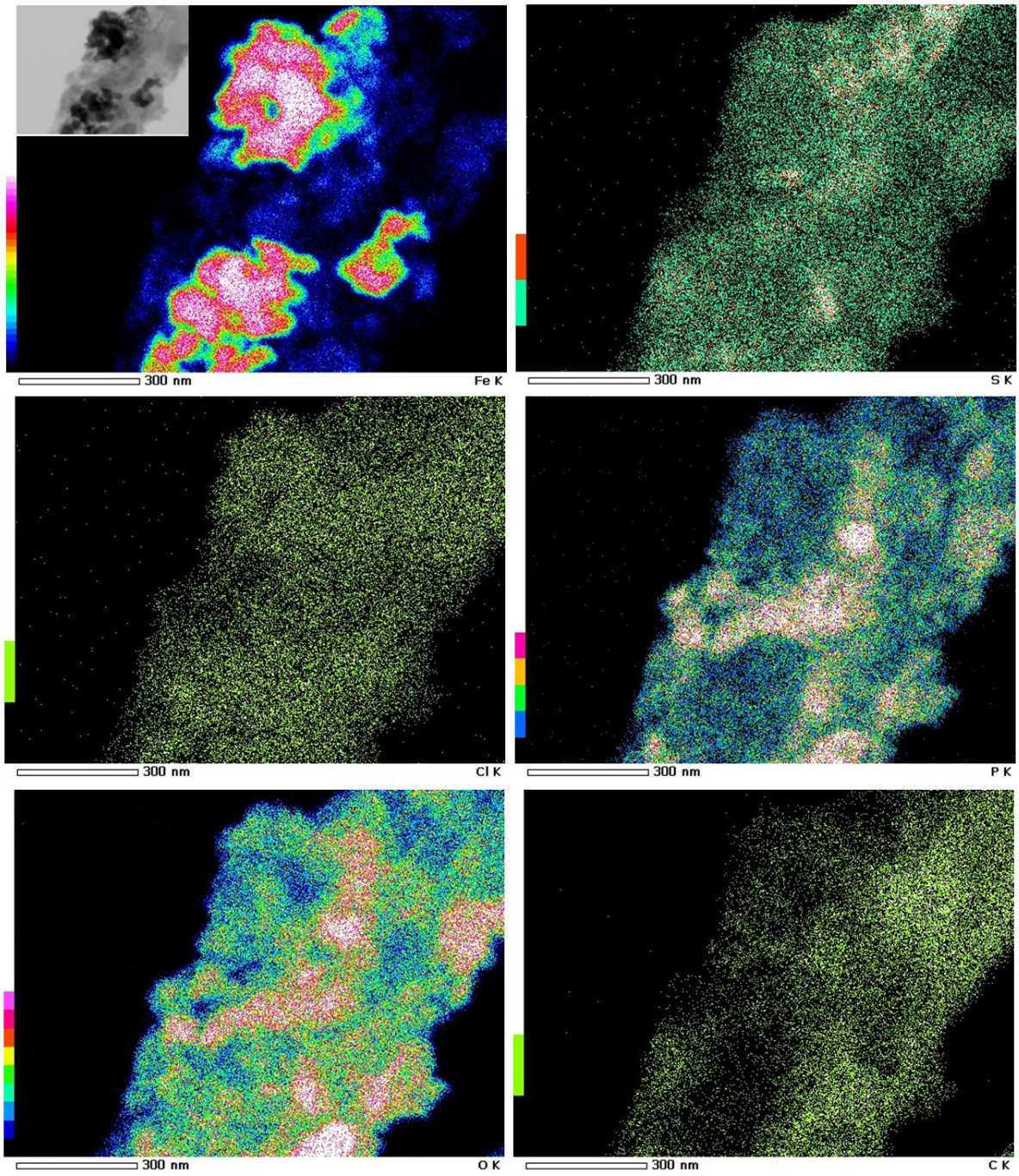

Figure S3.8 EDS maps of iron (Fe), sulfur (S), chlorine (Cl), Phosphorus (P), oxygen (O) and carbon (C) in activated sludge after dosing of NZVI. Greater color intensity indicates higher X-ray counts. Corresponding STEM images appear in the gray insets.

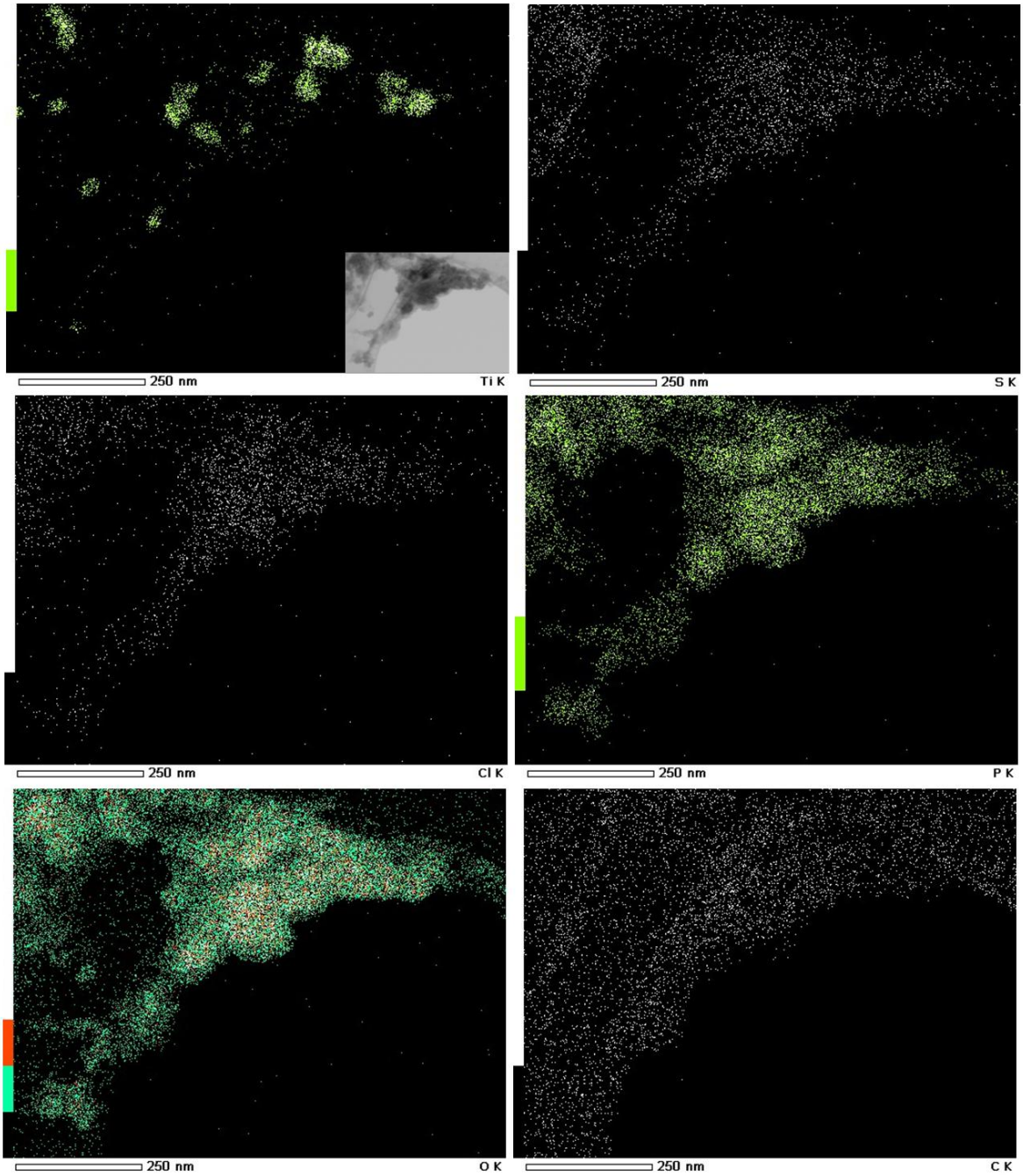

Figure S3.9 EDS maps of titanium (Ti), sulfur (S), chlorine (Cl), Phosphorus (P), oxygen (O) and carbon (C) in activated sludge after dosing of nanoTiO_2. Greater color intensity indicates higher X-ray counts. Corresponding STEM images appear in the gray insets.

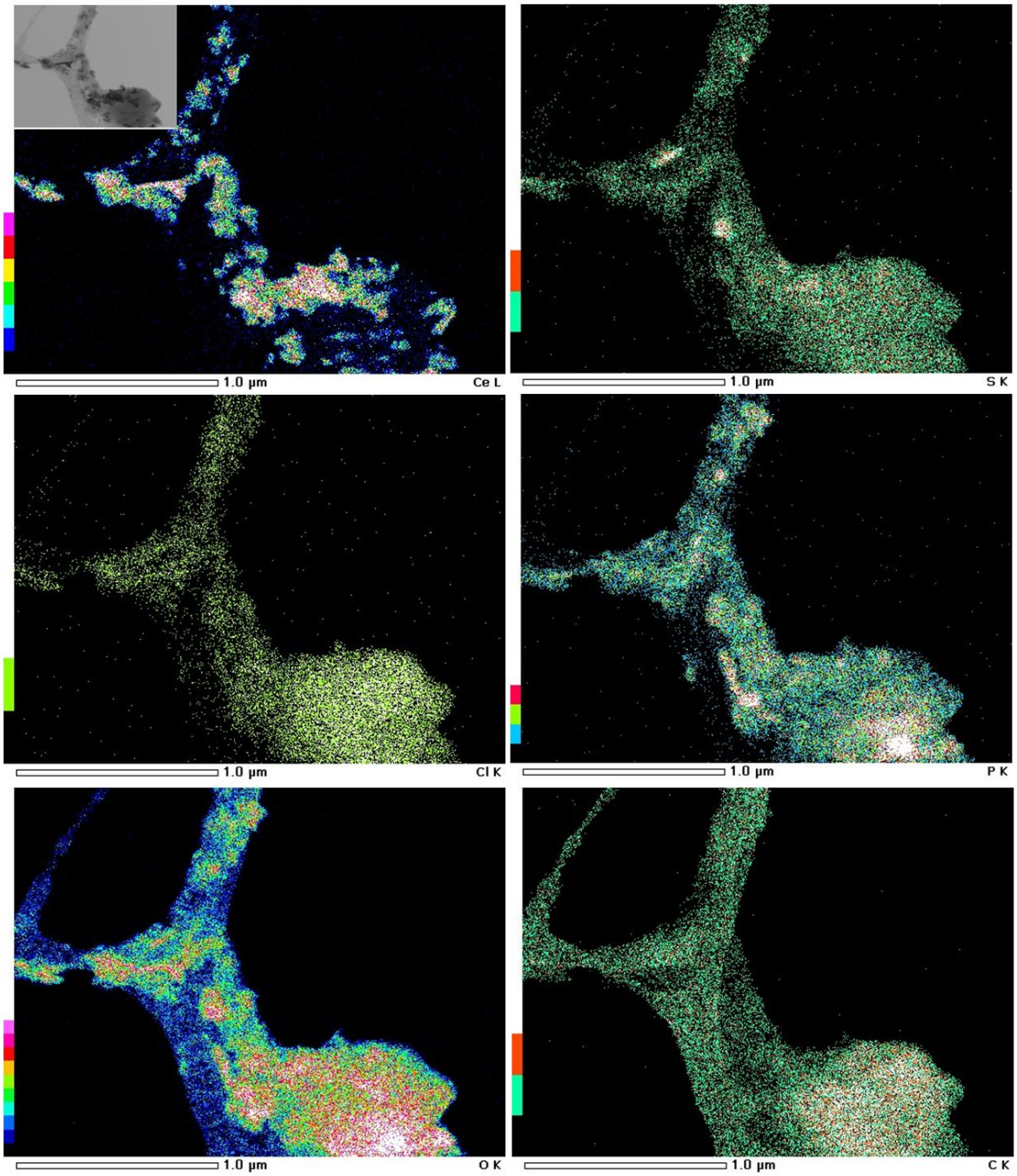

Figure S3.10 EDS maps of cerium (Ce), sulfur (S), chlorine (Cl), Phosphorus (P), oxygen (O) and carbon (C) in activated sludge after dosing of nanoCeO_2. Greater color intensity indicates higher X-ray counts. Corresponding STEM images appear in the gray insets.

CHAPTER 4: Toxicity of Engineered Nanomaterials and their Transformation Products following Wastewater Treatment on A549 Human Lung Epithelial Cells

Yanjun Ma, Subbiah Elankumaran, Linsey C. Marr, Eric P. Vejerano, and Amy Pruden

4.1 Abstract

Here we characterize the toxicity of environmentally-relevant forms of engineered nanomaterials (ENMs), which can transform during wastewater treatment and persist in aqueous effluents and biosolids. In an aerosol exposure scenario, cytotoxicity and genotoxicity of effluents and biosolids from lab-scale sequencing batch reactors (SBRs) to A549 human lung epithelial cells were examined. The SBRs were dosed with nanoAg, nano zero-valent iron (NZVI), nanoTiO_2 and nanoCeO_2 at sequentially increasing concentrations from 0.1 to 20 mg/L. Toxicities were compared to outputs from SBRs dosed with ionic/bulk analogs, undosed SBRs, and pristine ENMs. Pristine nanoAg and NZVI showed significant cytotoxicity to A549 cells in a dose-dependent manner from 1 to 67 μg/mL, while nanoTiO_2 and nanoCeO_2 only exerted cytotoxicity at 67 μg/mL. Only nanoAg induced a genotoxic response, at 9, 33 and 53 μg/mL. However, no significant cytotoxic or genotoxic effects of the SBR effluents or biosolids containing nanomaterials were observed.

4.2 Introduction

The concern that engineered nanomaterials (ENMs) may have adverse effects on human health is increasing as application of nanotechnology in consumer products expands.[1,2] Humans can be exposed to ENMs in the workplace and during use of nano-products, and also through

contact with water, soil, or air to which ENMs may have been released.[3] Comprehensive risk assessment of ENMs requires characterization of the toxicity of ENMs under a wide range of exposure conditions, including environmental routes. Cytotoxicity and genotoxicity of common metal and carbon nanomaterials, such as nanoAg, nanoTiO_2, and carbon nanotubes have been widely studied in human lung, dermal and visceral cells.[4-7] However, in assessing the risks of ENMs released into the natural environment, available data on the toxicity of environmentally-relevant forms of ENMs is lacking.[8,9] Extrapolation of toxicity data based on testing of pristine ENMs may not be appropriate because ENMs are highly reactive by nature and can be chemically, physically and biologically transformed in the environment, potentially altering their toxicity.[10,11]

Wastewater treatment plants (WWTPs) are a critical route of ENM receipt and release into the natural environment.[12-14] The complex wastewater matrix is likely to favor transformation of ENMs. A small portion of ENMs will remain in the wastewater effluent, while the majority will associate with the sludge[15,16] and eventually be disposed of by land-application, landfill, or incineration.[12] During the reuse of treated wastewater and land-application of waste sludge (biosolids), there is potential for humans to be exposed to transformed ENMs, especially through inhalation of aerosols generated.[17,18] However, to the knowledge of the authors, impacts of human exposure to transformed ENMs following wastewater treatment has not previously been reported.

This study examined cytotoxicity and genotoxicity of effluents and biosolids from lab-scale sequencing batch reactors (SBRs) receiving ENMs to A549 human lung epithelial cells. The SBRs were dosed with nanoAg, nano zero-valent iron (NZVI), nanoTiO_2 and nanoCeO_2 at sequentially increasing concentrations from 0.1 to 20 mg/L. Toxicities were compared to outputs

from SBRs dosed with ionic/bulk analogs (Ag^+, Fe^{2+}, bulkTiO_2 and bulkCeO_2), outputs from undosed SBRs, and pristine ENMs.

4.3 Materials and Methods

4.3.1 Preparation of Samples

NanoAg (52 ±12 nm, prepared using citrate reduction method), NZVI (46 ±10 nm, NANOFER 25S, Rajhrad, Czech Republic), nanoTiO_2 (21 ±12 nm, anatase nanopowder, Sigma-Aldrich, Saint Louis, MO), nanoCeO_2 (33 ±12 nm, Sigma-Aldrich) and their ionic/bulk analogs [Ag^+ as $AgNO_3$ (Fisher, Suwanee, GA), Fe^{2+} as $FeSO_4$ (Fisher), bulkTiO_2 (Sigma-Aldrich) and bulkCeO_2 (Sigma-Aldrich)] were prepared/purchased and characterized as described in Ma et al.[19] As previously reported,[19] lab-scale nitrifying SBRs fed with synthetic wastewater were set up and operated at steady state under three conditions in duplicate: (1) SBRs dosed with nanoAg, NZVI, nanoTiO_2, or nanoCeO_2; (2) SBRs dosed with Ag^+, Fe^{2+}, bulkTiO_2, or bulkCeO_2; and (3) undosed SBRs. The dosing was initiated at 0.1 mg/L and sequentially increased to 1, 10 and 20 mg/L. The SBRs were actively nitrifying at the time of this study; further details on SBR performance are reported in Ma et al.[19] Aqueous effluents and biosolids were sampled at the end of 20 mg/L dosing. In preparation for toxicity tests, samples from duplicate SBRs were combined and sterilized, as described in the Supporting Information. Concentrations of nanomaterials in SBR effluents and biosolids were quantified by inductively coupled plasma mass spectrometry (ICP-MS) as described elsewhere.[19]

4.3.2 Cell Culture and Treatment

Human lung alveolar epithelial cells A549 were obtained from ATCC (#CCL-185, Manassas, VA). Cells were cultured in Dulbecco's Modified Eagle Medium (DMEM, Thermo

Scientific HyClone, Logan, UT) containing 10% heat inactivated fetal bovine serum (FBS, Atlanta Biologicals, Flowery Branch, GA) and 1% penicillin-streptomycin (Thermo Scientific HyClone, Logan, UT), and were maintained in a humidified incubator at 37 ℃ and 5% CO_2. Cells were seeded at a density of 1×10^4 in 100 μL culture medium in each well of 96-well plates. At 80% confluency of adherent cells, they were treated for 24 h either with pristine nanomaterials, ionic/bulk analogs, SBR aqueous effluents, or SBR biosolids as indicated. The exposure concentrations of the pristine materials (Table S4.1) varied from 1 to 67 μg/mL for the cytotoxicity assay to estimate IC_{50} values. Genotoxicity assays were carried out at key concentration points according to results of the cytotoxicity assays (Table S4.1). The exposure concentrations of nanomaterials and ionic/bulk materials in SBR effluents and biosolids are shown in Table 4.1. All the samples were diluted with the culture medium to target concentrations.

4.3.3 Cytotoxicity Assay

Cell viability was measured using the WST-1 assay (Roche, Indianapolis, IN) based on quantification of mitochondrial activity as an indicator of cytotoxicity. After the A549 cells were treated with the samples for 24h, WST-1 reagent was added to each well at 1/10 volume of the medium. The absorbance was quantified after incubating at 37 ℃ for 3 h using a Tecan Safire^2 Microplate Reader (Tecan US In., Research Triangle Pa, NC) at 440 nm with a reference wavelength of 660 nm. All samples treated with A549 cells *(a)* were tested in triplicate in three independent experiments with three controls: *(b)* untreated A549 cells in culture medium; *(c)* samples in culture medium without A549 cells; and *(d)* culture medium only. In a single experiment, cell viability was calculated as percentage of the average absorbance derived from triplicate runs of treated cells relative to untreated control cells, with absorbances of

corresponding controls subtracted out to address possible matrix interferences: fraction cell viability = [(a-c)/(b-d)].

Table 4.1 Concentration of nanomaterials and ionic/bulk materials in SBR effluents and biosolids, and exposure concentration in cytotoxicity and genotoxicity assays.

	SBR effluents (μg/L)	Exposure concentration (μg/L)[a]	Biosolids (μg/g total solids)	Exposure concentration (μg/mL)[b]
NanoAg	28.43	9.48	2332.34	0.47
Ag^+	43.67	14.56	2212.61	0.44
NZVI	7.10	2.37	38327.68	7.67
Fe^{2+}	4.70	1.57	48061.38	9.61
NanoTiO_2	0.95[c]	0.32	49201.98	9.84
BulkTiO_2	1.02[c]	0.34	67649.03	13.53
NanoCeO_2	0.25	0.08	22360.00	4.47
BulkCeO_2	0.86	0.29	26454.21	5.29

[a] SBR effluents were diluted approximately 1:3 in the culture medium.
[b] SBR biosolids were exposed to A549 cells at 200 μg total solids/mL.
[c] Concentrations of nanoTiO_2 and bulkTiO_2 in SBR effluents were near the detection limit of Ti by ICP-MS and not significantly different from concentrations in the undosed SBR.

4.3.4 Genotoxicity Assay

DNA damage in A549 cells was detected using immunofluorescent labeling of γH2AX foci as described elsewhere.[20] At sites of DNA double strand breaks, H2AX, a minor nucleosomal histone protein, is rapidly phosphorylated and forms γH2AX.[21] The experimental and imaging procedures are provided in the Supporting Information. Three independent experiments were conducted with at least 200 cells imaged in a single test. Untreated cells and

cells treated with 100 μM H_2O_2 for 10 min were included as negative and positive controls, respectively. Images were analyzed using ImageJ 1.47 (http://rsbweb.nih.gov/ij/) with a macro designed to subtract background and count the number of foci within the defined nucleus masks.

4.3.5 Statistical Analysis

The data were presented as mean ± standard deviation of three independent experiments. The student's *t* test or pairwise *t* test was conducted in R-2.8.1 (http://cran.r-project.org/bin/windows/base/old/2.8.1/) to determine statistical differences between samples at a significance level of 0.05 ($p < 0.05$).

4.4 Results and Discussion

4.4.1 Toxicity of Pristine Nanomaterials

Based on the WST-1 assay, the viability of cells exposed to nanoAg, Ag^+, NZVI and Fe^{2+} for 24 h decreased significantly ($p < 0.05$) in a dose-dependent manner (Figure S4.1). The IC_{50} values for these materials were estimated to be 53±2, 21±0.1, 38±2 and 55±2 μg/mL, respectively. In particular, the IC_{50} of Ag^+ was significantly lower than that of nanoAg ($p = 5\times10^{-4}$), a result that is in agreement with other studies using A549 cell targets.[4,22] By contrast, NZVI was more toxic than its ionic analog, Fe^{2+} ($p = 6\times10^{-4}$). In another study, the cytotoxicty of NZVI (synthesized through reduction of $FeCl_3$ by $NaBH_4$ and coated with Pd) and Fe^{2+} to human bronchial epithelial cells 16HBE14o was not significantly different.[23] Differences between the studies could relate to differences in NZVI coatings (manufacturer in present study reports biodegradable organic and inorganic stabilizers) or the different cells used in the assays (A549 versus 16HBE14o). The viability of cells exposed to nanoTiO_2, nanoCeO_2 and their bulk analogs only decreased at 67 μg/ml by 10-20% (Figure S4.1, $p < 0.05$). But in a few other studies, no

significant cytotoxicity of nanoTiO_2 and nanoCeO_2 to A549 cells was observed even at concentrations up to 100 μg/ml. [5,24,25]

Only cells that were exposed to 33 and 53 μg/mL nanoAg and 21 μg/mL Ag^+ showed significantly higher levels of average γH2AX foci per cell (Figure S4.2A) and greater percentages of cells containing γH2AX foci (Figure S4.2B) ($p < 0.05$) relative to untreated control cells, suggesting genotoxicity resulting from DNA double strand breaks. The number of γH2AX foci per cell exposed to 9 μg/mL nanoAg was not significantly different from that of the control cells (Figure S4.2A, $p = 0.12$), but the percentage of cells containing γH2AX foci was significantly higher than the control cells (Figure S4.2B, $p = 0.03$). Although IC_{50} concentrations of NZVI and Fe^{2+} (38 and 55 μg/mL, respectively), and nanoTiO_2, nanoCeO_2 and the bulk analogs at 67 μg/ml induced significant cytotoxicity to A549 cells, the number of γH2AX foci were not significantly different in cells treated with these materials (Figure S4.2, $p > 0.05$). To the authors' knowledge, genotoxicity of NZVI to human cells has not been investigated previously. Genotoxicities at concentrations of 2.5-15 μg/mL of nanoAg[4], 10-50 μg/mL of nanoTiO_2[26], and 0.5-100 μg/mL of nanoCeO_2[25] have been observed in A549 cells in previous studies. However, in this study, the genotoxicity of nanoAg could be demonstrated, but not nanoTiO_2 or nanoCeO_2 at 67 μg/mL.

4.4.2 Toxicity of SBR Effluents and Biosolids

Based on a previous study,[19] >99% of nanomaterials and ionic/bulk analogs dosed into the SBRs partitioned into the sludge relative to the influent concentrations. Concentrations of nanomaterials in SBR aqueous effluents and biosolids, as well as exposed to A549 cells are shown in Table 4.1. No significant decrease of cell viability or induction of γH2AX foci were observed in A549 cells treated with SBR effluents (Figure 4.1A, Figure 4.2, $p > 0.05$). The

exposure concentration of nanoAg in this study (9.48 μg/L) was much higher than predicted concentrations in WWTP effluents (< 0.5 μg/L),[12-14] while the exposure concentrations of NZVI (2.37 μg/L), nanoTiO_2 (0.32 μg/L) and nanoCeO_2 (0.08 μg/L) were within or lower than the lower bound concentrations predicted (0.7-20 μg/L for NZVI[14], 1-70 μg/L for nanoTiO_2[12-14], and 0.5×10^{-4}-2 μg/L for nanoCeO_2[13-14]). Results of this study indicated limited toxicity of nanoAg in wastewater effluents at higher than environmentally-relevant concentrations to A549 cells, while the effects of higher concentrations of NZVI, nanoTiO_2 and nanoCeO_2 remains to be determined.

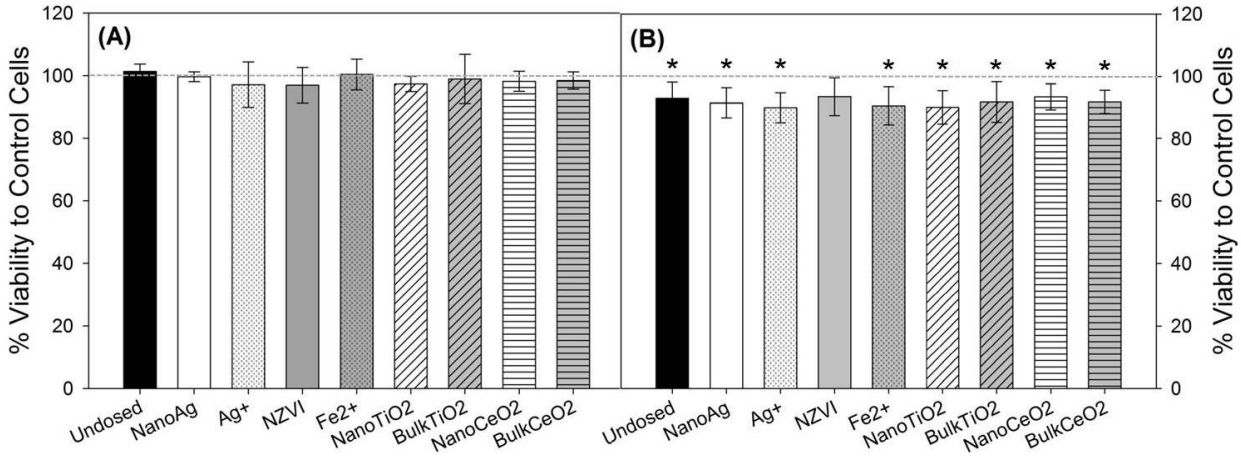

Figure 4.1 Characteristic cytotoxicity of A549 cells exposed to (A) wastewater effluents and (B) biosolids from undosed SBR, and SBRs dosed with nanoAg, Ag^+, NZVI, Fe^{2+}, nanoTiO_2, bulkTiO_2, nanoCeO_2 and bulkCeO_2 for 24 h by WST-1 assay. Exposure concentrations of materials are shown in Table 4.1. Error bars represent standard deviations of three independent experiments. "*" indicates significant decrease of viability compared with untreated control cells ($p < 0.05$).

The concentrations of nanomaterials in biosolids in this study (>2000 μg/g dry mass, Table 4.1) were significantly higher than concentrations predicted in biosolids from WWTP (<1000 μg/g dry mass).[12-14] Moreover, 200 μg total solids/mL represented a higher rate of

exposure relative to other studies of effects of aerosolized biosolids to human lung cells.[27] The viability of cells exposed to biosolids at 200 µg total solids/mL decreased by 7-10% relative to untreated control cells ($p < 0.05$), except for biosolids containing NZVI ($p = 0.08$) (Figure 4.1B). But, there was no significant difference between cells exposed to biosolids from undosed versus dosed SBRs ($p > 0.05$), indicating that the decrease in cell viability was unlikely due to the nanomaterials or ionic/bulk materials, but probably due instead to the high concentration of total solids. Cytotoxicity of biosolids was also examined at 50 and 100 µg total solids/mL, and no significant effects were observed relative to control cells ($p > 0.05$, Figure S4.3).

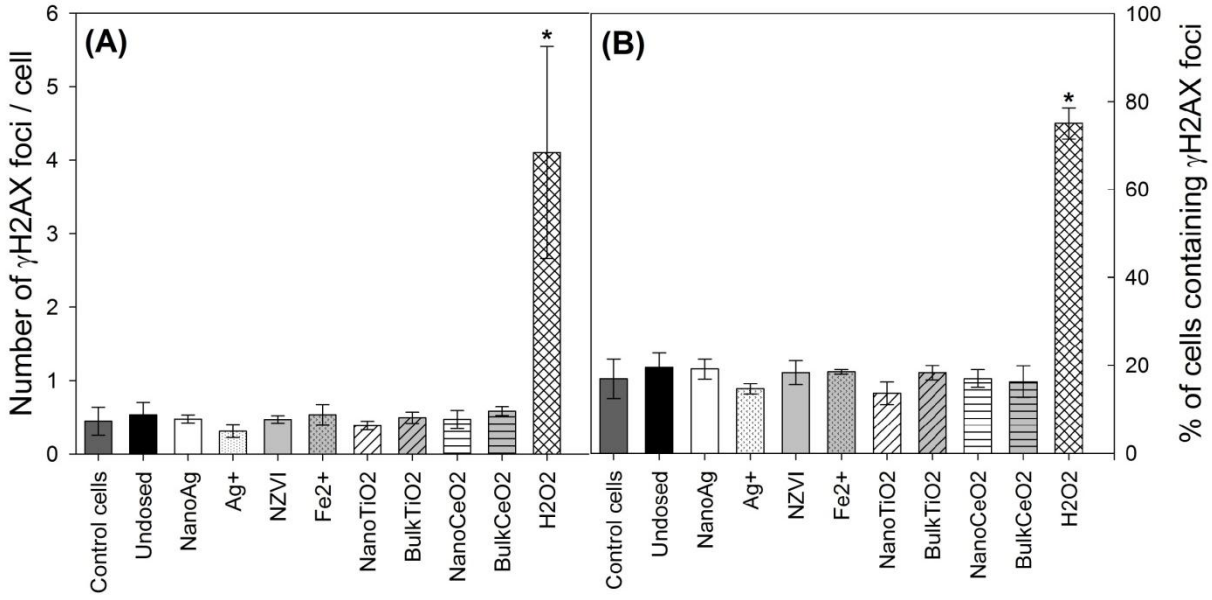

Figure 4.2 γH2AX foci in untreated control A549 cells; cells treated with wastewater effluents from undosed SBR and SBRs dosed with nanoAg, Ag^{+}, NZVI, Fe^{2+}, nanoTiO_2, bulkTiO_2, nanoCeO_2 and bulkCeO_2 for 24 h; and cells treated with 100 µM H_2O_2 for 10 min. Exposure concentrations of materials are shown in Table 4.1. Data are presented as (A) number of γH2AX foci per cell, and (B) percentage of cells containing γH2AX foci. Error bars represent standard deviations of three independent experiments. "*" indicates significant difference compared with untreated control cells ($p < 0.05$).

Genotoxicity of biosolids was examined at 200 µg total solids/mL. However, no significant differences were observed in terms of the number of γH2AX foci per cell or in the percentage of cells containing γH2AX foci in cells treated with biosolids relative to untreated control cells (Figure 4.3, $p > 0.05$), suggesting little or no DNA damage to A549 cells even at concentrations exceeding most likely aerosol exposure levels.

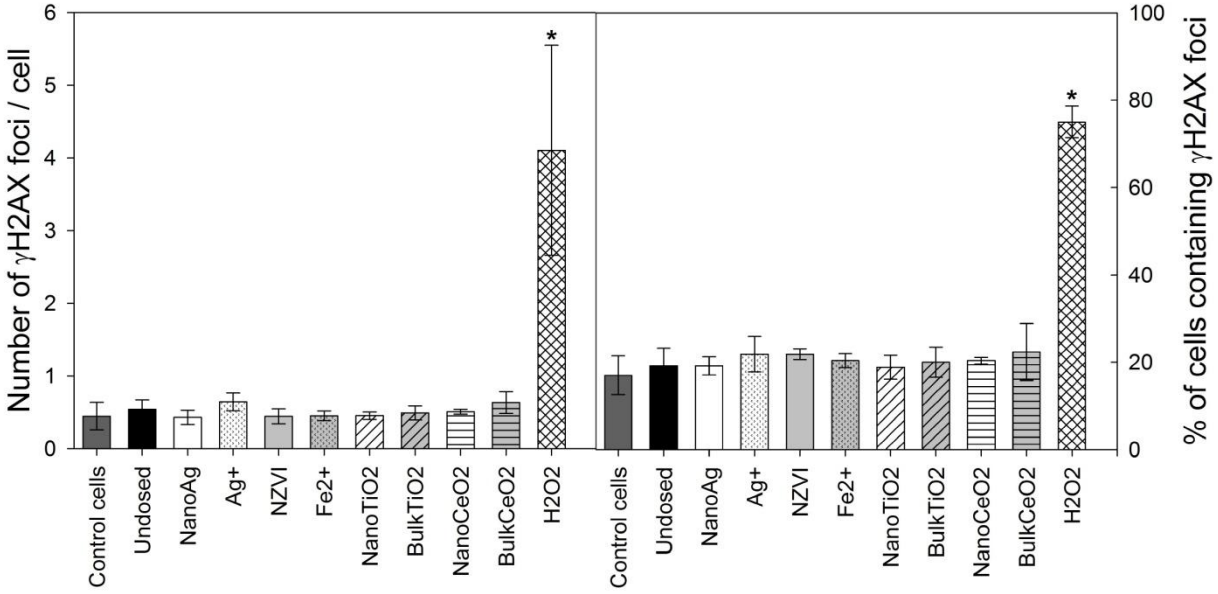

Figure 4.3 γH2AX foci in untreated control A549 cells; cells treated with biosolids from undosed SBR and SBRs dosed with nanoAg, Ag^{+}, NZVI, Fe^{2+}, nanoTiO_2, bulkTiO_2, nanoCeO_2 and bulkCeO_2 for 24 h; and cells treated with 100 µM H_2O_2 for 10 min. Exposure concentrations of materials are shown in Table 4.1. Data was presented as (A) number of γH2AX foci per cell, and (B) percentage of cells containing γH2AX foci. Error bars represent standard deviations of three independent experiments. "*" indicates significant difference compared with untreated control cells ($p < 0.05$).

Uptake of pristine nanoAg, nanoTiO_2, and nanoCeO_2 by human cells,[5,22,24,28] and NZVI by mammalian nerve cells[29] has been observed in previous studies and the most commonly identified mechanism of toxicity was the generation of reactive oxygen species, which induced

oxidative stress[4,23,26,28]. Release of Ag^+ was considered another potential cuase of nanoAg toxicity.[30] Based on TEM-EDS mapping carried out in a previous study of the SBR biosolids,[19] while a large portion of nanoAg remained dispersed, it mainly formed Ag-S complexes. Sulfidation has been reported to reduce toxicity of nanoAg to microbes, aquatic and terrestrial eukaryotic organisms due to low solubility of Ag-S complexes.[31,32] Similarly, transformation of nanoAg in this study may limit their reactivity and result in little toxicity of SBR biosolids to A549 cells. The majority of NZVI, nanoTiO_2 and nanoCeO_2 were aggregated, but not chemically modified. Epithelial cells are impervious to aggregated nanomaterials by diffusion or macropinocytosis.[33] Therefore, the absence of cytotoxicity and genotoxicity of SBR biosolids in this study could be attributed to the inability of aggregated NZVI, nanoTiO_2 and nanoCeO_2 to enter cells. However, the size of the nanomaterial aggregate can affect its physiological distribution and kinetics, cellular distribution (for example within the draining lymph node for an aerosolized particle), cellular uptake and intracellular processing pathways.[34] Also, it is difficult to ascertain the fate of aerosolized nanomaterials from biosolids in the respiratory tract as particles can diffuse and convect during interstitial transport depending on their size.[35] Thus, future work may consider the toxicity under *ex vivo* and *in vivo* conditions.

4.5 Acknowledgments

Funding was provided by the U.S. Environmental Protection Agency Star Grant #834856, the National Science Foundation Center for the Environmental Implications of Nanotechnology (CIENT) (EF-0830093), and the Virginia Tech Institute for Critical Technology and Applied Science.

4.6 References

(1) Papp, T.; Schiffmann, D.; Weiss, D.; Castranova, V.; Vallyathan, V.; Rahman, Q., Human health implications of nanomaterial exposure. *Nanotoxicology* **2008,** *2* (1), 9-27.

(2) Xia, T.; Li, N.; Nel, A. E., Potential Health Impact of Nanoparticles. *Annu Rev Publ Health* **2009,** *30*, 137-150.

(3) Colvin, V. L., The potential environmental impact of engineered nanomaterials. *Nat Biotechnol* **2003,** *21* (10), 1166-1170.

(4) Foldbjerg, R.; Dang, D. A.; Autrup, H., Cytotoxicity and genotoxicity of silver nanoparticles in the human lung cancer cell line, A549. *Arch Toxicol* **2011,** *85* (7), 743-750.

(5) Lankoff, A.; Sandberg, W. J.; Wegierek-Ciuk, A.; Lisowska, H.; Refsnes, M.; Sartowska, B.; Schwarze, P. E.; Meczynska-Wielgosz, S.; Wojewodzka, M.; Kruszewski, M., The effect of agglomeration state of silver and titanium dioxide nanoparticles on cellular response of HepG2, A549 and THP-1 cells. *Toxicol Lett* **2012,** *208* (3), 197-213.

(6) Lindberg, H. K.; Falck, G. C. M.; Suhonen, S.; Vippola, M.; Vanhala, E.; Catalan, J.; Savolainen, K.; Norppa, H., Genotoxicity of nanomaterials: DNA damage and micronuclei induced by carbon nanotubes and graphite nanofibres in human bronchial epithelial cells in vitro. *Toxicol Lett* **2009,** *186* (3), 166-173.

(7) Lewinski, N.; Colvin, V.; Drezek, R., Cytotoxicity of nanoparticles. *Small* **2008,** *4* (1), 26-49.

(8) Blaser, S. A.; Scheringer, M.; MacLeod, M.; Hungerbuhler, K., Estimation of cumulative aquatic exposure and risk due to silver: Contribution of nano-functionalized plastics and textiles. *Sci Total Environ* **2008,** *390* (2-3), 396-409.

(9) Klaine, S. J.; Koelmans, A. A.; Horne, N.; Carley, S.; Handy, R. D.; Kapustka, L.; Nowack, B.; von der Kammer, F., Paradigms to assess the environmental impact of manufactured nanomaterials. *Environ Toxicol Chem* **2012,** *31* (1), 3-14.

(10) Wiesner, M. R.; Lowry, G. V.; Alvarez, P.; Dionysiou, D.; Biswas, P., Assessing the risks of manufactured nanomaterials. *Environ Sci Technol* **2006,** *40* (14), 4336-4345.

(11) Nowack, B.; Ranville, J. F.; Diamond, S.; Gallego-Urrea, J. A.; Metcalfe, C.; Rose, J.; Horne, N.; Koelmans, A. A.; Klaine, S. J., Potential scenarios for nanomaterial release and subsequent alteration in the environment. *Environ Toxicol Chem* **2012,** *31* (1), 50-59.

(12) Gottschalk, F.; Sonderer, T.; Scholz, R. W.; Nowack, B., Modeled Environmental Concentrations of Engineered Nanomaterials (TiO2, ZnO, Ag, CNT, Fullerenes) for Different Regions. *Environ Sci Technol* **2009,** *43* (24), 9216-9222.

(13) Gottschalk, F.; Sun, T. Y.; Nowack, B., Environmental concentrations of engineered nanomaterials: Review of modeling and analytical studies. *Environ Pollut* **2013,** *181*, 287-300.

(14) Keller, A. A.; Lazareva, A., Predicted Releases of Engineered Nanomaterials: From Global to Regional to Local. *Environ Sci Technol Lett* **2014**, dx.doi.org/10.1021/ez400106t.

(15) Limbach, L. K.; Bereiter, R.; Mueller, E.; Krebs, R.; Gaelli, R.; Stark, W. J., Removal of oxide nanoparticles in a model wastewater treatment plant: Influence of agglomeration and surfactants on clearing efficiency. *Environ Sci Technol* **2008,** *42* (15), 5828-5833.

(16) Kiser, M. A.; Westerhoff, P.; Benn, T.; Wang, Y.; Perez-Rivera, J.; Hristovski, K., Titanium Nanomaterial Removal and Release from Wastewater Treatment Plants. *Environ Sci Technol* **2009,** *43* (17), 6757-6763.

(17) Bausum, H. T.; Schaub, S. A.; Kenyon, K. F.; Small, M. J., Comparison of Coliphage and Bacterial Aerosols at a Wastewater Spray Irrigation Site. *Appl Environ Microb* **1982,** *43* (1), 28-38.

(18) Paez-Rubio, T.; Ramarui, A.; Sommer, J.; Xin, H.; Anderson, J.; Peccia, J., Emission rates and characterization of aerosols produced during the spreading of dewatered class B biosolids. *Environ Sci Technol* **2007,** *41* (10), 3537-3544.

(19) Ma, Y.; Metch, J. W.; Vejerano, E. P.; Miller, I. J.; Leon E. C.; Marr L. C.; Pruden, A., Microbial Community Response of Nitrifying Sequencing Batch Reactors to Silver, Zero-Valent Iron, Titanium Dioxide and Cerium Dioxide Nanomaterials. *Environ Sci Technol* (In review).

(20) Yu, Y. K.; Zhu, W.; Diao, H. L.; Zhou, C. X.; Chen, F. Q. F.; Yang, J., A comparative study of using comet assay and gamma H2AX foci formation in the detection of N-methyl-N '-nitro-N-nitrosoguanidine-induced DNA damage. *Toxicol in Vitro* **2006,** *20* (6), 959-965.

(21) Rogakou, E. P.; Pilch, D. R.; Orr, A. H.; Ivanova, V. S.; Bonner, W. M., DNA double-stranded breaks induce histone H2AX phosphorylation on serine 139. *J Biol Chem* **1998,** *273* (10), 5858-5868.

(22) Cronholm, P.; Karlsson, H. L.; Hedberg, J.; Lowe, T. A.; Winnberg, L.; Elihn, K.; Wallinder, I. O.; Moller, L., Intracellular Uptake and Toxicity of Ag and CuO Nanoparticles: A Comparison Between Nanoparticles and their Corresponding Metal Ions. *Small* **2013,** *9* (7), 970-982.

(23) Keenan, C. R.; Goth-Goldstein, R.; Lucas, D.; Sedlak, D. L., Oxidative Stress Induced by Zero-Valent Iron Nanoparticles and Fe(II) in Human Bronchial Epithelial Cells. *Environ Sci Technol* **2009,** *43* (12), 4555-4560.

(24) Moschini, E.; Gualtieri, M.; Colombo, M.; Fascio, U.; Camatini, M.; Mantecca, P., The modality of cell-particle interactions drives the toxicity of nanosized CuO and TiO_2 in human alveolar epithelial cells. *Toxicol Lett* **2013,** *222* (2), 102-116.

(25) De Marzi, L.; Monaco, A.; De Lapuente, J.; Ramos, D.; Borras, M.; Di Gioacchino, M.; Santucci, S.; Poma, A., Cytotoxicity and Genotoxicity of Ceria Nanoparticles on Different Cell Lines in Vitro. *Int J Mol Sci* **2013,** *14* (2), 3065-3077.

(26) Srivastava, R. K.; Rahman, Q.; Kashyap, M. P.; Singh, A. K.; Jain, G.; Jahan, S.; Lohani, M.; Lantow, M.; Pant, A. B., Nano-titanium dioxide induces genotoxicity and apoptosis in human lung cancer cell line, A549. *Hum Exp Toxicol* **2013,** *32* (2), 153-166.

(27) Viau, E.; Levi-Schaffer, F.; Peccia, J., Respiratory Toxicity and Inflammatory Response in Human Bronchial Epithelial Cells Exposed to Biosolids, Animal Manure, and Agricultural Soil Particulate Matter. *Environ Sci Technol* **2010,** *44* (8), 3142-3148.

(28) Eom, H. J.; Choi, J., Oxidative stress of CeO2 nanoparticles via p38-Nrf-2 signaling pathway in human bronchial epithelial cell, Beas-2B. *Toxicol Lett* **2009,** *187* (2), 77-83.

(29) Phenrat, T.; Long, T. C.; Lowry, G. V.; Veronesi, B., Partial Oxidation ("Aging") and Surface Modification Decrease the Toxicity of Nanosized Zerovalent Iron. *Environ Sci Technol* **2009,** *43* (1), 195-200.

(30) AshaRani, P. V.; Mun, G. L. K.; Hande, M. P.; Valiyaveettil, S., Cytotoxicity and Genotoxicity of Silver Nanoparticles in Human Cells. *Acs Nano* **2009,** *3* (2), 279-290.

(31) Reinsch, B. C.; Levard, C.; Li, Z.; Ma, R.; Wise, A.; Gregory, K. B.; Brown, G. E.; Lowry, G. V., Sulfidation of Silver Nanoparticles Decreases *Escherichia coli* Growth Inhibition. *Environ Sci Technol* **2012,** *46* (13), 6992-7000.

(32) Levard, C.; Hotze, E. M.; Colman, B. P.; Dale, A. L.; Truong, L.; Yang, X. Y.; Bone, A. J.; Brown, G. E.; Tanguay, R. L.; Di Giulio, R. T.; Bernhardt, E. S.; Meyer, J. N.; Wiesner, M. R.; Lowry, G. V., Sulfidation of Silver Nanoparticles: Natural Antidote to Their Toxicity. *Environ Sci Technol* **2013,** *47* (23), 13440-13448.

(33) Albanese, A.; Chan, W. C. W., Effect of Gold Nanoparticle Aggregation on Cell Uptake and Toxicity. *Acs Nano* **2011,** *5* (7), 5478-5489.

(34) Oberdorster, G.; Ferin, J.; Lehnert, B. E., Correlation between Particle-Size, in-Vivo Particle Persistence, and Lung Injury. *Environ Health Persp* **1994,** *102*, 173-179.

(35) Semmler-Behnke, M.; Takenaka, S.; Fertsch, S.; Wenk, A.; Seitz, J.; Mayer, P.; Oberdorster, G.; Kreyling, W. G., Efficient elimination of inhaled nanoparticles from the alveolar region: Evidence for interstitial uptake and subsequent reentrainment onto airway epithelium. *Environ Health Persp* **2007,** *115* (5), 728-733.

4.7 Supplemental Materials

Preparation of SBR effluents and biosolids for toxicity assays

Wastewater effluents from SBRs were filtered through 0.45 μm mixed-cellulose ester membrane filters (EMD Millipore, Billerica, MA) to remove bacteria, and biosolids were freeze-dried (FreeZone Plus 4.5, Labconco, Kansas City, MO). A subsample of 1.6 mg freeze-dried biosolids was sterilized with 0.5 mL 100% ethanol and air-dried in a fume hood. The ethanol-treated biosolids were suspended in 1.6 mL 0.1% PBS-Tween solution by sonication for 30 min.

Immunofluorescent labeling of γH2AX foci

A549 cells were exposed to samples for 24 h, followed by washing with PBS and fixation in 4% paraformaldehyde for 15 min and permeabilization in 0.25% Triton X-100 for 15 min. After being blocked with 1% bovine serum albumin in PBS for 1 h, cells were incubated with a rabbit

polyclonal anti-γH2AX antibody (1:500; Santa Cruz Biotechnology Inc., Paso Robles, CA) for 1 h. Following washing with PBS 3x, the cells were incubated with Alexa Fluor 488 Goat Anti-Rabbit IgG (H+L) Antibody (1:500, Life Technologies Corporation, Grand Island, NY) and Hoechst 33342 (10 μg/mL, Life Technologies Corporation, Grand Island, NY) for 1 h. After washing the cells three times with PBS, fluorescence was visualized under 40× objective of an EcLipse TS 100 fluorescent microscopy (Nikon, Melville, NY). γH2AX foci emitted green fluorescent and the nuclei were stained blue with Hoechst 33342 .

Supporting tables and figures

Table S4.1 Exposure concentration of pristine nanomaterials and ionic/bulk materials to A549 cells

Assay	**Exposure concentration**							
	NanoAg	Ag^{+}	NZVI	Fe^{2+}	Nano TiO_2	Bulk TiO_2	Nano CeO_2	Bulk CeO_2
Cytotoxicity (μg/mL)	1, 9, 33, 50, 60 and 67							
Genotoxicity* (μg/mL)	9,33,53	21	38	55	67	67	67	67

*Genotoxicity of nanoAg, Ag^{+}, NZVI and Fe^{2+} was examined at IC_{50} obtained from cytotoxicity assay (53, 21, 38 and 55 μg/mL, respectively); nanoAg was also examined at 9 and 33 μg/mL because significant genotoxicity were observed at 53 μg/mL; nanoTiO_2, bulkTiO_2, nanoCeO_2 and bulkCeO_2 were examined at 67 μg/mL, because cytotoxicity was only observed at 67 μg/mL.

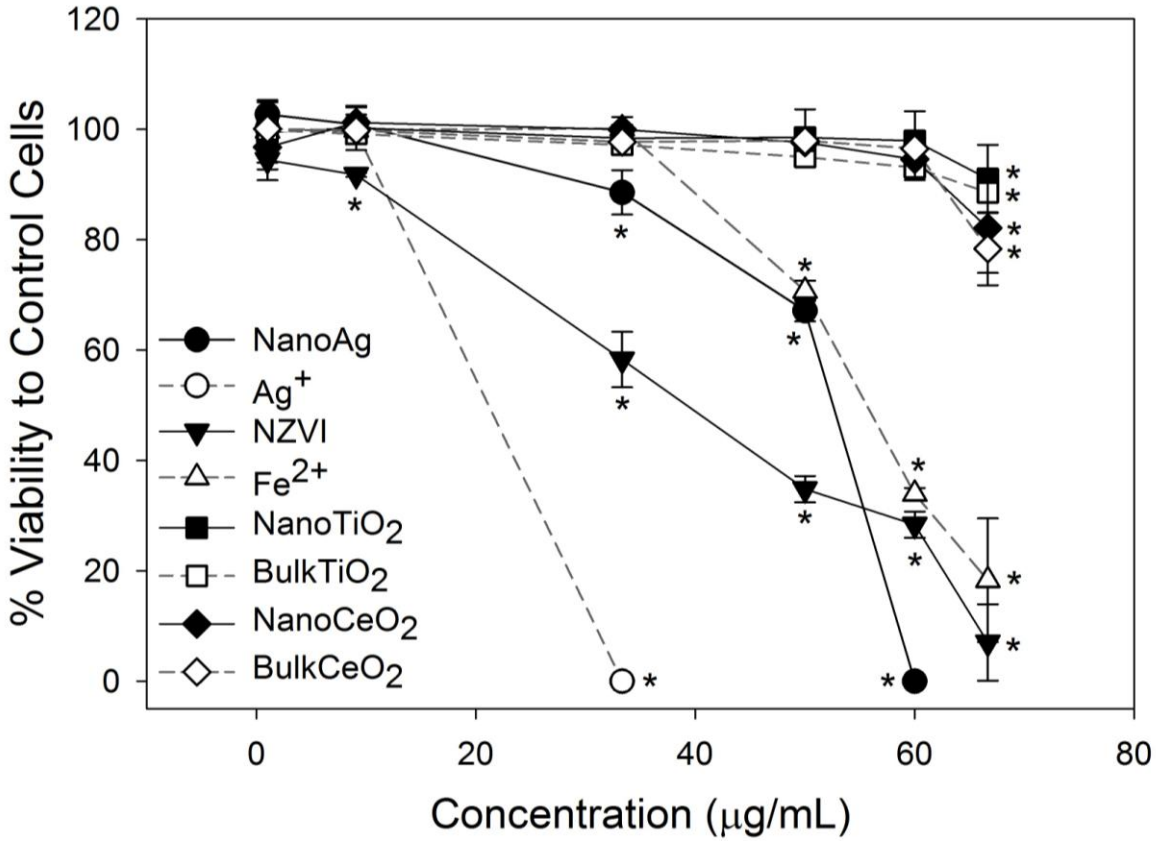

Figure S4.1 Characteristic cytotoxicity of A549 cells exposed to nanoAg, Ag^{+}, NZVI, Fe^{2+}, nanoTiO_2, bulkTiO_2, nanoCeO_2 and bulkCeO_2 for 24 h by WST-1 assay. Six concentrations were tested: 1, 9, 33, 50, 60 and 67 μg/mL. Error bars represent standard deviations of three independent experiments. "*" indicates significant decrease of viability compared with untreated control cells ($p < 0.05$).

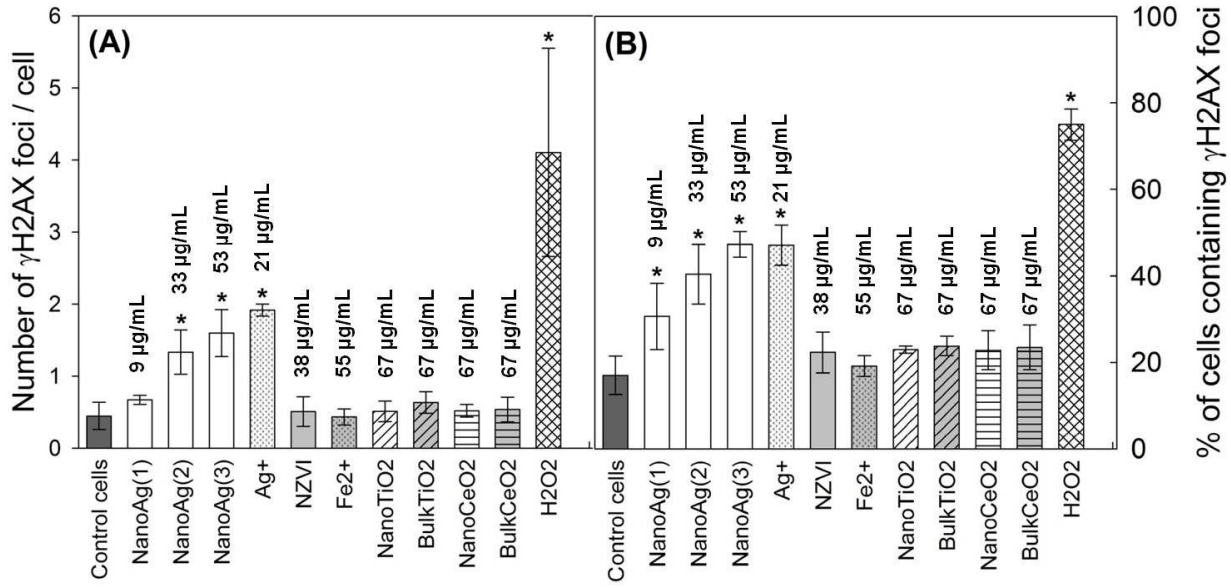

Figure S4.2 γH2AX foci in untreated A549 control cells; cells treated with nanoAg, Ag^{+}, NZVI, Fe^{2+}, nanoTiO_2, bulkTiO_2, nanoCeO_2 and bulkCeO2 at different concentrations for 24 h; and cells treated with 100 µM H_2O_2 for 10 min. Data are presented as (A) number of γH2AX foci per cell, and (B) percentage of cells containing γH2AX foci. Error bars represent standard deviations of three independent experiments. "*" indicates significant difference compared with untreated control cells ($p < 0.05$).

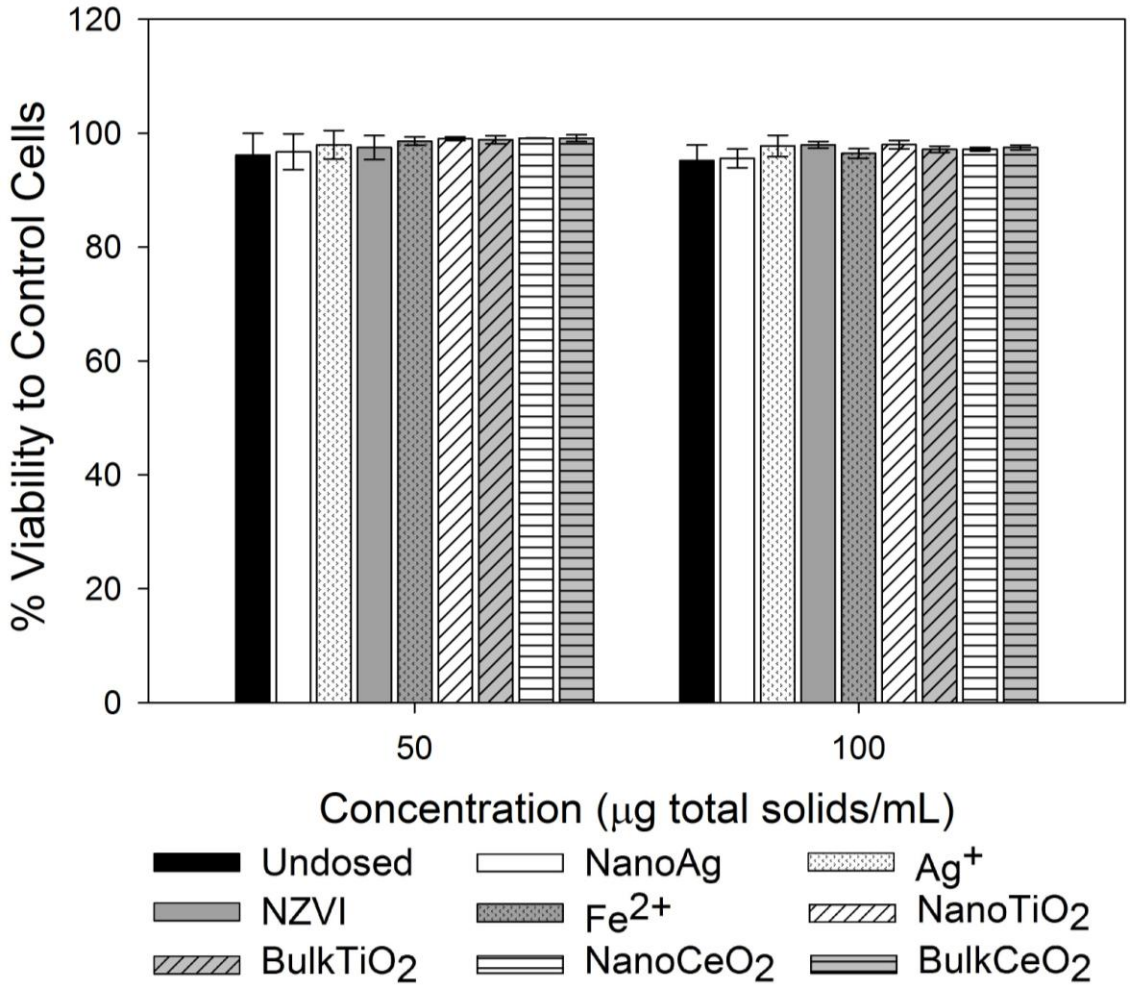

Figure S4.3 Characteristic cytotoxicity of A549 cells exposed to 50 and 100 μg total solids/mL biosolids from undosed SBR, and SBRs dosed with nanoAg, Ag^{+}, NZVI, Fe^{2+}, nanoTiO_2, bulkTiO_2, nanoCeO_2 and bulkCeO_2 for 24 h by WST-1 assay. Error bars represent standard deviations of three independent experiments. There were no significant differences of viability between cells treated with biosolid samples compared with untreated control cells ($p > 0.05$).

CHAPTER 5: Conclusions

Antibiotic resistance genes (AGRs) and engineered nanomaterials (ENMs) were recently identified as contaminants of emerging concern. Their fate in the environment and potential impacts on human and ecosystem health have not been fully characterized. This study aimed to improve understanding of the fate of ARGs and ENMs during wastewater treatment processes, which is an important recipient, reservoir, and source of ARGs and ENMs to the natural environment. The toxicity of ENMs during biological wastewater treatment was further examined with respect to impacts on the functionality of microbial communities, as well as toxicity of ENMs transformed during wastewater treatment to human lung epithelial cells in an aerosol exposure scenario. The study explored a variety of advanced molecular biological tools and toxicity indicators to facilitate quantification of ARGs, characterize the profile of microbial communities, and assess toxicity of ENMs. Specific contributions of this study to further understanding of the fate and impacts of ARGs and ENMs during wastewater treatment processes include:

1) *Identification of the important role of bacterial community composition of sludge digestion processes in driving the distribution of ARGs present in the produced biosolids.* Response of nine representative ARGs to various sludge digestion conditions revealed that ARG removal did not follow a simple trend: Similar performance was observed among mesophilic anaerobic digesters at 10 and 20 day SRT, and also among thermophilic anaerobic digesters at 47 ℃, 52 ℃ and 59 ℃, with thermophilic digestion exhibit more effective reduction to *erm*(B), *erm*(F), *tet*(O), and *tet*(w). Thermal hydrolysis pretreatment remarkably reduced all the ARGs; however, in the downstream anaerobic digestion, all the ARGs rebounded, and in the following aerobic digestion, different behavior of ARGs was observed. DGGE and sequencing analysis

verified distinct diversities and bacterial community compositions in the mesophilic, thermophilic digesters and digesters following thermal hydrolysis pretreatment, which supported the argument that bacterial community compositions in the digesters played an important role in driving the response of ARGs.

2) *Thermophilic anaerobic digestion and thermal hydrolysis pretreatment are promising for reducing ARGs present in produced biosolids.* Thermophilic anaerobic digesters operated at 47 ℃, 52 ℃ and 59 ℃ provided more effective removal of *erm*(B), *erm*(F), *tet*(O), and *tet*(w) compared with mesophilic digesters. The reduction of ARGs by thermal hydrolysis pretreatment was remarkable. Although ARGs rebounded in the following anaerobic and aerobic digesters, the final concentration of most ARGs was still lower than in the produced biosolids of mesophilic anaerobic digesters. The advantages of thermophilic anaerobic digestion and thermal hydrolysis pretreatment were likely due to the lower diversity of bacterial communities which provided a narrower host range of ARGs.

3) *Limited adverse effects of silver (Ag), zero-valent iron (NZVI), titanium dioxide (nanoTiO_2) and cerium dioxide (nanoceO_2) nanomaterials during and following simulated nitrifying activated sludge system.* In sequential loading of nanoAg, NZVI, nanoTiO_2 and nanoCeO_2 to SBRs from 0.1 to 20 mg/L for 56 days, and high loading of nanoAg and nanoCeO_2 at 20 mg/L for 42 days, nitrification function was not measurably inhibited by any of the nanomaterials, although decreased nitrifier gene abundances and distinct bacterial communities were observed in SBRs receiving nanoAg and nanoCeO_2. Also, no significant cytotoxicity and genotoxicity were observed to A549 human lung epithelial cells for SBR effluents and biosolids containing nanomaterials. The Ag-S complexes transformed from nanoAg and the aggregated NZVI, nanoTiO_2 and nanoCeO_2 appeared to be generally stable in the activated sludge, which

may have limited their effects on nitrification function, microbial community structure and A549 cells.

4) *Diversity of microbial community is likely to be a superior indicator of shift in wastewater treatment performance than specific microbial compositions.* One result of interest in this study was the variation of initial microbial community structures when SBRs were re-started for the testing of subsequent nanomaterials, although stable nitrification was achieved in all the SBRs at the beginning of each experiment, which indicated functional redundancy. Moreover, while many of the materials impacted the microbial community structure, only Ag^+ significantly decreased the microbial diversity and inhibited nitrification function.

Overall, results of this study will assist characterizing release of ARGs and ENMs from WWTPs to the environment, and assessing potential risks of ENMs to biological wastewater treatment and human health. Based on this work, the following research is suggested as next steps:

1) *Further investigate horizontal transfer of ARGs during sludge digestion.* Response of ARGs to various sludge digestion conditions in this study indicated an important role of horizontal gene transfer, especially rebound of ARGs in anaerobic digesters following thermal hydrolysis pretreatment, and the correlation of occurrence of *sul*I genes with class I integron gene *int*I1. Future research may be conducted in conditions which the seed culture is carefully selected to be devoid of ARGs, with the feed concentration of ARGs systematically manipulated. Better understanding of horizontal gene transfer will facilitate innovation of current sludge treatment processes for extensive removal of ARGs.

2) *Examine long-term effects of nanomaterials in nitrifying activated sludge systems.* Although inhibition to nitrification function by nanomaterials was not observed in the time

period examined in this study (42-56 days), decrease of nitrifier gene abundances and distinct bacterial communities in SBRs dosed with nanoAg and nanoCeO_2 should be of concern. Long-term study is necessary to verify if continuous exposure to nanomaterials will eventually exert adverse effects on the nitrification.

3) *Examine effects of nanomaterials on nitrifying activated sludge systems in more complex wastewater matrix.* This study used simplified synthetic wastewater during operation of SBRs and dosing of nanomaterials. However, behavior of nanomaterials in real-world wastewater streams may be impacted by a broader range of chemicals. It is necessary that the research is extended to a more complicated wastewater matrix to identify potential effects of nanomaterials associated with other wastewater constituents.

4) *Extend study of transformation and toxicities of ENMs to other groups.* The list of ENMs is expanding with the rapid development of nanotechnolology. This study only examined four metal and metal oxide nanomaterials. For thoroughly assessing the risks of ENMs, it is necessary to extend the study to other groups, and with a variety of properties.